Highly Sensitive Indirect Photometric Detection of Anions and Cations in Capillary Electrophoresis

by

Cameron Anthony Johns

Chemistry

A thesis submitted in fulfilment of the requirements for the degree

of

Doctor of Philosophy

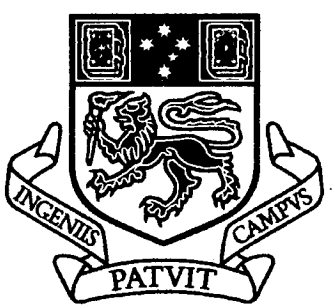

UNIVERSITY
OF TASMANIA

Submitted 31 March 2003

DECLARATION

To the best of my knowledge, this thesis contains no copy or paraphrase of material previously published or written by another person, except where due reference is made in the text of the thesis.

Cameron Anthony Johns
31 March 2003

This thesis may be available for loan and limited copying in accordance with the Copyright Act 1968.

Cameron Anthony Johns
31 March 2003

Acknowledgments

There are a number of people I would like to thank for making this work possible.

Firstly, I sincerely thank Professor Paul Haddad and Dr. Mirek Macka for their supervision of this project. Their input, ideas and guidance throughout my study have made this thesis a reality.

The contribution of all past and present members of the Australian Centre for Research on Separation Science must be acknowledged. Many valuable ideas have come from discussions throughout the group and the support and friendship of everyone involved in the group has been deeply appreciated. Thanks to Helmy Cook, Baoguo Sun, Joe Hutchinson, Andrew Grosse, John O'Reilly, John Madden, Emily Hilder, Michael Breadmore, Kai Ling Ng, Phil Doble, Matt Shaw, Phil Zakaria, Narumol Vachirapatama, Greg Dicinoski and others for making it such an enjoyable place to be.

I would also like to thank the staff of the School of Chemistry and fellow Postgraduate and Honours students for their help and valued friendships throughout the years.

Finally, I must thank my family and friends for their wonderful support throughout my studies. Without them, none of this would have been possible.

LIST OF PUBLICATIONS

Type of Publication	Number	Reference
Papers in refereed journals	8	1-8
Oral presentations at international meetings	1	9
Posters at international meetings	3	10-12

1. C. Johns, M. Macka and P.R. Haddad, Enhancement of detection sensitivity for indirect photometric detection of anions and cations in capillary electrophoresis, *Electrophoresis*, accepted (2003).
   (Chapter 1)

2. C. Johns, M. Macka and P. R. Haddad, Indirect photometric detection of anions in capillary electrophoresis using dyes as probes and electrolytes buffered with an isoelectric ampholyte, *Electrophoresis*, 21, (2000) 1312-1319.
   (*Chapter 3*)

3. C. Johns, M. Macka, P.R. Haddad, M. King and B. Paull, Practical method for evaluation of linearity and effective pathlength of on-capillary photometric detectors in capillary electrophoresis, *J. Chromatogr. A*, 927, (2001), 237-241.
   (*Chapter 4*)

4. C. Johns, M. Macka and P.R. Haddad, Optimisation of probe concentration in indirect photometric detection in capillary electrophoresis using highly absorbing dyes, *Electrophoresis*, 23, (2002) 43-48.
   (*Chapter 5*)

5. C. Johns, M.J. Shaw, M. Macka and P.R. Haddad, Sensitive indirect photometric detection of inorganic and small organic anions by capillary electrophoresis using Orange G as a probe ion, *Electrophoresis*, 24, (2003) 557-566.
   (Chapter 6)

6. C. Johns, M. Macka and P.R. Haddad, Highly sensitive indirect photometric detection of cations by capillary electrophoresis using the cationic dye chrysoidine, *J. Chromatogr. A*, accepted (2002).
   (*Chapter 7*)

7. C. Johns, M. Macka and P.R. Haddad, Measurement of detection linearity and effective pathlength of a high sensitivity detection cell and extended light path capillary for capillary

electrophoresis, *LC-GC*, submitted (2002).
(*Chapter 4*)

8. M. Macka, C. Johns, P. Doble and P. R. Haddad, Indirect photometric detection in CE using buffered electrolytes-Part II, Practical rules, LC-GC, 19 (2001) 178-188.
(Chapter 4)

9. C. Johns, M. Macka and P. R. Haddad, What are the benefits for optimising the probe concentration in electrolytes for indirect photometric detection in capillary electrophoresis?, Oral, *International Ion Chromatography Symposium IICS 2001*, Chicago, IL, USA.

10. C. Johns, M. Macka and P.R. Haddad, Indirect Photometric Detection of Anions in CE Using Dyes as Probes and Electrolytes Buffered with Isoelectric Ampholytes, Poster, *12th International Symposium on High Performance Capillary Electrophoresis & Related Microscale Techniques (HPCE 1999)*, Palm Springs, CA, USA.

11. C. Johns, M. Macka and P.R. Haddad, What is the optimal probe concentration in electrolytes for indirect photometric detection in capillary electrophoresis?, Poster, *International Ion Chromatography Symposium IICS 2000*, Nice, France.

12. C. Johns, M. Macka, M. King, B. Paull and P.R. Haddad, Detection Linearity and Effective Pathlength in On-Capillary Photometric Detection: Evaluation of Five Commercial Detectors, Poster, *25th International Symposium on High Performance Liquid Phase Separations & Related Techniques HPLC 2001*, Maastricht, Holland.

Abstract

The aim of this work was to substantially improve the detection sensitivity and corresponding limits of detection (LODs) of methods for separation of anions and cations by capillary electrophoresis using indirect photometric detection. The approach taken in this project was to employ highly absorbing dyes as indirect detection probes as an effective way to increase the detection sensitivity.

The benefits of using dyes as indirect detection probes in electrolytes buffered with isoelectric ampholytic buffers to enhance detection sensitivity have been demonstrated. Electrolytes containing the dyes, tartrazine and naphthol yellow S (ε= 21,350 and 23,125 L mol^{-1} cm^{-1} respectively), were properly buffered without the addition of co-ions by the use of the ampholytic buffer histidine at its isoelectric point. The increased absorptivity offered by both dyes in comparison to traditionally used anionic probes was reflected by the very low limits of detection (typically sub μM) achieved. Excellent peak shapes and separation efficiencies (up to 300,000 theoretical plates) were observed.

When electrolytes were buffered with low conductivity buffers, such as an ampholyte at its isoelectric point, the limiting factor regarding the probe concentration was the background absorbance and not the separation current. A detailed study on detection linearity of various CE instruments and detection configurations showed that most modern instruments retained a linear absorbance response far in excess of the absorbance range normally used for indirect photometric detection. The upper detector linearity limit (absorbance at which 95% of sensitivity is retained) of five commercially available instruments fitted with a 75 μm ID capillary ranged from 0.3 to 1.2 AU. An estimate of effective pathlengths of each system gave values ranging from 49.7 to 64.6 μm for a 75 μm ID capillary. Upper detector linearity limits and effective pathlengths of an Agilent Extended Light Path Capillary and High Sensitivity Detection Cell were also determined, with values of 1.49 and 2.19 AU, and 128 and 1068 μm, respectively being obtained.

The effects of increasing the probe concentration whilst still remaining within the linear response range of the detector were investigated. The concentration of tartrazine as probe was increased from 0.5 to 3 mM, which resulted in improved resolution between peaks, enhanced peak shapes, extension of the linear analyte response range and the ability to handle more highly concentrated samples without loss of high detection sensitivity.

The combination of high sensitivity and improved stacking effects from the use of dyes at increased concentration were demonstrated by the use of a new dye, Orange G (ε= 24,345 L mol^{-1} cm^{-1}) for the analysis of a range of inorganic and small organic anions. After optimisation, a concentration of 4 mM was found to provide the highest sensitivity. Limits of detection with the optimised system varied from 0.22-0.91 μM. The increased probe concentration resulted in more efficient separations with efficiencies ranging from 128,000-297,000 theoretical plates. A novel approach was used to minimise adsorption problems associated with the use of the dye at high concentrations. A combination of a polyethylenimine coated capillary, addition of a neutral polymer to the BGE and the use of a 50 μm ID capillary provided flat baselines at high Orange G concentrations. The optimised system was used for the determination of anions present in air filter samples and good agreement was obtained with results from ion chromatography.

The use of cationic dyes for the detection of cations is performed even less than for the detection of anions. Based on previous experience and principles gained from work on separation and detection of anions, a new cationic dye, chrysoidine (ε= 23,427 L mol^{-1} cm^{-1}) was investigated. In conjunction with the use of 2-hydroxyisobutyric acid (HIBA) and lactic acid as complexing agents, a mixture of alkaline earth metals, transition metals and lanthanides was separated with limits of detection from 0.22-0.61 μM (for HIBA) and 0.12-1.43 μM (for lactic acid). The use of complexing agents with cationic dyes had not been previously reported. Separation efficiencies ranged from 40,000 to 153,000 theoretical plates.

Table of Contents

Chapter 1

Introduction and Literature Review

1.1 Introduction

1.1.1 Scope of Review

The detection of analytes in capillary electrophoresis (CE) is usually performed by direct photometric detection which involves monitoring a wavelength at which analytes absorb. The major restriction of this approach is that not all analytes will be sufficiently highly absorbing. Indirect photometric detection is an effective alternative detection technique for such cations and anions which lack a suitable chromophore. Unlike direct detection this is a universal, non-selective detection mode in which analytes are detected by their *lack of absorbance.* A strongly absorbing ion, typically called the probe, is added to the background electrolyte (BGE). The probe is displaced by analyte ions of the same charge as the probe, resulting in a decrease in the background absorbance. While indirect detection has a number of advantages over direct detection, including its universality, the sensitivity of the technique remains its major restriction. The focus of this review is on factors relating to the concentration sensitivity of indirect detection, together with previous approaches that have been used to improve sensitivity.

1.1.2 Previous Reviews in the Field

A small number of reviews in the area of indirect photometric detection have appeared. Indirect detection has been reviewed as a sub-area of general detection methods for CE and particularly when photometric detection is emphasised [1-4]. Doble and Haddad [5] presented a comprehensive review on indirect detection of anions in CE. Factors relating to limits of detection, buffering, and determination of inorganic ions, organic acids, carbohydrates, phosphates and phosphonates were discussed in detail. In this Chapter this topic is updated and expanded to include the indirect photometric detection

of cations, with special emphasis on the limits of detection, detector linearity, and buffering aspects.

1.2 Theory and Background

1.2.1 The Kohlrausch Regulating Function and Transfer Ratio

Transfer ratio (R) is defined as the number of moles of probe displaced by one mole of analyte ions. On first inspection, it would be expected that this displacement process would occur on an equivalent-per-equivalent basis. For example R between a singly charged analyte and singly charged probe would be one, between a doubly charged analyte and singly charged probe the R would be two, and so on. If this situation occurred in practice the peak areas of all analytes of the same charge and concentration would be the same. However, this does not hold true. Transfer ratios depend not only on the charges of the probe and analyte, but also on their electrophoretic mobilities. Ackermans *et al.* [6] showed a non-linear relationship between mobility and peak areas which can be rationalised using Kohlrausch's Regulating Function (KRF) [7]

$$\omega = \sum_i \frac{c_i.z_i}{\mu_i} = \text{constant} \qquad (1.1)$$

where c_i, z_i, and μ_i are the ionic concentrations, absolute values of the charge, and absolute values of the effective mobilities of all ionic constituents, respectively.

One single ω function will dictate the movement of ions in a capillary filled with a uniform electrolyte. Two ω functions will determine the movement of ions if a sample plug containing one analyte is introduced, the first being associated with the sample plug, and the second with the bulk electrolyte. Both ω functions must be constant, therefore the concentration distributions of the ions for the bulk electrolyte and the sample plug remain as they were prior to the application of voltage. It follows that in order for this to occur, R is dependent on the mobilities of the probe, the analyte, and the counter-ions. This relationship can be derived directly from the ω function [8, 9] or by applying an eigenvalue approach [9, 10].

Let an electrolyte consist of a single ion A, and its corresponding counter-ion, C. From Eqn. (1.1) the ω function describing the electrolyte is:

$$\omega_1 = \frac{c_A z_A}{\mu_A} + \frac{c_C z_C}{\mu_C} \tag{1.2}$$

where c_A and c_C are the concentrations of A and C in the background electrolyte.

For the electroneutrality condition to hold true:

$$c_A z_A = c_C z_C \tag{1.3}$$

$$\therefore \quad \omega_1 = c_A z_A \left(\frac{1}{\mu_A} + \frac{1}{\mu_C}\right) = \frac{c_A z_A}{\mu_A \mu_C}(\mu_A + \mu_C) \tag{1.4}$$

Now consider injection of an ionic analyte, BC, dissociated into a co-ion B, and conter-ion C. The sample zone will then consist of A, B, and C. From Eqn. (1.1) the ω function describing the sample zone is:

$$\omega_2 = \frac{c'_A z_A}{\mu_A} + \frac{c_B z_B}{\mu_B} + \frac{c'_C z_C}{\mu_C} \tag{1.5}$$

where c'_A and c'_C are the concentrations of A, and C in the sample zone.

For the electroneutrality condition to hold true:

$$c'_A z_A + c_B z_B = c'_C z_C \tag{1.6}$$

$$\therefore \quad \omega_2 = \frac{c'_A z_A}{\mu_A} + \frac{c_B z_B}{\mu_B} + \frac{c'_A z_A}{\mu_C} + \frac{c_B z_B}{\mu_C} \tag{1.7}$$

$$= c'_A z_A \left(\frac{1}{\mu_A} + \frac{1}{\mu_C}\right) + c_B z_B \left(\frac{1}{\mu_B} + \frac{1}{\mu_C}\right) \tag{1.8}$$

Now $\omega_1 = \omega_2$

$$\therefore \quad c_A z_A \left(\frac{1}{\mu_A} + \frac{1}{\mu_C}\right) = c'_A z_A \left(\frac{1}{\mu_A} + \frac{1}{\mu_C}\right) + c_B z_B \left(\frac{1}{\mu_B} + \frac{1}{\mu_C}\right) \tag{1.9}$$

$$(c_A - c'_A) z_A \left(\frac{1}{\mu_A} + \frac{1}{\mu_C}\right) = c_B z_B \left(\frac{1}{\mu_B} + \frac{1}{\mu_C}\right) \tag{1.10}$$

Let $\Delta c_A = c_A - c'_A$

$$\therefore \quad \frac{\Delta c_A}{c_B} = \frac{z_B}{z_A} \frac{\left(\frac{1}{\mu_B} + \frac{1}{\mu_C}\right)}{\left(\frac{1}{\mu_A} + \frac{1}{\mu_C}\right)} \tag{1.11}$$

$$= \frac{z_B}{z_A} \frac{(\mu_B + \mu_C)}{(\mu_A + \mu_C)} \cdot \frac{\mu_A \ \mu_C}{\mu_B \ \mu_C} \tag{1.12}$$

$$= \frac{z_B}{z_A} \cdot \frac{\mu_A}{\mu_B} \frac{(\mu_B + \mu_C)}{(\mu_A + \mu_C)} = R \tag{1.13}$$

Attempts to validate the applicability of Eqn. (1.13) in practical situations (with samples containing more than one analyte) have been made. Predictions made using Eqn (1.13) by Nielen [11] corresponded well with the response factors of alkylsulfate surfactants, analysed with veronal as the probe. Cousins *et al.* [12, 13] used a number of probes to experimentally determine R values for a series of anions. However, experimentally determined values did not match predicted values very well. Nevertheless, the general trend predicted by Eqn. (1.13), matched the values found experimentally. Doble *et al.* [14] found Eqn. (1.13) to be valid for electrolytes containing only a probe anion and counter-ion. The introduction of another co-ion, for example bromide from tetradecyltrimethylammonium bromide (TTAB) (used to modify the electroosmotic flow (EOF)), caused a decrease in R and deviation from predicted values. Maximum values of R occurred when the probe and analyte had very similar mobilities. It should be noted that although EOF plays an important role in CE separations, the EOF mobility does not participate in the equations describing KRF.

It is also possible to detect analytes via the displacement of a counter-ion. This indirect detection mode is based on the principle that the difference in mobility between the analyte ion and the co-ion will result in a change in the counter-ion concentration. If the co-ion is transparent, an absorbing counter-ion can be used for detection, but a strong dependence of the detection sensitivity upon the mobility difference between the analyte and the co-ion (with zero sensitivity occurring for matching mobilities) makes this detection mode somewhat impractical. Collet and Gareil [15] performed indirect detection of cations using anionic probes (benzoate, anisate). Negative and positive peaks were observed depending on the relative mobilities of the analyte and co-ion. If the mobility of the analyte was greater than the mobility of the co-ion, then a positive peak was observed, and if the mobility of the analyte was less than the co-ion mobility then a negative peak occurred [16]. This detection mode relies on a non-absorbing

analyte being detected in a BGE consisting of a non-absorbing co-ion and an absorbing counter-ion, which acts as the probe. If the mobilities of the analyte ion and the co-ion are identical then no peak will be observed. It was found that the response factor depended on the absolute mobilities of the analyte ion, co-ion and counter-ion.

1.2.2 Peak Shapes

Peak shapes of analytes will depend on the relative mobilities of the probe and analyte. A number of papers on this subject have been published [10, 17-20]. Mikkers *et al.* [21, 22] described analyte zone concentration distributions using a mathematical model derived from the KRF. Concentration distributions of the analyte bands were found to depend on the relative mobilities of the probe and analyte. This can be summarised as follows. Analytes which have a mobility higher than the probe will have a concentration distribution which is diffuse at the front and sharp at the back of the sample zone, which will result in a fronted peak (observed relative to the vectors of electrophoretic mobilities of the analyte and co-ion). The direction of EOF and whether the separation is run in the co- or counter-EOF mode will then determine which side of the sample zone moves through the detector first and consequently whether the peak appears as fronted or tailed in the electropherogram. Similarly, analytes with mobilities lower than the probe will have a concentration distribution which is sharp at the front of the zone and diffuse at the rear of the zone, causing tailing peaks (observed relative to the vectors of electrophoretic mobilities of the analyte and co-ion). If the probe and analyte have the same mobilities, a symmetrical peak will occur.

This zone broadening mechanism, which is generally referred to as electromigrational dispersion [23], also depends on another parameter, namely the relative concentrations of the sample ion and the electrolyte co-ion. Electromigrational dispersion can be minimised by manipulating the concentrations of the electrolyte and sample such that the electrolyte concentration is more than two orders of magnitude greater [21]. Therefore, the two main approaches to minimise electromigrational dispersion are to match the mobilities of the analyte(s) and the co-ion as closely as possible, and to keep the electrolyte concentration as high and the injected sample amount as low as possible.

1.2.3 Sensitivity of Indirect Photometric Detection

A non-absorbing analyte will have a limit of detection given by [3, 24-27]:

$$C_{LOD} = \frac{C_p}{R D_r} = \frac{N_{BL}}{R \varepsilon \ell} \tag{1.14}$$

where C_{LOD} is the concentration limit of detection, C_p is the probe concentration, R is the transfer ratio, D_r is the dynamic reserve (the ratio of background absorbance to noise), N_{BL} is the baseline noise, ε is the molar absorptivity of the probe, and ℓ is the detection cell path length. It can be seen that increases in sensitivity may be made through decreasing the probe concentration C_p or baseline noise N_{BL}, or increasing the transfer ratio R, dynamic reserve D_r, probe molar absorptivity ε, or detection cell path length ℓ. However, D_r and C_p are not independent of each another. Decreasing C_p also reduces D_r, which negates any sensitivity increases. Previous attempts at sensitivity enhancements have therefore focussed on reduction of baseline noise, increases in pathlength and increased molar absorptivity of the probe.

1.2.3.1 Baseline Noise

There are various factors which contribute to the overall baseline noise, and these can be divided into 'instrumental' and 'chemical' factors. The first category includes factors such as spatial and intensity stability of the light source, output of the light source at a given wavelength, and other instrumental parameters (electronic noise, temperature stability, mechanical rigidity of the optics, etc.). The 'chemical' noise is caused by undesirable fluctuations in the probe concentration leading to changes in the background absorbance of the BGE.

Attempts have been made to reduce the baseline noise by optimal choice of the light source. Light sources for indirect photometric detection are usually operated at either the emission maximum of the source or the absorption maximum of the probe. Light sources such as deuterium, zinc and cadmium lamps are used most commonly. Such lamps are typically operated in the UV range where their light output and noise are

optimal. An alternative is the use of light emitting diodes (LEDs), which offer a highly stable, nearly monochromatic light source. They also offer the possibility of excellent performance in the visible region of the spectrum where the light output is relatively low for the deuterium lamp. LEDs have been used successfully for indirect detection, and typically result in significant reductions of baseline noise, leading to improvements in detection limits [28, 29]. However, no LEDs in the low-UV range which are suitable for use with the typically used strongly UV absorbing probes are available commercially.

1.2.3.2 Detection Pathlength

The very short optical pathlengths involved in CE with on-capillary detection limit the detection sensitivity. The detection pathlength will be equivalent to the capillary internal diameter (ID) only in an ideal situation where the optics are such that all the individual rays of the light beam pass through the centre of the capillary. In reality, the effective pathlength will be shorter than the capillary ID. Capillary diameters ranging from 50-100 μm are typically used for indirect detection. Increasing the capillary ID, and hence the optical pathlength, results in increases in Joule heating and baseline noise, which counterbalance potential increases in sensitivity. Ma and Zhang [30] investigated the effect of capillary ID on signal-to-noise ratio (S/N) and found that over a range of 25 to 75 μm the ID did not exert a critical influence on sensitivity. They speculated that this was due to increased baseline noise caused by increased Joule heating with larger capillary IDs. However Steiner *et al.* [31] calculated S/N for capillaries ranging in ID from 10 to 10000 μm and showed that S/N increased with capillary ID. This debate is clouded by the fact that the authors measured the background absorbance of the BGE in each capillary without the application of voltage. This approach therefore did not consider the effects of Joule heating on baseline noise.

The use of capillaries with extended pathlengths only at the detection window itself can offer a combination of extended optical pathlength without increases in Joule heating. Weston *et al.* [32] used a capillary of 75 μm ID with a bubble of 300 μm at the detection point. Despite increasing the pathlength by a factor of 4, they reported only a two-fold increase in S/N, due mainly to a resultant increase in baseline noise caused by

the extended pathlength. Doble *et al.* [33] used a Z-cell arrangement with an optical pathlength of 3 mm. By comparison with a 75 μm capillary, S/N was increased by a factor of 3. The less than expected gains can be explained by the increases in baseline noise. The probe concentration was also reduced by a factor of 4 to maintain a background absorbance of 0.127 AU, which additionally negatively influenced the electromigrational dispersion resulting in broader peaks and smaller peak heights. It can be concluded that unlike direct photometric detection, increasing the pathlength for indirect detection will result only in marginal improvements in S/N and corresponding concentration LODs.

1.2.3.3 Probe Absorptivity

The remaining parameter in Eqn. (1.14) that can be optimised in order to achieve lower detection limits is the absorptivity of the probe. Indeed, improvements in detection limits have been achieved in this area mainly through use of this approach. The majority of work has been applied to the detection of anions. Increasing the probe absorptivity results in an increase in the dynamic reserve. The probe concentration may also have to be reduced to keep the BGE absorbance within instrumental limits (see Section 1.2.5), although lowering the probe concentration is undesirable as it will normally result in increased electromigrational dispersion. The mobility of the probe should match the analyte mobility as closely as possible to improve peak shapes and maximise the transfer ratio and hence sensitivity. Foret *et al.* [34] observed a 50 fold increase in sensitivity by using sorbate (ε= 24,120 L.mol^{-1} cm^{-1} at 254 nm) as a probe compared to the use of benzoate (ε= 809 L.mol^{-1} cm^{-1} at 254 nm) for the detection of aspartate, butyrate, chlorate, chloride, dichloroacetate, dimethylmalonate, gluconorate, glutamate, hydroxyisobutyrate, lactate, malonate, methylmalonate and phosphate. Beck and Engelhardt [35] observed that the most sensitive detection of organic and inorganic cations occurred when cationic probes of the highest absorptivity and mobility closest to the analytes were used. Weston *et al.* [32] reported that changing cationic probes from UV Cat 1 to UV Cat 2 improved detection limits of inorganic cations by two to four times, due to the higher absorptivity of UV Cat 2 and its better mobility match to the analytes.

1.2.4 Buffering of Electrolytes for Indirect Photometric Detection

The necessity for BGEs to be well buffered has been clearly demonstrated by numerous authors [36-39]. The application of high voltages to conducting solutions and the resultant electrolysis can result in a pH decrease at the anode, where hydrogen ions are formed, and an increase in pH at the cathode where hydroxyl ions form. Kenndler and Friedl [36] have reported that pH changes as small as 0.03 pH units can cause a loss of resolution and changes in selectivity. As the EOF, and hence also the analyte migration times, are dependent on the electrolyte pH, electrolytes must contain some degree of buffering in order to provide suitable reproducibility and ruggedness of the method. Unfortunately many BGE systems used in CE provide little or no buffering. Investigations into the effects of pH variations provide compelling arguments for the necessity of well buffered systems. Zhu *et al.* [37] observed that the use of BGEs with lower buffering capacities caused faster pH changes. Strege and Lagu [38] highlighted the need for BGE replenishment to prevent poor migration time reproducibility caused by pH variations. Experimentally measured pH changes agreed well with calculated values [40, 41]. Visualisation of pH changes around a capillary and electrode and measurement of those changes in the capillary have been achieved by the addition of pH indicators to BGEs by Macka *et al.* [39], again emphasising the need for proper buffering.

Buffering electrolytes for indirect detection may be performed in four ways. In the first approach, the probe itself can be used as a buffer. For example, for anion detection a weak acid such as phthalate [42] or benzoate [43] is used at or near the pK_a of the probe. However there are three major limitations to this approach. First, the pH range of the BGE is confined to about plus or minus one pH unit from the pK_a of the probe. Second, the buffering capacity of the BGE is dependent on the probe concentration, and third the probe must be only partially ionised (to provide suitable buffering) and will therefore have low mobility. This means that this approach will be suited only to the analysis of analytes with low to moderate mobility.

A second approach is to add a co-ion as a buffer. This method has been used with addition of phosphate [44], carbonate [45], acetate [46], 2-

(cyclohexylamino)ethanesulfonic acid [47] and borate [42, 48-52] to BGEs for detection of anions. Whilst this may provide adequate buffering capacity, the introduction of a co-ion and the resultant competitive displacement can lead to a loss of detection sensitivity and the occurrence of system peaks which can interfere with detection of analytes. This approach may be used successfully only if the mobilities of the probe, co-ion and analyte fall in the appropriate regions so that system peaks will occur at migration times not interfering with analytes.

A third means of providing buffering for indirect detection is the use of a counter-ionic buffer as this provides suitable buffering without the addition of a co-ion. This approach has been used to provide buffering to chromate-based BGEs for detection of anions by the addition of buffering cations such as Tris [26, 53-61] and triethanolamine [62-66]. The use of anionic buffers such as acetic acid with cationic probes for indirect detection of cations has also been performed.

The fourth and so far least commonly employed alternative is the use of isoelectric ampholytic buffers. An ampholyte at its isoelectric point will have zero (or very close to) overall charge and will not act as a competing co-ion. Providing the pK_a's of the functional groups on the ampholyte are sufficiently close (within 2 pH units) to the p*I*, the ampholyte will provide buffering [67, 68]. Unfortunately, few ampholytes that are suitable as BGE buffers fulfil this requirement. Doble *et al.* [33] have used lysine and glutamic acid as buffers for indirect detection of anions. Bromocresol green was used as a probe and the BGE was buffered with 10 mM lysine at pH 9.7 for the indirect detection of C_2-C_8 alkanesulfonic acids. The moderately high EOF meant that separations were performed in a counter-EOF mode and detection of high mobility anions could not be performed with this approach. Such anions were determined using potassium indigotetrasulfonate (ITS) as the probe with the BGE buffered with 10 mM glutamic acid at pH 3.22. EOF was sufficiently low to allow the counter-EOF mode to be used with a negative voltage polarity. However, this system was restricted to the detection of relatively strong acid anions due to the low pH of the BGE. Isoelectric ampholytic buffers will have very low conductivity at their p*I* and can be added to the

BGE in sufficiently high concentrations to provide adequate buffering without increasing Joule heating effects.

1.2.5 Detector Linearity

Indirect photometric detection must be performed at a background absorbance which is within the linear range of the detector used in order to provide a linear response without a loss of detection sensitivity. Probes are typically used at concentrations which result in a background absorbance of around 0.05-0.15 AU. Some common examples are the use of chromate at concentrations ranging from 5-10 mM for detection of anions and imidazole from 5-10 mM for cation detection. As a result, more highly absorbing probes are often used at concentrations of roughly an order of magnitude less so as to keep the background absorbance below about 0.15 AU. In order to minimise electromigrational dispersion and to utilise the benefits of stacking effects, the ionic strength of the BGE should be as high as possible in comparison with the ionic strength of the sample. This is achieved with direct detection by increasing the buffer concentration until excessive separation current and Joule heating results. Practically, a simple plot of buffer concentration *versus* separation current (at constant voltage) can be used to determine the maximum acceptable buffer concentration. This is the concentration at which the above plot deviates substantially from linearity. The advantages of buffer concentration maximisation include narrower peaks, increased separation efficiency and resolution, increased peak heights and the ability to handle samples of higher ionic strength. Similar benefits can be expected to apply to the use of indirect detection.

By comparison, indirect detection has often been used with probe concentrations set at arbitrary values without rigorous investigation. Improvements in peak shapes and symmetries have been noted by increasing the concentration of pyromellitic acid [65]. Further increases in probe concentrations (and hence higher background absorbances) are generally avoided for fear of exceeding the linear range of the detector. Surprisingly little work has been performed on the linearity of detectors for use in CE [69-72]. The most common approach has been to measure the absorbance of a series of probe solutions and to plot absorbance *versus* probe concentration and to estimate the

absorbance at which deviation from linearity occurs [73]. Macka *et al.* [69] reported the use of an approach in which sensitivity (absorbance/concentration) was plotted *versus* absorbance and the linearity limit was defined as the concentration at which sensitivity decreased by a certain amount from its optimal value. Fitting curves to experimentally measured sensitivity data was used to derive the effective pathlength of the detector. This approach was applied successfully to the evaluation of linearity of various instruments and probes.

1.2.6 Highly Absorbing Probes

The most effective approach to improve detection sensitivity is to use more highly absorbing probes. The use of highly absorbing dyes as probes is an attractive option but to date has found limited application. Examples of this approach are reviewed below.

1.2.6.1 The Use of Anionic Dyes as Probes

Most work involving the use of dyes as probes has focussed on the detection of anions. Xue *et al.* [28] determined pyruvate using the anionic dye bromocresol green. A 0.5 mM bromocresol green, pH 8.0 unbuffered BGE was used, but unstable baselines were observed. Mala *et al.* [25] detected anions with the dyes indigo carmine and chlorphenol red. Unfortunately, both BGEs used in this work were buffered with a combination of Tris/acetic acid, and the acetate present would act as competing co-ions. This would account for the worse than expected sensitivity and LODs reported in this study. Siren *et al.* [74] used nitrosonaphthol dyes for detection of organic acids and inorganic anions. Attempts to buffer the BGE at pH 8 with phosphate were unsuccessful as sensitivity was compromised. Accordingly, the dyes were further used in unbuffered BGEs. Doble *et al.* [33] used bromocresol green for the detection of C_2-C_8 alkanesulfonic acids. BGEs buffered with the counter-ion diethanolamine (DEA) and the isoelectric ampholytic buffer lysine were compared. Detection limits with lysine as a buffer ranged from 1-2 μM and were approximately an order of magnitude greater than those obtained with the use of DEA as a buffer. The slopes of calibration curves with lysine were about 70% of those with DEA. The authors explained both observations by noting that lysine contained approximately 2% carbonate, which acted

as a co-ion and hence caused a decrease in sensitivity. The higher mobility dye potassium indigotetrasulfonate was used for detection of more mobile analyte anions [33], and excellent sensitivity (with detection limits ranging from 0.1-2 μM) was observed when the BGE was buffered with Bis/Tris. Use of the ampholytic buffer glutamic acid in the BGE was applicable only for detection of relatively strong acid anions due to the low BGE pH of 3.22. However, sensitivity was very good, with detection limits between 0.7 and 1 μM.

1.2.6.2 Use of Cationic Dyes as Probes

Cationic dyes have been used as probes even less than anionic dyes. Xue and Yeung [28] detected potassium with a 0.5 mM malachite green, pH 3 BGE. Mala *et al.* [25] used methyl green for the detection of caesium, potassium, calcium, magnesium, sodium and lithium ions. The BGE was buffered with 1 mM Tris titrated with acetic acid to pH 6.5. Tris would act as a competing co-ion at this pH and would therefore reduce detection sensitivity. It was noted that no separation was observed when the competing co-ion (Tris) was used at a concentration of 10 mM. This approach was adapted by Butler *et al.* [75] who substituted pyronine G for methyl green in order to better match the emission wavelength of an LED light source. Potassium, calcium, sodium and lithium ions were separated in a 0.15 mM pyronine G, 1 mM Tris, pH 4.0 BGE. Tetrazolium violet was used by Shamsi and Danielson [76] for separation of C_{12}-C_{18} dialkyldimethyl quaternary ammonium compounds and cis/trans adamantane isomers. Detection limits ranged from 0.05-1 mg/L. Buffering was provided at pH 6.0 by 100 mM borate. Significant amounts of methanol (50-85% v/v) were present in the BGEs used.

1.2.7 Separation and Indirect Photometric Detection of Cations

Many metal ions have very similar electrophoretic mobilities and cannot be easily separated by CE. The introduction of auxiliary ligands which can form complexes with metal ions can be used to achieve changes in selectivity. Two approaches are possible. A strongly complexing auxiliary ligand, such as cyanide [77-80], EDTA and CDTA [81-95], and metallochromic ligands [96-100], can be used to form highly stable

(usually anionic) complexes. Complexation is normally performed prior to injection, and this approach is referred to as *pre-capillary complexation*. Detection of the metal complexes is performed in the direct mode. As the majority of the metal ion is complexed, it is difficult to change the separation selectivity. An alternative is the use of weakly complexing ligands where the metal is only partially complexed, so that selectivity changes can be accomplished by varying the degree of complexation using changes in pH or ligand concentration. Complexation is normally performed after the injection and occurs when the sample contacts the BGE containing the auxiliary ligand. This is referred to as *on-capillary complexation*. Detection of the complexes is normally performed indirectly. This is the most common technique for the separation of metal ions, typically using weak acid ligands such as 2-hydroxyisobutyric acid (HIBA), citric acid, lactic acid, acetic acid, glycolic acid, succininic acid and acetic acid.

The first demonstration of this approach was by Foret *et al.* [101] who separated all 14 lanthanides by the addition of HIBA. Jandik and others [102-104] separated 15 alkali, alkaline earth and transition metals and 13 lanthanides using 4-methylbenzylamine (UV Cat 1) as a probe with HIBA and citric acids as complexing agents. Chen and Cassidy [105] achieved baseline separation of 26 metals with N,N'-dimethylbenzylamine as probe and HIBA as complexing agent. Shi and Fritz [106] separated 27 metals using 4-methylbenzylamine and lactic acid. Lin *et al.* [107] investigated the use of 10 carboxylic acids (acetic, glycolic, lactic, HIBA, oxalic, malonic, malic, tartaric, succininic and citric) as complexing agents. It was found that oxalic and citric acid caused the largest selectivity changes. The optimum pH in terms of separation selectivity was found to be near the pK_{a1} of the complexing agent. Optimisation of separations involving large numbers of metals have been thoroughly investigated [106, 108].

1.2.8 Simultaneous Separation and Indirect Photometric Detection of Anions and Cations

The simultaneous separation and detection of anions and cations poses a number of difficulties. Firstly, anions and cations must be transported pass the detection window in such a way to allow separation and secondly the BGE must contain suitable probes to allow the detection of the ions. A small number of approaches have been used to

address this task. It is possible to employ an EOF which has sufficient velocity to transport ions which are migrating in the opposite direction to the EOF past the detection point. The simplest way to increase the magnitude of the EOF is to increase the BGE pH. However, this may not be suitable for the detection of cations as alkaline earth metal ions may form hydroxide complexes. Additionally, cationic probes may not be protonated at higher pH values. Alternatively, external pressure can be applied to provide a flow in addition to the EOF, as demonstrated by Haumann *et al.* [109]. The most successful means of simultaneous detection involves the use of sample injection at both ends of the capillary. Cations and anions can then be allowed to migrate past the detector due to their electrophoretic mobilities. The BGE should contain both an anionic and cationic probe in order to provide detection. Clearly, from indirect detection principles the presence of competing co-ions should be minimised. This suggests that probes should be present as free acids and bases. The BGE must be at a pH at which both probes will be charged.

Padarauskas *et al.* [110] used two different BGEs for simultaneous detection. Imidazole (cationic probe) and nitrate (anionic probe) were used at pH 4 to separate and detect potassium, chloride, sulfate, calcium, sodium and magnesium ions. Buffering was provided by fumaric acid. An electrolyte containing copper(II)-ethylenediamine and nitrate at pH 8.5 allowed detection of chloride, sulfate, potassium, ammonium, hydrogencarbonate, calcium, sodium and magnesium ions. Fumaric acid was utilised as a complexing agent to improve separation selectivity between calcium and sodium. Triethanolamine was used as a buffer, which resulted in a system peak occurring in a mobility region away from that of the analytes. The sample was injected electrokinetically at both ends of the capillary and a detection window near the middle of the capillary was used.

This approach was further developed by Padarauskas *et al.* [111] using a BGE containing copper(II)-ethylenediamine as the cationic probe and chromate (in the form of chromic trioxide) as the anionic probe. Potassium, calcium, magnesium, sodium,

ammonium, chloride, hydrogencarbonate, sulfate and nitrate ions were separated. Triethanolamine provided buffering at pH 8.0. This method was used for the analysis of tap, river and mineral waters.

Kuban and Karlberg [112] used a BGE containing 4-aminopyridine and chromic acid at pH 8.0 for detection of cations and anions respectively. The sample was injected hydrodynamically at both capillary ends and again a detection window in the middle of the capillary was used. Separation of 22 small inorganic and organic anions and alkali and alkaline earth metal ions was achieved in less than five minutes. Transition metal cations and barium could not be analysed as hydroxide formation and/or precipitation with chromate occurred.

Xiong and Li [113] investigated the use of benzylamine and imidazole (cationic probes) and benzenesulfonic acid, sulfosalicylic acid and pyromellitic acid (anionic probes) in BGEs for simultaneous detection of anions and cations. Sample was injected hydrostatically at the anodic end of the capillary and ions were transported past the detection window by a high velocity EOF. A BGE containing imidazole and sulfosalicyclic acid was used to detect potassium, sodium, lithium, hydrogen phosphate, fluoride, hydrogen carbonate, chlorate and perchlorate ions. A benzylamine-pyromellitic acid BGE was used to detect potassium, sodium, lithium, acetate, hydrogen phosphate, fluoride, chlorate, perchlorate, nitrate, nitrite, chloride and sulfate ions.

Xiong and Li [114] further developed this approach by studying the use of imidazole, 1,2-dimethylimidazole, benzylamine (cationic probes) and sulfosalicylic acid, trimellitic acid and pyromellitic acid (anionic probes). They found that a BGE consisting of 1,2-dimethylimidazole/trimellitic acid was the best combination. Imidazole was eliminated as it was desired to perform separations at a pH higher than the pK_a of imidazole, meaning it would not function as a probe. Benzylamine was discarded due to its lower absorptivity (between 200 and 230 nm) compared with 1,2-dimethylimidazole.

Trimellitic acid was selected as the anionic probe based on superior detection sensitivity and peak shapes compared with the other anionic probes. This electrolyte was then optimised, allowing the separation and detection of four alkali metal ions and 12 organic acids in six minutes. Detection limits ranged from 0.08-5 μg/mL. The method was used successfully for the analysis of apple, grape and orange juices.

Raguenes *et al.* [115] used a BGE containing Tris/1,5-naphthalenedisulfonic acid to separate and detect potassium, ammonium, sodium, lithium, ascorbate, sorbate, benzoate, lactate, acetate, hydrogencarbonate, phosphate, formate and fluoride ions in less than nine minutes with detection limits between 0.1 and 1 ppm. The analysis of a real sample yielded results comparable with inductively-couple plasma mass spectroscopy and ion chromatography.

Haumann *et al.* [109] used imidazole-thiocyanate and dimethyldiphenylphosphonium iodide-trimesic acid BGEs in conjunction with hydrodynamic sample injection at both capillary ends for detection of inorganic anions and cations, small organic acids and aliphatic amines. The analysis of drinking water, mineral water and an alcoholic beverage demonstrated the utility of this system.

1.3 Tabular Summary of the Literature

Tables 1.1-1.7 provide a comprehensive overview of indirect detection methods for anions and cations. Due to the large number of entries using chromate as a probe, these are listed together in Table 1.1. The remaining Tables are used to group various probe types, with benzene carboxylate probes being listed in Table 1.2, naphthalene carboxylate probes listed in Table 1.3, aromatic sulfonate probes listed in Table 1.4, and miscellaneous anionic probes listed in Table 1.5. In a similar fashion, cationic probe data are collected in Tables 1.6 and 1.7, with methods using imidazole as probe being given in Table 1.6 and other cationic probes listed in Table 1.7. Each entry contains information on the probe concentration which has been used, detection wavelength(s), ions analysed and LODs (where given in the original publication) and the method of buffering. The complexing agent and mode of complexation (if any) is also given for

all cationic probe entries. Absorptivities of anionic probes are given where possible in Table 1.8 and cationic probe absorptivities are collated in Table 1.9.

Inspection of these tables allows some general comments to be made regarding previous approaches to indirect detection. First, the majority of work has been performed using low or moderately absorbing probes. In the rare cases when highly absorbing probes have been used, they have been utilised at low BGE concentrations. Second, most BGEs have been unbuffered or incorrectly buffered with the addition of co-ions. Very few BGEs have been buffered using an isoelectric ampholytic buffer. Third, most detection has been performed at wavelengths in the low UV region. There has been little use of detection of probes at longer wavelengths, such as in the visible region. Fourth, the small amount of work on the detection of cations using highly absorbing probes has been severely restricted as no complexing agents have been used to allow separation of a range of metal ions. Finally, concentration detection limits are generally at the micromolar level.

1.4 Aims

As is evident from Tables 1.1-1.9, indirect photometric detection has been generally performed using moderately absorbing probes. The advantages and disadvantages of using highly absorbing probes have yet to be explored fully. Importantly, the use of such probes at similar concentrations used for less absorbing probes has been avoided due to a lack of knowledge regarding detector linearity. Many BGEs have also been incorrectly buffered, or not buffered at all. Even less work in these areas has been accomplished for the detection of cations. Based on these considerations, the aims of this work were as follows:

- To investigate the use of previously unexploited highly absorbing dyes in properly buffered BGEs for the determination of anions;
- To evaluate the performance and linearity of various detection cells and instruments for capillary electrophoresis in order to determine the maximum workable absorbance background levels;

- To demonstrate the advantages and disadvantages associated with the use of highly absorbing probes at higher concentrations;
- To develop a highly sensitive, rugged and reproducible method for the indirect photometric detection of anions;
- To utilise the knowledge gained from anion investigations to establish a highly sensitive method for indirect photometric detection of cations using a highly absorbing cationic dye.

Table 1.1 Chromate electrolytes for indirect detection of anions

[chromate] in BGE (mM)	Detection wavelength (nm)	Buffering method	LODs	Analytes	Ref.
3	214, 254	Counter-ion (Tris)	2-4 μM	sulfate, sulfide, tetrathionate, thiosulfate	[54]
5	254, 270, 300	Counter-ion (Tris)	1 -2.5 μM	C_2-C_{14} fatty acids	[56]
5	254	None (probe only)	0.3 - 0.8 ppb	acetate, chloride, fluoride, formate, nitrate, oxalate, phosphate, propionate, sulfate	[116]
10	254	None (probe only)	0.1 - 0.4 µg/ml	acetate, carbonate, chlorate, citrate, fluoride, formate, malonate, oxalate, phosphate, succinate, sulfate, tartrate	[117]
7-10	254	None (probe only)	0.4 - 1.2 µg/l (EMI)	chloride, fluoride, nitrate, oxalate, phosphate, sulfate	[118]
5	260	None (probe only)	20-50 μM	citrate, diethylenetriaminepentacetic acid, ethylenediaminetetraacetic acid, nitrilotriacetic acid, phosphate, pyrophosphate, tripolyphosphate	[119]
6	254	None (probe only)	3.5-15 pg	arsenate, arsenite, dimethylarsinate, monomethylarsonate	[120]
10	254	None (probe only)	0.32 µg/ml	acetate, borate, bromide, butyrate, carbonate, chloride, citrate, fluoride, formate, molybdate, nitrate, nitrite, oleate, phosphate, propionate, sulfate, thiosulfate, tungstate	[121]

Table 1.1 Chromate electrolytes for indirect detection of anions

[chromate] in BGE (mM)	Detection wavelength (nm)	Buffering method	LODs	Analytes	Ref.
5	214, 254	Counter-ion (Tris)	25-50 μ*M*	arsenate, arsenite	[59]
5	220, 276	None (probe only)	3-450 ng/ml	acetate, carbonate, chlorate, chloride, formate, nitrate, sulfate	[122]
5	254	None (probe only)	< 10 μ*M*	sulfate, fluoride, nitrite, nitrate, chloride, bromide	[123]
5	254	Counter-ion (Tris)	N/A	chloride, sulfate, nitrate, chlorate, phosphate, carbonate	[124]
5	254	None (probe only)	200 - 1000 μg/l	bromide, chloride, nitrate, nitrite, phosphate, sulfate	[125]
5	185, 254	None (probe only)	150-320 ng/ml	acetate, chloride, citrate, fumarate, nitrate, phosphate, sulfate	[126]
2-12	254	None (probe only)	0.12 - 0.84 ppm	acetate, bromide, carbonate, chloride, fluoride, molybdate, nitrate, phosphate, sulfate, thiosulfate	[127]
7	254	None (probe only)	< 5 μg/ml	carbonate, chloride, nitrate, sulfate	[128]
5,10	255	None (probe only)	5-70 ppm	chloride, morpholine, nitrate, N-morpholine, N-morpholine-N-oxide, sulfate	[129]
10	254	None (probe only)	0.1-0.4 μg/ml	chloride, fluoride, monofluorophosphate, nitrate, phosphate, sulfate, tungstate	[130]

Table 1.1 Chromate electrolytes for indirect detection of anions

[chromate] in BGE (mM)	Detection wavelength (nm)	Buffering method	LODs	Analytes	Ref.
2.5	254, 270	Co-ion (borate)	200 ng/ml	bisinositol phosphate, hexakisinositol phosphate, monoinositol phosphate, trisinositol phosphate	[42]
5	254	Co-ion (CHES)	0.10-0.32 ppm	chloride, bromide, sulfate, nitrate, fluoride, phosphate, carbonate	[47]
5	254	Co-ion (borate)	1-3 mg/l	bromide, chloride, fluoride, nitrate, nitrite, phosphate, sulfate, thiosulfate	[63]

Table 1.2 Benzene Carboxylate Probes for Indirect Detection of Anions

Probe	BGE Range (mM)	Detection wavelength (nm)	Buffering method	LOD	Analytes	Ref
p-aminobenzoate	7.5-20	250, 264	None (probe only)	10-40 nM	(large volume injection) chloride, sulfate, nitrite, nitrate, formate, acetate, propionate, methanesulfonate, oxalate, malonate, maleate, succinate, glutarate, adipate, pimelate, suberate, azelate, sebacate	[131]
Anisate	10	254, 270, 300	Counter-ion (Tris)	1-2.5 μM	C_2-C_{14} fatty acids	[56]
Benzoate	100	254	Counter-ion (Tris)	50 μM	α,β,γ cyclodextrins	[55]
	20	228	Counter-ion (Tris)	0.3-1.1 fmol	bromide, chloride, nitrate, sulfate	[30]
	40	254, 270, 300	None (probe only)	1-2.5 μM	C_2-C_{14} fatty acids	[56]
o-benzylbenzoic acid	20	228	None (probe only)	0.3-1.1 fmol	bromide, chloride, nitrate, sulfate	[30]
2,3-dihydroxybenzoic acid	10	254, 270, 300	Counter-ion (Tris)	1-2.5 μM	C_2-C_{14} fatty acids	[56]
3,5-dimethoxybenzoate	100	254	Counter-ion (Tris)	50 μM	α,β,γ cyclodextrins	[55]
3,4-dimethoxycinnamic acid	12	256, 267, 310	None (probe only)	0.01-0.04 mM	fructose, glucose, maltose, sucrose	[132]
2,4-dimethylbenzoate	100	254	Counter-ion (Tris)	50 μM	α,β,γ cyclodextrins	[55]

Table 1.2 Benzene Carboxylate Probes for Indirect Detection of Anions (cont)

Probe	BGE Range (mM)	Detection wavelength (nm)	Buffering method	LOD	Analytes	Ref
2,5-dimethylbenzoate	100	254	Counter-ion (Tris)	50 μM	α,β,γ cyclodextrins	[55]
3,5-dimethylbenzoate	100	254	Counter-ion (Tris)	50 μM	α,β,γ cyclodextrins	[55]
3,5-dinitrobenzoate	5	200, 254	Co-ion (phosphate)	6 μM	caprylate, laurate, myristate, oleate, palmitate, stearate	[44]
Hydroxybenzoate	4	220, 450	None (probe only)	0.1 μg/mL	acetate	[133]
p-hydroxybenzoate	5	254	None (probe only)	N/A	bromide, butanesulfonate, carbonate, chloride, citrate, ethanesulfonate, hexanesulfonate, molybdate, nitrate, nitrite, pentanesulfonate, phthalate, propanesulfonate, sulfate, tungstate	[134]
Phenylacetic acid	0.1	222	None (probe only)	0.1 mM	carbohydrates	[135]
Phthalate	3	214, 254	Counter-ion (Tris)	2-4 μM	sulfate, disulfide, tetrathionate, thiosulfate	[54]
	5	254	Co-ion (borate)	12 μM	acetate, carbonate	[52]
	5	254, 270	Co-ion (borate)	200 ng/mL	bisinositol phosphate, hexakisinositol phosphate, monoinositol phosphate, trisinositol phopshate	[42]

Table 1.2 Benzene Carboxylate Probes for Indirect Detection of Anions (cont)

Probe	BGE Range (mM)	Detection wavelength (nm)	Buffering method	LOD	Analytes	Ref
Phthalate	5	230	None (probe only)	0.1-0.4 μg/mL	bromoacetate, chloroacetate, formate, monofluorioacetate	[136]
	5	254, 280	Co-ion (boric acid)	100-200 ng/mL	acetate, bromide, butyrate, chloride, formate, nitrate, nitrite, oxalate, propionate, sulfate	[62]
	1.5	230	Co-ion (carbonate)	60-360 pg	adipate, α-ketoglutarate, citrate, ethylmalonate, glutarate, lactate, malonate, methylmalonate, methylsuccinate, oxalate, pyruvate, succinate, tartrate	[137]
	5	185	None (probe only)	0.7-1.1 mg/L	acetate, citraconate, citrate, crotonate, hydroxyisobutyrate, itaconate, mesaconate, methacrylate, pyruvate	[138]
Pyromellitate	1.5	214, 254	Counter-ion (Tris)	2-4 μM	sulfate, sulfide, tetrathionate, thiosulfate	[54]
	2.25	254	Counter-ion (triethanolamine)	1-3 mg/L	bromide, chloride, fluoride, nitrate, nitrite, phosphate, sulfate, thiosulfate	[63]
	3	220	Counter-ion (diethylenetriamine)	0.01-1.0 mg/L	acetate, chloride, citrate, lactate, malate, nitrate, oxalate, phosphate, succinate, sulfate, tartrate	[139]

Table 1.2 Benzene Carboxylate Probes for Indirect Detection of Anions (cont)

Probe	BGE Range (mM)	Detection wavelength (nm)	Buffering method	LOD	Analytes	Ref
Pyromellitate	2.25	254, 280	Counter-ion (triethanolamine)	100-200 ng/mL	acetate, bromide, butyrate, chloride, formate, nitrate, nitrite, oxalate, propionate, sulfate	[62]
	2.25	254	Counter-ion (triethanolamine)	0.04-0.15 mg/L	bromide, chloride, nitrate, nitrite, oxalate, sulfate	[140]
	2.25	254	Counter-ion (triethanolamine)	0.01-0.04 mg/L	bromide, chloride, sulfate, nitrite, nitrate, fluoride, phosphate	[141]
Salicylate	7.5	222-288	Counter-ion (Tris)	0.2-2 μM	ascorbate, carbonate, chloride, citrate, formate, fumarate, glutarate, lactate, malate, nitrate, oxalate, phosphate, pyruvate, succinate, sulfate	[26]
	5	230	Co-ion (acetate)	0.6 pmol	alkane sulfonates, alkyl sulfates	[142]
2-sulfobenzoic acid	20	228	None (probe only)	0.3-1.1 fmol	bromide, chloride, nitrate, sulfate	[30]
5-sulfosalicylic acid	5	214	None (probe only)	5 fmol	heparin fragments	[143]
	0.1	214	None (probe only)	100-900 ppb	phosphate, fluoride, carbonate, chlorate, perchlorate	[113]
1,2,4-tricarboxybenzoic acid	5	214	None (probe onl)y	5 fmol	heparin fragments	[143]
Trimellitate	5	220, 240, 265	None (probe only)	N/A	acetate, ascorbate, citrate, glucanate, glutamate, lactate, malate, oxalate, tartrate	[144]

Table 1.2 Benzene Carboxylate Probes for Indirect Detection of Anions (cont)

Probe	BGE Range (mM)	Detection wavelength (nm)	Buffering method	LOD	Analytes	Ref
Trimellitate	5	254	None (probe only)	N/A	bromide, chloride, citrate, fluoride, phosphate, sulfate	[12]
	1	254	Counter-ion (Tris)	N/A	chloride, citrate, hexanoate, malonate, propionate, tartrate	[53]
	0.5	210	Counter-ion (Tris)	N/A	hexanoate, propionate	[61]
Trimesic acid	Unknown	230	Unknown	50 mg/L	bromide, carbonate, chlorate, chloride, fluoride, nitrate, nitrite, perchlorate, phosphate, sulfate	[145]

Table 1.3 Naphthalene Carboxylate Probes for Indirect Detection of Anions

Probe	BGE Range (mM)	Detection wavelength (nm)	Buffering method	LODs	Analytes	Ref
2,6-naphthalenedicar-boxylate	1	240	None (probe only)	0.025 mg/l	acetate, butyrate, propionate	[146]
	2	280	None (probe only)	20 μg/ml	acetate, adipate, azelate, benzoate, butyrate, carbonate, chloroacetate, dichloroacetate, formate, fumarate, glutarate, methanesulfonate, phthalate, pimelate, propionate, sebacate, suberate	[147]
	2	254, 280	None (probe only)	100-200 ng/ml	acetate, bromide, butyrate, chloride, formate, nitrate, nitrite, oxalate, propionate, sulfate	[62]
	4	214	Counter-ion (Bis/Tris)	47-180 mg/L	oxalate, malonate, formate, malate, succinate, phthalate, methanesulfonate, glutarate, glycolate, pyruvate, suberate, acetate, glyoxylate, lactate, propionate, benzoate	[148]
Naphthoate	10	254, 270, 300	Counter-ion (Tris)	1-2.5 μ*M*	C_2-C_{14} fatty acids	[56]
1-naphthylacetic acid	0.1 - 2	222	None (probe only)	0.1 m*M*	carbohydrates	[135]

Table 1.4 Aromatic Sulfonate Probes for Indirect Detection of Anions

Probe	BGE Range (mM)	Detection wavelength (nm)	Buffering method	LODs	Analytes	Ref
1,3-benzene-disulfonate	3	214, 254	Counter-ion (Tris)	2-4 μ*M*	sulfate, sulfide, tetrathionate, thiosulfate	[54]
1,5-naphthalene-disulfonate	3	214, 254	Counter-ion (Tris)	2-4 μ*M*	sulfate, sulfide, tetrathionate, thiosulfate	[54]
	4-8.3	214, 284, 288	Co-ion (borate)	10-275 μg/L (Inorganic anions), 30-60 μg/L (organic acids)	Inorganic anions, organic acids	[149]
Naphthalenesulfonate	5	214, 274	Co-ion (borate)	0.5-2.0 mg/L	C_4-C_{14} alkanesulfonates and alkyl sulfates	[149]
2-naphthalenesulfonate	4-10	254, 270, 300	Counter-ion (Tris)	1-2.5 μ*M*	C_2-C_{14} fatty acids	[56]
2-naphthalenesulfonic acid	0.1	222	None (probe only)	0.1 m*M*	carbohydrates	[135]
1,3,6-naphthalene-trisulfonate	2	214, 254	Counter-ion (Tris)	2-4 μ*M*	sulfate, sulfide, tetrathionate, thiosulfate	[54]
1,3,6-naphthalene-trisulfonate	4-8.3	214, 284, 288	Co-ion (borate)	8-250 μg/L (Inorganic anions), 20-50 μg/L (organic acids)	Inorganic anions, organic acids	[149]

Table 1.4 Aromatic Sulfonate Probes for Indirect Detection of Anions (cont)

Probe	BGE Range (mM)	Detection wavelength (nm)	Buffering method	LODs	Analytes	Ref
1-naphthol-3,6-disulfonic acid	0.5	214	Co-ion (acetic acid)	4-22 μM	inositol phosphates	[150]
1-nitroso-2-naphhthol-3,6-disulfonate	0.5	254	None (probe only)	$2x10^{-8}$ -$9x10^{-7}$ *M*	acetate, butyrate, chloride, clodronate, fluoride, hippurate, isovalerate, malonate, nitrate, nitrite, oxalate, phosphate, phosphite, propionate, pyruvate, sulfate	[74]
1-nitroso-2-naphthol-6-sulfonate	0.5	254	None (probe only)	$2x10^{-8}$ - $9x10^{-7}$ *M*	acetate, butyrate, chloride, clodronate, fluoride, hippurate, isovalerate, malonate, nitrate, nitrite, oxalate, phosphate, phosphite, propionate, pyruvate, sulfate	[74]
2-nitroso-1-naphthol-6-sulfonate	0.5	254	None (probe only)	$2x10^{-8}$ - $9x10^{-7}$ *M*	acetate, butyrate, chloride, clodronate, fluoride, hippurate, isovalerate, malonate, nitrate, nitrite, oxalate, phosphate, phosphite, propionate, pyruvate, sulfate	[74]
p-toluenesulfonate	5	220	Co-ion (borate)	N/A	anionic and cationic surfactants	[50]

Table 1.5 Miscellaneous Probes for Indirect Detection of Anions

Probe	BGE Range (mM)	Detection wavelength (nm)	Buffering method	LODs	Analytes	Ref
Adenosine monophosphate	5	259, 261	Co-ion (borate)	1.2 - 11 μ*M*	polyphosphates and polyphosphonates	[49]
	5	254, 259, 280, 300	Co-ion (borate)	0.05 - 3.0 mg/l	alkyl sulfates and sulfonates	[76]
Bromocresol green	0.5	633	None (probe only)	2x 10^{-16} mol	pyruvate	[28]
	0.5	618	Ampholytic (lysine), counter-ion (diethanolamine)	0.1-0.2 μM	C_2-C_8 alkanesulfonic acids	[33]
Chlorphenol red	0.5	578, 620, 635	Co-ion (acetic acid)	2 x10^{-13} - 8x 10^{-16} mol	bromide, chloride, citrate, fumarate, glutamate, malonate, nitrate, sulfate	[25]
p-cresol	0.1	222	None (probe only)	0.1 m*M*	carbohydrates	[135]
1,3-dihydroxynaphthalene	0.1	222	None (probe only)	0.1 m*M*	carbohydrates	[135]
Indigo carmine	0.5	578, 620, 635	Co-ion (acetic acid)	2x10^{-13}- 8x10^{-16} mol	bromide, chloride, citrate, fumarate, glutamate, malonate, nitrate, sulfate	[25]
Permanganate	20	635, 670	None (probe only)	3.5 μ*M*	chlorate, chloride, fluoride, nitrate, sulfate	[151]

Table 1.5 Miscellaneous Probes for Indirect Detection of Anions (cont)

Probe	BGE Range (mM)	Detection wavelength (nm)	Buffering method	LODs	Analytes	Ref
Phenylphosphonic acid	10	200	Co-ion (borate)	0.15 - 0.21 pmol	butylphosphonic acid, ethylphosphonic acid, methylphosphonic acid, propylphosphonic acid	[51]
	1	214	Ampholytic (glutamic acid)	2 μM	methylphosphonic acid	[152]
Potassium indigotetrasulfonate	0.5	314	Counter-ion (Bis-Tris)	0.1-2 μM	bromide, chloride, sulfate, thiocyanate, chlorate, malonate, tartrate, bromate, formate, succinate, phthalate, iodate, phosphate	[33]
	0.5	314	Ampholytic (glutamic acid)	0.7-1 μM	sulfate, nitrate, perchlorate, chlorate, bromate	[33]
2,6-pyridinedicarboxylate	5	214	None (probe only)	1-2.5 mg/l	acetate, bromide, butyrate, citrate, formate, heptanoate, hexanoate, iodide, lactate, malate, nitrate, octanoate, oxalate, pyruvate, succinate, tartrate, valerate	[153]
	20	230	None (probe only	6-12 mg/L	inorganic and organic anions, amino acids	[154]
	20	230	None (probe only)	23-37 mg/L	carbohydrates	[154]
Riboflavin	12	256, 267, 310	None (probe only)	0.01 to 0.04 m*M*	fructose, glucose, maltose, sucrose	[132]

Table 1.5 Miscellaneous Probes for Indirect Detection of Anions (cont)

Probe	BGE Range (mM)	Detection wavelength (nm)	Buffering method	LODs	Analytes	Ref
Sorbate	6	256	None (probe only)	0.23-0.29 m*M*	D-fructose, L-fucose, D-galactose, D-glucose, D-glucuronic acid, galacturonate, N-acetyl-galactosamine, N-acetyl-glucosamine, N-acetyl-neuraminic acid	[155]
	6	256	None (probe only)	2 pmol	carbohydrates	[156]
	6	254	None (probe only)	2000 fmol	2-deoxy-d-galactose, 2-deoxy-d-ribose, cellobiose, d-arabonic acid, d-fructose, d-fucose, d-galactonic acid, d-galactose, d-galacturonic acid, d-gluconic acid, d-glucose, d-glucuronic acid, d-lyxose, d-mannonic acid, d-mannose, d-mannuronic acid, d-ribonic acid, d-ribose, d-xylose, lactose, lactulose, l- arabinose, l-rhamnose, l-sorbose, maltose, maltotriose, melibiose, raffinose, saccharose	[157]
	12	256, 267, 310	None (probe only)	0.01 - 0.04 m*M*	fructose, glucose, maltose, sucrose	[132]

Table 1.5 Miscellaneous Probes for Indirect Detection of Anions (cont)

Probe	BGE Range (mM)	Detection wavelength (nm)	Buffering method	LODs	Analytes	Ref
Tryptophan	1.0	280	None (probe only)	N/A	1-naphthylacetic acid, anthraquinone-2-sulfonic acid, cellobiose, d-arabinose, d-fructose, d-fucose, d-galactonic acid, d-galactosamine, d-galactose, d-gluconic acid, d-glucosamine, d-glucose, d-lyxose, d-mannitol, d-mannose, d-ribose, d-sorbitol, d-sorbose, d-tagatose, d-xylose, furanarcrylic acid, gentiobiose, lactose, maltose, meleziose, melibiose, muconic acid, raffinose, sorbate, stachyose, sucrose, tryptophan	[158]
Uridine monophosphate	5	259, 261	Co-ion (borate)	1.2 -11 μM	polyphosphates and polyphosphonates	[49]

Table 1.6 Imidazole Electrolytes for Indirect Detection of Cations

Complexing agent	Complex Formation	[imidazole] in BGE (mM)	Detection wavelength (nm)	Buffering method	LODs	Analytes	Ref
Sulfate	ON	20	214	None (probe only)	N/A	sodium, potassium, magnesium, calcium	[159]
None	None	3-5	214	None (probe only)	0.05-0.1ppm	potassium, sodium, lithium, barium, calcium, magnesium	[35]
None	None	5	214	None (probe only)	10nM	Al^{3+} , AlF^{2+}, AlF_2^{+}, Al-oxalate	[160]
Acetate, glycolate, lactate, HIBA, oxalate, malonate, malate, tartrate, succinate, citrate	ON	5	215	None (probe only)	~ sub-ppm	lithium, sodium, potassium, magnesium, calcium, barium	[107]
Sulfate	ON	5	214	None (probe only)	50-100 ppb	sodium, potassium, magnesium, calcium, manganese	[161]
Sulfate	ON	100	214	None (probe only)	70 μM	calcium, sodium, potassium, magnesium	[162]
None	None	10	214	None (probe only)	17-82 μM	sodium, potassium, magnesium, calcium	[163]

Table 1.6 Imidazole Electrolytes for Indirect Detection of Cations (cont)

Complexing agent	Complex Formation	[imidazole] in BGE (mM)	Detection wavelength (nm)	Buffering method	LODs	Analytes	Ref
HIBA + 18C6	ON	5	214	Counter-ion (HIBA)	0.4ppb – 1ppm (EMI)	lithium, sodium, potassium, magnesium, calcium, strontium, barium, manganese, nickel, zinc, copper, ammonium	[164]
None	None	6	214	Counter-ion (formate)	0.5 ppm	potassium	[165]
None	None	6	214	Counter-ion (formate)	N/A	sodium	[166
HIBA	ON	5	214	Counter-ion (HIBA)	N/A	lithium, sodium, potassium, magnesium, calcium, strontium, barium, chromium, manganese, nickel, zinc, copper, ammonium	[167]
18C6	ON	1-15	214	None (probe only)	N/A	lithium, sodium, potassium, magnesium, calcium, ammonium	[168]
HIBA + 18C6	ON	5	214	Counter-ion (HIBA)	0.1-0.4 ppm	sodium, potassium, magnesium, calcium	[169]
Lactate	ON	1-15	214	Counter-ion (lactate)	N/A	lithium, sodium, potassium, caesium, magnesium, calcium, strontium, barium, manganese, $iron^{II}$, $cobalt^{II}$, nickel, copper, zinc, cadmium, lead, ammonium	[170]
HIBA + 18C6	ON	5	214	Counter-ion (HIBA)	50-400 ppb	sodium, potassium, magnesium, calcium, manganese, zinc, ammonium	[171]

Table 1.6 Imidazole Electrolytes for Indirect Detection of Cations (cont)

Complexing agent	Complex Formation	[imidazole] in BGE (mM)	Detection wavelength (nm)	Buffering method	LODs	Analytes	Ref
HIBA, or CDTA	ON	5	200	Counter-ion (borate)	N/A	strontium, copper, mercury, aluminium, lead	[93]
Sulfate	ON	25-75	214	None (probe only)	7 μM	lithium, sodium, potassium, magnesium, calcium, barium	[31]
None	None	12.5	215	Counter-ion (HIBA, acetate)	N/A	sodium, potassium, magnesium, calcium, manganese, cobalt^{II}, nickel, zinc, ammonium	[172]
HIBA	ON	6	214	Counter-ion (HIBA	N/A	lithium, sodium, potassium, magnesium, calcium, strontium, barium, manganese, iron, cobalt^{II}, copper	[173]
None	None	20	214	Counter-ion (acetate)	7-20 μM	lithium, sodium, potassium, rubidium, caesium, magnesium, calcium, strontium, barium, ammonium	[174]
Sulfate	ON	5	214	None (probe only)	50-100 ppb	sodium, potassium, magnesium, calcium, manganese	[175]
None	None	10	204, 214	None (probe only)	~ 50 ppb	lithium, sodium, potassium, magnesium, calcium, barium, ammonium	[176]

Table 1.6 Imidazole Electrolytes for Indirect Detection of Cations (cont)

Complexing agent	Complex Formation	[imidazole] in BGE (mM)	Detection wavelength (nm)	Buffering method	LODs	Analytes	Ref
Glycolate	ON	10	214	Counter-ion (glycolic acid)	N/A	potassium, barium, strontium, sodium, calcium, magnesium, manganese, iron, cadmium, lithium, cobalt, nickel, zinc, copper	[177]
Tartrate	ON	6	214	Counter-ion (HIBA)	N/A	lithium, sodium, potassium, magnesium, calcium, strontium, barium, copper, zinc, cadmium, manganese, iron^{II}, cobalt^{II}, nickel	[178]
Citrate	ON	10	210	Counter-ion (citrate)	N/A	calcium, barium	[179]

Table 1.7 Miscellaneous Probes for Indirect Detection of Cations

Probe	Complexing agent	Complex Formation	BGE Range (mM)	Detection Wavelength (nm)	Buffering method	LODs	Analytes	Ref
$CuSO_4$	18C6	ON	4	215	Counter-ion (formate)	0.06 –1 ppm	lithium, potassium	[180]
	Sulfate	ON	4	215	Counter-ion (formate)	N/A	sodium, potassium, magnesium, calcium	[181]
	Sulfate or SDS	ON	5	214	None (probe only)	N/A	lithium, sodium, potassium, rubidium, caesium, magnesium, calcium, strontium, barium, zinc, manganese, $cobalt^{II}$, nickel	[182]
	Sulfate + 18C6	ON	4	215	Counter-ion (formate)	0.6-13 ppm	lithium, sodium, potassium, magnesium, calcium, strontium, barium, ammonium	[183]
	18C6	ON	4	215	Counter-ion (formate)	1-8 ppb	lithium, sodium, potassium, rubidium, caesium, magnesium, calcium, strontium, barium, zinc, manganese, $cobalt^{II}$, nickel	[66]

Table 1.7 Miscellaneous Probes for Indirect Detection of Cations (cont)

Probe	Complexing agent	Complex Formation	BGE Range (mM)	Detection Wavelength (nm)	Buffering method	LODs	Analytes	Ref
UV Cat 1	HIBA	ON	10	214	Counter-ion (HIBA, acetate)	~ ppb range	lithium, sodium, potassium, rubidium, magnesium, calcium, 13 lanthanides	[103]
	Citrate, HIBA	ON	10	214	Counter-ion (MES, HIBA)	18-397 ppb	alkali, alkaline earth, manganese, cadmium, $iron^{II}$, cobalt, lead, nickel, zinc, copper, 13 lanthanides	[104]
	HIBA	ON	10	214	Counter-ion (HIBA)	N/A	potassium, barium, strontium, calcium, sodium, magnesium, manganese, cadmium, chromium, cobalt, lithium, lead, nickel, zinc, copper	[177]
	HIBA	ON	5	214	Counter-ion (HIBA)	N/A	sodium, potassium	[184]
	HIBA	ON	5	214	Counter-ion (HIBA)	5-20ppm	potassium	[185]
	HIBA	ON	5	185, 214	Counter-ion (HIBA, tropolone)	30-267 ppt (EMI)	lithium, sodium, potassium, magnesium, calcium, strontium, barium	[32]

Table 1.7 Miscellaneous Probes for Indirect Detection of Cations (cont)

Probe	Complexing agent	Complex Formation	BGE Range (mM)	Detection Wavelength (nm)	Buffering method	LODs	Analytes	Ref
UV Cat 1	HIBA	ON	5	185	Counter-ion (tropolone, HIBA)	0.5-3.3 ppb	sodium, potassium, magnesium, calcium, manganese	[186]
	HIBA	ON	5	185	Counter-ion (HIBA)	N/A	sodium, nickel, ammonium	[187]
	HIBA	ON	5	185, 214	Counter-ion (HIBA)	70-200 ppb	magnesium, zinc, copper, aluminium, sodium	[188]
	HIBA	ON	5	214	Counter-ion (HIBA)	N/A	sodium, potassium	[189]
	Phthalate, tartrate, lactate, HIBA	ON	2	214	Counter-ion (tartrate)	50-500 ppb	lithium, sodium, potassium, magnesium, calcium, strontium, barium, manganese, cadmium, cobalt^{II}, nickel, zinc, lead, copper, 13 lanthanides	[106]
	HIBA	ON	5-10	214	Counter-ion (HIBA, acetate)	N/A	lithium, sodium, potassium, magnesium, calcium, strontium, barium, manganese, iron^{II}, cobalt^{II}, nickel, copper, zinc, cadmium, lead, lanthanides	[190]

Table 1.7 Miscellaneous Probes for Indirect Detection of Cations (cont)

Probe	Complexing agent	Complex Formation	BGE Range (mM)	Detection Wavelength (nm)	Buffering method	LODs	Analytes	Ref
UV Cat 1	HIBA	ON	5	214	Counter-ion (HIBA)	N/A	sodium, calcium, potassium, magnesium	[191]
UV Cat 2	18C6 (or 15C5 or 12C4)	ON	1.0	185	Counter-ion (tropolone)	N/A	lithium, sodium, potassium, magnesium, calcium, barium, ammonium	[192]
	Tropolone	ON	1.2	185	Counter-ion (tropolone)	N/A	sodium, potassium, magnesium, calcium	[193]
Benzylamine	HIBA	ON	4	214	Counter-ion (HIBA, acetate)	N/A	14 lanthanides	[194]
	None	None	10	204, 214	None (probe only)	~ 50 ppb	lithium, sodium, potassium, magnesium, calcium, barium, ammonium	[195]

Table 1.7 Miscellaneous Probes for Indirect Detection of Cations (cont)

Probe	Complexing agent	Complex Formation	BGE Range (mM)	Detection Wavelength (nm)	Buffering method	LODs	Analytes	Ref
4-methyl benzylamine	Lactate + 18C6	ON	7.5	214, 254	Counter-ion (lactate)	~ 0.1 ppm	lithium, sodium, potassium, magnesium, calcium, strontium, barium, copper, zinc, cadmium, lead, manganese, iron^{II}, nickel, aluminium^{3+}, VO^{2+}, ammonium, UO_2^{2+}, chromium^{3+}, silver	[196]
N,N-dimethyl-benzylamine	HIBA	ON	6	214	Counter-ion (HIBA)	0.1-1 ppm	lithium, sodium, potassium, magnesium, calcium, barium, manganese, iron^{II}, cobalt^{II}, nickel, zinc, copper, 14 lanthanides	[105]
Creatinine	HIBA	ON	10	214	Counter-ion (acetate, HIBA)	40 ppb	lanthanum, cerium, gadolilium, terbium	[197]
	HIBA	ON	30	220	Counter-ion (acetate)	0.1 μM, 10 fmol	14 lanthanides, lithium, sodium, potassium, magnesium	[101]

Table 1.7 Miscellaneous Probes for Indirect Detection of Cations (cont)

Probe	Complexing agent	Complex Formation	BGE Range (mM)	Detection Wavelength (nm)	Buffering method	LODs	Analytes	Ref
Creatinine	Lactate or HIBA	ON	30	214	Counter-ion (lactate, HIBA)	N/A	13 lanthanides, sodium, potassium, magnesium	[198]
	HIBA	ON	10	214	Counter-ion (HIBA)	N/A	lanthanum, cerium, gadolilium, terbium	[199]
	PEG200 + tartrate	ON	30	254	Counter-ion (tartrate)	N/A	lithium, sodium, potassium, rubidium, caesium, magnesium, calcium, strontium, barium, ammonium	[200]
	HIBA, or HQSA, or EDTA	ON	5	200	Counter-ion (HIBA)	N/A	$iron^{II}$, $iron^{III}$, nickel, copper, zinc, lead	[95]
	PEGs (MW 200-20·10^6)	ON	10	214	Counter-ion (acetate)	N/A	lithium, sodium, potassium, magnesium, calcium, barium, zinc, lead, lanthanum, samarium, europium, dysprosium	[201]
	HIBA	ON	30	220	Counter-ion (HIBA)	2-10 ppb	sodium, potassium, magnesium, calcium	[202]

Table 1.7 Miscellaneous Probes for Indirect Detection of Cations (cont)

Probe	Complexing agent	Complex Formation	BGE Range (mM)	Detection Wavelength (nm)	Buffering method	LODs	Analytes	Ref
Pyridine	Tartrate + 18C6	ON	5	255	Counter-ion (tartrate)	~ 25 μM	calcium, lithium, sodium, potassium, magnesium, barium, ammonium, creatinine	[203]
	EDTA	ON	10	254	None (probe only)	N/A	magnesium, lithium, sodium, potassium, calcium, strontium, barium	[88]
2-aminopyridine	None	None	15	214	Counter-ion (acetate)	0.04-0.6 ppm	lithium, sodium, potassium, magnesium, calcium, barium, manganese, chromium, zinc, cadmium	[204]
	HIBA	ON	15	214	Counter-ion (acetate)	20-350 ppb	lithium, sodium, potassium, magnesium, calcium, strontium, barium, chromium^{III}, manganese, nickel, zinc, cadmium	[205]
4-aminopyridine	18C6, HIBA	ON	5-15	254	Counter-ion (HIBA, acetate)	~ low ppm	lithium, sodium, potassium, ammonium, manganese, iron^{II}, cobalt^{II}, cadmium, nickel, zinc	[206]

Table 1.7 Miscellaneous Probes for Indirect Detection of Cations (cont)

Probe	Complexing agent	Complex Formation	BGE Range (mM)	Detection Wavelength (nm)	Buffering method	LODs	Analytes	Ref
4-aminopyridine	HIBA	ON	10	214	Counter-ion (HIBA)	92-454 ppb	potassium, sodium, barium, strontium, calcium magnesium, manganese, lithium, iron, cobalt, cadmium nickel, zinc, lead, chromium, copper	[177]
	Cry22	ON	5	254	Counter-ion (acetate)	N/A	sodium, potassium, ammonium	[207]
Malachite green	None	None	0.5	632.8	None (probe only)	1 μM	potassium	[28]
4-methylamino-phenol	DFO	PRE	4	UV	None (probe only)	N/A	aluminium (lithium, sodium, potassium, caesium, magnesium, calcium	[208]
4-methyl-aminophenol-sulfate	18C6	ON	4	220	None (probe only)	N/A	potassium, magnesium (mono- & divalent	[209]
$Cu(en)_2$	Acetate	ON	7.5	230	Counter-ion (triethanolamine)	0.09-0.54 mg/L	potassium, ammonium, barium, strontium, calcium, sodium, magnesium, lithium	[210]

Table 1.7 Miscellaneous Probes for Indirect Detection of Cations (cont)

Probe	Complexing agent	Complex Formation	BGE Range (mM)	Detection Wavelength (nm)	Buffering method	LODs	Analytes	Ref
Benzimidazole	Tartrate + 18C6	ON	5	254	Counter-ion (tartrate)	N/A	lithium, sodium, potassium, rubidium, caesium, magnesium, calcium, strontium, barium, ammonium	[211]
2-ethylimadazole	EDTA	ON	10	214	Counter-ion (HIBA)	~ 0.5 ppm (EMI)	lanthanum, praseodymium, europium, terbium, dysprosium	[89]
Dimethyldiphenyl-phosphonium hydroxide	18C6	ON	5	215	Counter-ion (MES)	1-8 ppb	lithium, sodium, potassium, rubidium, caesium, magnesium, calcium, strontium, barium, zinc, manganese, cobalt^{II}, nickel	[66]
	18C6 + HIBA or citrate	ON	5-7	210	Counter-ion (HIBA, citrate)	N/A	Group I, II, transitional metal cations, (ammonium	[212]
	HIBA	ON	5	210	Counter-ion (HIBA)	~ 2 ppb	lithium, sodium, potassium, magnesium, calcium, strontium, barium, ammonium	[213]

Table 1.7 Miscellaneous Probes for Indirect Detection of Cations (cont)

Probe	Complexing agent	Complex Formation	BGE Range (mM)	Detection Wavelength (nm)	Buffering method	LODs	Analytes	Ref
Dimethyldiphenyl-phosphonium iodide	HIBA +18C6	ON	12	220	Counter-ion (HIBA, trimesic acid)	2-5 μM	potassium, sodium, magnesium	[109]
Ephedrine	HIBA	ON	5.2	204	Counter-ion (HIBA)	N/A	aluminium, lithium, sodium, potassium, magnesium, calcium, strontium, titanium, chromium, manganese, nickel, cobalt, copper, zinc, cadmium, cerium	[214]
Tetrazolium violet	None	None	5-10	300	Counter-ion (borate)	0.05-0.50 mg/L	chloroethyltrimethyl-ammonium, tetrabutylammonium, tetrahexylammonium, didodecyldimethyl-ammonium	[76]
Pyronine G	None	None	0.15	525	Co-ion (HIBA)	N/A	potassium, calcium, sodium, lithium	[75]
Methyl green	None	None	0.1	630	Co-ion (Tris)	0.8 fmol	lithium, sodium, potassium, caesium, magnesium, calcium	[25]

Table 1.7 Miscellaneous Probes for Indirect Detection of Cations (cont)

Probe	Complexing agent	Complex Formation	BGE Range (mM)	Detection Wavelength (nm)	Buffering method	LODs	Analytes	Ref
1,1'-di-n-heptyl-4,4'-bipyridinium hydroxide (DHBPOH)	Glycine	ON	5	280	Counter-ion (glycine)	9-60 ppb	lithium, sodium, potassium, rubidium, caesium, magnesium, calcium, strontium, barium, manganese, cadmium, ammonium	[215]
4-N-methylamino-phenol	18C6	ON	4	220	None (probe only)	fmol range	sodium, potassium, magnesium, calcium, zinc, ammonium	[216]
	18C6	ON	4	220	None (probe only)	40-80 fmol	sodium, potassium, magnesium, calcium, zinc, manganese, lead, ammonium	[217]

Table Abbreviations

Tris	tris(hydroxymethyl)aminomethane
EMI	electromigration injection
N/A	not available
Bis/Tris	2,2-bis(hydroxymethyl)-2,2',2''-nitrilotriethanol
CHES	(cyclohexylamino)ethanesulfonic acid
HIBA	2-hydroxyisobutyric acid
18C6	18-Crown-6
15C5	15-Crown-5
12C4	12-Crown-4
CDTA	*trans*-1,2-diaminocyclohexane-*N,N,N',N'*-tetraacetic acid
SDS	sodium dodecyl sulfate
MES	morpholineethanesulfonic acid
PEG	poly(ethylene glycol)
HQSA	8-hydroxyquinoline-5-sulfonic acid
EDTA	ethylenediaminetetraacetic acid
Cry22	polyether cryptand-22
DFO	desferrioximine

Table 1.8 Absorptivity data for probes for detection of anions

Probe	**Absorptivity ($L.mol^{-1}$ cm^{-1})**
Chromate	(1) 2,640, 254 nm, pH 8.1 [54] (2) 3,180, 254 nm, pH 8.0 [12]
p-aminobenzoate	(1) 13,600, 264 nm, pH 9.6 [131]
Benzoate	(1) 44,480, 194 nm, pH 6.5 [153] (2) 11,900, 228 nm, pH 6.5 [30] (3) 809, 254 nm, pH 8.0 [12]
o-benzylbenzoic acid	(1) 19,000, 228 nm, pH 6.5 [30]
3,4-dimethoxycinnamic acid	(1) 27,000, 310 nm, N/A [132]
p-hydroxybenzoate	(1) 10,299, 254 nm, pH 8.0 [12]
Phenylacetic acid	(1) 7,600, 209 nm, pH 12.1 [135]
Phthalate	(1) 9,950, 214 nm, pH 8.1 [54] (2) 37,160, 196 nm, pH 6.5 [153] (3) 1,357, 254 nm, pH 8.0 [12]
Pyromellitate	(1) 26,200, 214 nm, pH 8.0 [54] (2) 23,900, 214 nm, pH 6.5 [153] (3) 7,062, 254 nm, pH 8.0 [12] (4) 24,000, 210 nm, N/A [218]
2-sulfobenzoic acid	(1) 40,000, 228 nm, pH 6.5 [30]
5-sulfosalicylic acid	(1) 44,000, 210 nm, N/A [218] (2) 22,000, 217 nm, N/A [218] (3) 9,200, 226 nm, N/A [218]
Trimellitate	(1) 7,147, 254 nm, pH 8.0 [12]
2,6-naphthalenedicarboxylate	(1) 7,667, 254 nm, N/A [147] (2) 10,020, 280 nm, N/A [147]
1-naphthylacetic acid	(1) 81,100, 222 nm, pH 12.1 [135]
1,3-benzenedisulfonate	(1) 9,950, 214 nm, pH 8.05 [54]
1,5-naphthalenedisulfonate	(1) 31,000, 214 nm, pH 8.1 [54] (2) 16,420, 288 nm, N/A [149] (3) 89,000, 224 nm, N/A [218]
Naphthalenesulfonate	(1) 6,200, 274 nm, N/A [149]
2-naphthalenesulfonate	(1) 11,520, 206 nm, pH 6 [50]
1,3,6-naphthalenetrisulfonate	(1) 31,600, 214 nm, pH 8 [54] (2) 7,750, 284 nm, N/A [149]

Probe	**Absorptivity ($L.mol^{-1} cm^{-1}$)**
p-toluenesulfonate	(1) 7,520, 221 nm, pH 6.0 [50] (2) 344, 254 nm, pH 8.0 [12]
Adenosine monophosphate	(1) 9,335, N/A, N/A [49]
Bromocresol green	(1) 45,000, 618 nm, pH 9.2 [33]
Chlorphenol red	(1) 28,000, 578 nm, pH 6.5 [25] (2) 33,000, 578 nm, pH 7.3 [25]
p-cresol	(1) 8,320, 236 nm, pH 12.1 [135]
1,3-dihydroxynaphthalene	(1) 14,680, 256 nm, pH 12.1 [135]
Indigo carmine	(1) 12,000, 620 nm, pH 4.2-7.3 [25]
Potassium indigotetrasulfonate	(1) 32,100, 314 nm, pH 6.8 [33]
2,6-pyridinedicarboxylate	(1) 43,680, 192 nm, pH 6.5 [153]
Riboflavin	(1) 30,000, 267 nm, N/A [132]
Sorbate	(1) 24,120, 254 nm, pH 12.1 [135] (2) 28,800, 254 nm, pH 12.1 [158]
Tryptophan	(1) 5,630, 280 nm, pH 12.1 [158]
Uridine monophosphate	(1) 7,240, 261 nm, pH 7.8 [49]

Table 1.9 Absorptivity data for probes for detection of cations

Probe	**Absorptivity ($L.mol^{-1} cm^{-1}$)**
Imidazole	(1) 3,300, 211 nm, pH 4.5 [170] (2) 4,770, 211 nm, N/A [219]
Creatinine	(1) 9,200, 214 nm, pH 4.6 [105]
Copper ethylenediamine	(1) 6,340, 230 nm, pH 8.0 [210]
1,1'-di-n-heptyl-4,4'-bipyridinium hydroxide (DHBPOH)	(1) 24,000, 252 nm, N/A [220]
Methyl green	(1) 15,000, 635 nm, pH 4.2 [25]
Ephedrine	(1) 5,660, 204 nm, N/A [214]
Pyridine	(1) 2,000, 254 nm, N/A [50]
N,N-dimethylbenzylamine	(1) 6,000, 214 nm, pH 4.6 [105]
Benzylamine	(1) 4,300, 214 nm, pH 4.6 [105] (2) 5,440, 204 nm, N/A [50] (3) 7,200, 210 nm, N/A [218]
4-aminopyridine	(1) 18,500, 261 nm, N/A [221] (2) 16,000, 210 nm, N/A [218]
Tetrazolium violet	(1) 5,800, 300 nm, N/A [76] (2) 18,000, 254 nm, N/A [76] (3) 9,700, 280 nm, N/A [76]

1.5 References

1 V. Pacakova and K. Stulik, *J. Chromatogr. A,* **789** (1997) 169.

2 J.S. Fritz, *J. Chromatogr. A,* **884** (2000) 261.

3 M. Macka and P.R. Haddad, *Electrophoresis*, **18** (1997) 2482.

4 K. Swinney and D.J. Bornhop, *Electrophoresis*, **21** (2000) 1239.

5 P. Doble and P.R. Haddad, *J. Chromatogr. A,* **834** (1999) 189.

6 M. T. Ackermans, F.M. Everaerts and J.L. Beckers, *J. Chromatogr.*, **549** (1991) 345.

7 R. Kuhn and S. Hoffstetter-Kuhn, *Capillary Electrophoresis: Principles and Practice*, Springer Laboratory (1993).

8 T. Rabiloud, *Electrophoresis*, **15** (1994) 278.

9 G.J.M. Bruin, A.C. van Asten, X. Xu and H. Poppe, *J. Chromatogr.*, **608** (1992) 97.

10 H. Poppe, *Anal. Chem.*, **64** (1992) 1908.

11 M.W.F. Nielen, *J. Chromatogr.*, **588** (1991) 321.

12 S.M. Cousins, P.R. Haddad and W. Buchberger, *J. Chromatogr. A,* **671** (1994) 397.

13 W. Buchberger, S.M. Cousins and P.R. Haddad, *TrAC*, **13** (1994) 313.

14 P. Doble, P. Andersson and P.R. Haddad, *J. Chromatogr. A,* **770** (1997) 291.

15 J. Collet and P. Gariel, *J. Chromatogr. A,* **716** (1995) 115.

16 J.L. Beckers, *J. Chromatogr. A,* **679** (1994) 153.

17 X. Xu, W.T. Kok and H. Poppe, *J. Chromatogr. A,* **742** (1996) 211.

18 J.L. Beckers, *J. Chromatogr. A,* **693** (1995) 347.

19 J.L. Beckers, *J. Chromatogr. A,* **741** (1996) 265.

20 J.L. Beckers, *J. Chromatogr. A,* **764** (1997) 111.

21 F.E.P. Mikkers, F.M. Everaerts and T.P.E.M. Verheggen, *J. Chromatogr.*, **169** (1979) 1.

22 F.E.P. Mikkers, F.M. Everaerts and T.P.E.M. Verheggen, *J. Chromatogr.*, **169** (1979) 11.

23 F. Foret, L. Krivankova and P. Bocek, *Capillary Zone Electrophoresis*, VCH Publishers, Weinheim, (1993)

24 P. Jandik and G. Bonn, *Capillary Electrophoresis of Small Molecules and Ions*, VCH Publishers, Weinheim, (1993).

25 Z. Mala, R. Vespalec, P. Bocek, *Electrophoresis,* **15** (1994) 1526.

26 A. Bazzanella, H. Lochmann, A. Mainka and K. Bachmann, *Chromatographia*, **45** (1997) 59.

27 T. Takeuchi and E.S. Yeung, *J. Chromatogr.*, **370** (1986) 83.

28 Y.J. Xue and E.S. Yeung, *Anal. Chem.*, **65** (1993) 2923.

29 M. Macka, B. Paull, P. Andersson and P.R. Haddad, *J. Chromatogr. A,* **767** (1997) 303.

30 Y.F. Ma and R.L. Zhang, *J. Chromatogr.*, **625** (1992) 341.

31 F. Steiner, W. Beck and H. Engelhardt, *J. Chromatogr. A*, **738** (1996) 11.

32 A. Weston, P.R. Brown, P. Jandik, A.L. Heckenberg and W.R. Jones, *J. Chromatogr.*, **608** (1992) 395.

33 P. Doble, M. Macka and P.R. Haddad, *J. Chromatogr. A,* **804** (1998) 327.

34 F. Foret, S. Fanali, L. Ossicini and P. Bocek, *J. Chromatogr.*, **470** (1989) 299.

35 W. Beck and H. Engelhardt, *Chromatographia*, **33** (1992) 313.

36 E. Kenndler and W. Friedl, *J. Chromatogr.*, **608** (1992) 161.

37 T. Zhu, Y.L. Sun, C.X. Zhang, D.K. Ling and Z.P. Sun, *J. High Resolut. Chromatogr.*, **17** (1994) 563.

38 M.A. Strege and A.L. Lagu, *J. Liq. Chromatogr.*, **16** (1993) 51.

39 M. Macka, P. Andersson and P.R. Haddad, *Anal. Chem.*, **70** (1998) 743.

40 H. Corstjens, H.A.H. Billiet, J. Frank and K.C.A.M. Luyben, *Electrophoresis*, **17** (1996) 137.

41 M.S. Bello, *J. Chromatogr. A,* **744** (1996) 81.

42 A. Henshall, M.P. Harrold and J.M.Y. Tso, *J. Chromatogr.*, **608** (1992) 413.

43 C.O. Thompson, V.C. Trenerry and B. Kemmery, *J. Chromatogr. A*, **704** (1995) 203.

44 R. Neubert, K. Raith and J. Schiewe, *Pharmazie*, **52** (1997) 212.

45 S.A. Oerhle and P.C. Bossle, *J. Chromatogr. A*, **692** (1995) 247.

46 B.A.P. Buscher, U.R. Tjaden, H. Irth, E.M. Andersson and J. van der Greef, *J. Chromatogr. A*, **718** (1995) 413.

47 E. Santoyo, R. Garcia, J. Martinez-Frias, F. Lopez-Vera and S. Verma, *J. Chromatogr. A*, **956** (2002) 279.

48 L.K. Goebel, H.M. McNair, H.T. Rasmussen and B.P. McPherson, *J. Microcolumn Sep.*, **5** (1993) 47.

49 S.A. Shamsi and N.D. Danielson, *Anal. Chem.*, **67** (1995) 1845.

50 S.A. Shamsi and N.D. Danielson, *Anal. Chem.*, **67** (1995) 4210.

51 G.A. Pianetti, M. Taverna, A. Baillet, G. Mahuzier and D. Baylocq Ferrier, *J. Chromatogr.*, **630** (1993) 371.

52 R.W. Hepler and C.C. Yu Ip, *J. Chromatogr. A*, **680** (1994) 201.

53 T. Wang and R.A. Hartwick, *J. Chromatogr.*, **589** (1992) 307.

54 S. Motellier, K. Gurdale and H. Pitsch, *J. Chromatogr. A*, **770** (1997) 311.

55 K.L. Larsen, F. Mathiesen and W. Zimmerman, *Carbohydrate Research*, **298** (1997) 59.

56 R. Roldan Assad and P. Gareil, *J. Chromatogr. A*, **708** (1995) 339.

57 A. Nardi, S. Fanali and F. Foret, *Electrophoresis*, **11** (1990) 774.

58 E.V. Dose and G.A. Guichon, *Anal. Chem.*, **63** (1991) 1063.

59 C. Vogt, J. Vogt and H. Wittrisch, *J. Chromatogr. A*, **727** (1996) 301.

60 C. Vogt and G. Werner, *J. Chromatogr. A*, **686** (1994) 325.

61 T. Wang and R.A. Hartwick, *J. Chromatogr.*, **607** (1992) 119.

62 E. Dabek-Zlotorzynska and J.F. Dlouhy, *J. Chromatogr. A*, **671** (1994) 389.

63 M.M. Rhemrev Boom, *J. Chromatogr. A,* **680** (1994) 675.

64 T. Ehmann, K. Bachmann, L. Fabry, H. Rufer, S. Pahlke and L. Kotz, *Chromatographia*, **45** (1997) 301.

65 M.P. Harrold, M.J. Wojtusik, J. Riviello and P. Henson, *J. Chromatogr.*, **640** (1993) 463.

66 M.J. Wojtusik and M.P. Harrold, *J. Chromatogr. A*, **671** (1994) 411.

67 H. Rilbe, *Electrophoresis*, **13** (1992) 811.

68 H. Svensson, *Acta Chem. Scand.*, **16** (1962) 456.

69 M. Macka, P. Andersson and P.R. Haddad, *Electrophoresis*, **17** (1996) 1898.

70 Y. Walbroehl and J.W. Jorgenson, *J. Chromatogr.*, **315** (1984) 135.

71 A.E. Bruno, E. Gassmann, N. Pericle and K. Anton, *Anal. Chem.*, **61** (1989) 876.

72 G.J.M. Bruin, G. Stegeman, A.C. van Asten, X. Xu, J.C. Kraak and H. Poppe, *J. Chromatogr.*, **559** (1991) 163.

73 R. Cassidy and M. Janoski, LC-GC, ***10*** (1992) 692.

74 H. Siren, A. Maattanen and M.L. Riekkola, *J. Chromatogr. A,* **767** (1997) 293.

75 P.A.G. Butler, B. Mills and P.C. Hauser, *Analyst*, **122** (1997) 949.

76 S.A. Shamsi and N.D. Danielson, *J. Chromatogr. A*, **739** (1996) 405.

77 M. Aguilar, X. Huang and R.N. Zare, *J. Chromatogr.*, **480** (1989) 427.

78 M. Aguilar, A. Farran and M. Martinez, *J. Chromatogr.*, **635** (1993) 127.

79 W. Buchberger, O.P. Semenova and A.R. Timerbaev, *J. High Resolut. Chromatogr.*, **16** (1993) 153.

80 W. Buchberger and P.R. Haddad, *J. Chromatogr. A*, **687** (1994) 343.

81 A.R. Timerbaev, *J. Capillary Electrophor.*, **2** (1995) 165.

82 S. Motomizu, M. Oshima, S. Matsuda, Y. Obata and H. Tanaka, *Anal. Sci.*, **8** (1992) 619.

83 H. Kajiwara, A. Sato and S. Kaneko, *Biosci. Biotechnol. Biochem.*, **57** (1993) 1010.

84 P.L. Desbene and C. Morin, *Spectra 2000 [Deux Mille],* **181** *(1994)* 35.

85 A.R. Timerbaev, O.P. Semenova and G.K. Bonn, *Analyst*, **119** (1994) 2795.

86 P.L. Desbene, C.J. Morin, M.A.M. Desbene and R.S. Groult, *J. Chromatogr. A*, **689** (1995) 135.

87 A.R. Timerbaev and O.P. Semenova, *J. Chromatogr. A*, **690** (1995) 141.

88 T.L. Wang and S.F.Y. Li, *J. Chromatogr. A*, **707** (1995) 343.

89 B.A. Colburn, S.D. Starnes, M.J. Sepaniak and R. Hinton, R., *Separation Science & Technology.*, **30** (1995) 1511.

90 I. Haumann and K. Bächmann, *J. Chromatogr. A*, **717** (1995) 385.

91 A.R. Timerbaev, O.P. Semenova, W. Buchberger and G.K. Bonn, *Fresenius' J. Anal. Chem.*, **354** (1996) 414.

92 O.P. Semenova, A.R. Timerbaev, R. Gaegstadter and G.K. Bonn, *J. High Resolut. Chromatogr.*, **19** (1996) 177.

93 M. Norden and E. Dabek-Zlotorzynska, *J. Chromatogr. A*, **739** (1996) 421.

94 S. Schaffer, P. Gareil, C. Dezael and D. Richard, *J. Chromatogr. A*, **740** (1996) 151.

95 S. Conradi, C. Vogt, H. Wittrisch, G. Knobloch and G. Werner, *J. Chromatogr. A*, **745** (1996) 103.

96 D.H. Patterson, B.J. Harmon and F.E. Regnier, *J. Chromatogr. A*, **662** (1994) 389.

97 A.R. Timerbaev, O.P. Semenova, P. Jandik and G.K. Bonn, *J. Chromatogr. A*, **671** (1994) 419.

98 S. Motomizu, M. Kuwabara and M. Oshima, *Bunseki Kagaku.*, **43** (1994) 621.

99 Y. Liu, V. Lopez-Avila, J.J. Zhu, D.R. Wiederin and W.F. Beckert, *Anal. Chem.*, **67** (1995) 2020.

100 J. Xu and Y.F. Ma, *J. Microcolumn Sep.*, **8** (1996) 137.

101 F. Foret, S. Fanali, A. Nardi and P. Bocek, *Electrophoresis*, **11** (1990) 780.

102 G. Bondoux, P. Jandik, W.R. Jones, *Spectra-2000-[Deux-Mille]*, **158** (1991) 47.

103 P. Jandik, W.R. Jones, A. Weston and P.R. Brown, *LC-GC*, **9** (1991) 634-636, 638, 640, 642, 644.

104 A. Weston, P.R. Brown, P. Jandik, W.R. Jones and A.L. Heckenberg, *J. Chromatogr.*, **593** (1992) 289.

105 M. Chen and R.M. Cassidy, *J. Chromatogr.*, **640** (1993) 425.

106 Y.C. Shi and J.S. Fritz, *J. Chromatogr.*, **640** (1993) 473.

107 T.I. Lin, Y.H. Lee and Y.C. Chen, *J. Chromatogr. A*, **654** (1993) 167.

108 J.J. Corr and J.F. Anacleto, *Anal. Chem.*, **68** (1996) 2155.

109 I. Haumann, J. Boden, A. Mainka and U. Jegle, *J. Chromatogr. A*, **895** (2000) 269.

110 A. Padarauskas, V. Olsauskaite and G. Schedt, *J. Chromatogr. A*, **800** (1998) 369.

111 A. Padarauskas, V. Olsauskaite and V. Paliulionyte, *J. Chromatogr. A*, **829** (1998) 359

112 P. Kuban and B. Karlberg, *Anal. Chem.*, **70** (1998) 365.

113 X. Xiong and S.F.Y. Li, *Electrophoresis*, **19** (1998) 2243.

114 X. Xiong and S.F.Y. Li, *J. Chromatogr. A*, **822** (1998) 125.

115 C. Raguenes, X. Xiong, H.K. Lee and S.F.Y. Li, *J. Liq. Chromatogr. Relat. Technol.*, **22** (1999) 2353.

116 G. Bondoux, P. Jandik and W.R. Jones, *J. Chromatogr.*, **602** (1992) 79.

117 P.R. Haddad, A.H. Harakuwe and W.W. Buchberger, *J. Chromatogr. A*, **706** (1995) 571.

118 S.A. Oerhle, *J. Chromatogr. A*, **745** (1996) 81.

119 T.L. Wang, and S.F.Y. Li, *J. Chromatogr. A*, **723** (1996) 197.

120 L. Lin, J. Wang and J. Caruso, *J. Chromatogr. Sci.*, **33** (1995) 177.

121 M. Jimidar, C. Harmann, N. Cousement and D.L. Massart, *J. Chromatogr. A*, **706** (1995) 479.

122 K. Bachmann, I. Haag, T. Prokop, A. Roeder and P. Wagner, *J. Chromatogr.*, **643** (1993) 181.

123 C. Stathakis and R.M. Cassidy, *Anal. Chem.*, **66** (1994) 2110.

124 P. Doble, M. Macka, P. Andersson and P.R. Haddad, *Analytical Communications*, **34** (1997) 351.

125 M.T. Galceran, L. Puignou and M. Diez, *J. Chromatogr. A*, **732** (1996) 167.

126 M.E. Swartz, *J. Chromatogr.*, **640** (1993) 441.

127 K. Li and S.F.Y. Li, *J. Liq. Chromatogr.*, **17** (1994) 3889.

128 S.A. Oerhle, *J. Chromatogr. A*, **671** (1994) 383.

129 G.Y. Jung, T.H. Kim and H.B. Lim, *Anal. Sci.*, **12** (1996) 367.

130 P. Wang, S.F.Y. Li and H.K. Lee, *J. Chromatogr. A*, **765** (1997) 353.

131 A. Roder and K. Bachmann, *J. Chromatogr. A*, **689** (1995) 305.

132 X. Xu, W.T. Kok and H. Poppe, *J. Chromatogr. A*, **716** (1995) 231.

133 L. Zhou and A. Dovletoglou, *J. Chromatogr. A*, **763** (1997) 279.

134 W.R. Jones, *J. Chromatogr.*, **640** (1993) 387.

135 Y.H. Lee and T.I. Lin, *J. Chromatogr. B*, **681** (1999) 87.

136 F.Y. Guan, H.F. Wu and Y. Luo, *J. Chromatogr. A*, **719** (1996) 421.

137 H. Chen, Y. Xu, F. Van Lente and M.P.C. Ip, *J. Chromatogr. B*, **679** (1996) 49.

138 D. Volgger, A.J. Zemann, G.K. Bonn and M.J. Antal, *J. Chromatogr. A*, **758** (1997) 263.

139 M. Arellano, J. Andrianary, F. Dedieu, F. Couderc and P. Puig, *J. Chromatogr. A*, **765** (1997) 321.

140 E. Dabek-Zlotorzynska, J.F. Dlouhy, N. Houle, M. Piechowski and S. Ritchie, *J. Chromatogr. A*, **706** (1995) 469.

141 T. Hiissa, H. Siren, T. Kotiaho, M. Snellman and A. Hautojarvi, *J. Chromatogr. A*, **853** (1999) 403.

142 S. Chen and D.J. Pietrzyk, *Anal. Chem.*, **65** (1993) 2770.

143 J.B.L. Damm and G.T. Overklift, *J. Chromatogr. A*, **678** (1994) 151.

144 C.H. Wu, Y.S. Lo, Y.H. Lee and T.I. Lin, *J. Chromatogr. A*, **716** (1995) 291.

145 M. Van Holderbeke, H. Vanhoe, L. Moens and R. Dams, *Biomed. Chromatogr.*, **9** (1995) 281.

146 G.W. Tindall, D.R. Wilder and R.L. Perry, *J. Chromatogr.*, **641** (1993) 163.

147 E. Dabek-Zlotorzynska and J.F. Dlouhy, *J. Chromatogr. A*, **685** (1994) 145.

148 E. Dabek-Zlotorzynska, M. Piechowski, M. McGrath and E.P.C. Lai, *J. Chromatogr. A*, **910** (2001) 331.

149 S.A. Shamsi and N.D. Danielson, *Anal. Chem.*, **66** (1994) 3757.

150 B.A.P. Buscher, H. Irth, E. Andersson, U.R. Tjaden and J. van der Greef, *J. Chromatogr. A*, **678** (1994) 149.

151 W. Tong and E.S. Yeung, *J. Chromatogr. A*, **718** (1995) 177.

152 J.E. Melanson, B.L.Y. Wong, C.A. Boulet and C.A. Lucy, *J. Chromatogr. A*, **920** (2001) 359.

153 T. Soga and G.A. Ross, *J. Chromatogr. A*, **767** (1997) 223.

154 T. Soga and M. Imaizumi, *Electrophoresis*, **22** (2001) 3418.

155 A. Klockow, A. Paulus, V. Fihueredo, R. Amado and H.M. Widmer, *J. Chromatogr. A*, **680** (1994) 187.

156 A.E. Vorndran, P.J. Oefner, H. Scherz and G.K. Bonn, *Chromatographia*, **34** (1992) 308.

157 P.J. Oefner, A.E. Vorndran, E. Grill, C. Huber and G.K. Bonn, *Chromatographia*, **34** (1992) 308.

158 B. Lu and D. Westerlund, *Electrophoresis*, **17** (1996) 325.

159 H. Shi, R. Zhang, G. Chandrasekher and Y. Ma, *J. Chromatogr. A*, **680** (1994) 6.

160 N. Wu, W.J. Horvath, P. Sun and C.W. Huie, *J. Chromatogr.*, **635** (1993) 307.

161 Q. Yang, M. Jimidar, T.P. Hamoir, J. Smeyersverbeke and D.L. Massart, *J. Chromatogr. A*, **673** (1994) 275.

162 R. Zhang, H. Shi and Y. Ma, *J. Microcolumn Sep.*, **6** (1994) 217.

163 J.C. Transfiguracion, C. Dolman, D.H. Eidelman and D.K. Lloyd, *Anal. Chem.*, **67** (1995) 2937.

164 Q. Yang, J. Smeyersverbeke, W. Wu, M.S. Khots and D.L. Massart, *J. Chromatogr. A*, **688** (1994) 339.

165 K.D. Altria, T. Wood, R. Kitscha and A. Roberts-McIntosh, *J. Pharm. Biomed. Anal.*, **13** (1995) 33.

166 K.D. Altria, N.G. Clayton, R.C. Harden, J.V Makwana and M.J. Portsmouth, *Chromatographia*, **40** (1995) 47.

167 Q. Yang, Y. Zhuang, J. Smeyers-Verbeke and D.L. Massart, *J. Chromatogr. A*, **706** (1995) 503.

168 C. Francois, P. Morin and M. Dreux, *J. Chromatogr. A*, **706** (1995) 535.

169 M. Pantsar-Kallio and P.K.G. Manninen, *Anal. Chim. Acta.*, **314** (1995) 67.

170 C. Francois, P. Morin and M. Dreux, *J. Chromatogr. A*, **717** (1995) 393.

171 Q. Yang, C. Hartmann, J. Smeyers-Verbeke and D.L. Massart, *J. Chromatogr. A*, **717** (1995) 415.

172 H. Burt, D.M. Lewis and K.N. Tapley, *J. Chromatogr. A*, **736** (1996) 265.

173 H.A.H Billiet, P.E. Andersson and P.R. Haddad, *Electrophoresis.*, **17** (1996) 1367.

174 H. Salimi-Moosavi and R.M. Cassidy, *J. Chromatogr. A*, **749** (1996) 279.

175 Q. Yang, M. Jimidar, T.P. Hamoir, J. Smeyersverbeke and D.L. Massart, *J. Chromatogr. A*, **673** (1994) 275.

176 P. Morin, C. Francois and M. Dreux, *J. Liq. Chromatogr.*, **17** (1994) 3869.

177 N. Shakulashvili, T. Faller and H. Engelhardt, *J. Chromatogr. A*, **895** (2000) 205.

178 C.Y. Quang and M.G. Khaledi, *J. Chromatogr. A*, **659** (1994) 459.

179 J. Schiewe, M. Dabrunz and H.P. Abicht, *GIT Fachz. Lab.*, **38** (1994) 304.

180 J.M. Riviello and M.P. Harrold, *J. Chromatogr. A*, **652** (1993) 385.

181 R.R. Chadwick, J.C. Hsieh, K.S. Resham and R.B. Nelson, *J. Chromatogr. A*, **671** (1994) 403.

182 W. Buchberger, K. Winna and M. Turner, *J. Chromatogr. A*, **671** (1994) 375

183 J. Havel, P. Janos and P. Jandik, *J. Chromatogr. A*, **745** (1996) 127.

184 D.R. Salomon and J. Romano, *J. Chromatogr*, **602** (1992) 219.

185 M. Koberda, M.Konkowski, P. Youngberg, W.R. Jones and A. Weston, *J. Chromatogr.*, **602** (1992) 235.

186 R.A. Carpio, P. Jandik and E. Fallon, *J. Chromatogr. A*, **657** (1993) 185.

187 S.A. Oehrle, *J. Chromatogr. A*, **739** (1996) 413.

188 K.R. Cooper and R.G. Kelly, *J. Chromatogr. A*, **739** (1996) 183.

189 D.R. Salomon and J.P. Romano, *Process Control Qual.*, **3** (1992) 219.

190 B. Jones and Y. Takashi, *Kankyo Kagaku*, **3** (1993) 424.

191 M. Schmitt, F. Saulnier, L. Malhautier and G. Linden, *J. Chromatogr.*, **640** (1993) 419.

192 S.A. Oehrle, *J. Chromatogr. A*, **745** (1996) 87.

193 S.A. Oehrle, R.D. Blanchard, C.L. Stumpf and D.L. Wulfeck, *J. Chromatogr. A*, **680** (1994) 645.

194 M. Chen and R.M. Cassidy, *J. Chromatogr.*, **602** (1992) 227.

195 P. Morin, C. Francois and M. Dreux, *Analusis*, **22** (1994) 178.

196 Y.C. Shi and J.S. Fritz, *J. Chromatogr. A*, **671** (1994) 429.

197 M. Jimidar, T. Hamoir, W. Degezelle, D.L. Massart, S. Soykenc and P van de Winkel, *Anal. Chim. Acta*, **284** (1993) 217.

198 C. Vogt and S. Conradi, *Anal. Chim. Acta*, **294** (1994) 145.

199 M. Jimidar, B. Bourguignon and D.L. Massart, *J. Chromatogr. A*, **740** (1996) 109.

200 K. Ito and T. Hirokawa, *J. Chromatogr. A*, **742** (1996) 281.

201 C. Stathakis and R.M. Cassidy, *Analyst*, **121** (1996) 839.

202 E.L. Pretswell, B.A. McGaw and A.R. Morrisson, *Talanta*, **42** (1995) 283.

203 X. Xu, W.T. Kok, J.C. Kraak and H. Poppe, *J. Chromatogr. B*, **661** (1994) 35.

204 K.Z. Cheng, F.R. Nordmeyer and J.D. Lamb, *J. Capillary Electrophor.*, **2** (1995) 279.

205 K.Z. Cheng, Z.X. Zhao, R. Garrick, F.R. Nordmeyer, M.L. Lee and J.D. Lamb, *J. Chromatogr. A*, **706** (1995) 517.

206 W. Beck and H. Engelhardt, *Fres. J. Anal. Chem.*, **346** (1993) 618.

207 C.S. Chiou and J.S. Shih, *Analyst.*, **121** (1996) 1107.

208 K. Bächmann, T. Ehmann and I. Haumann, *J. Chromatogr. A*, **662** (1994) 434.

209 J. Boden, T. Ehmann, T. Groh, I. Haumann and K. Bächmann, *Fresenius J. Anal. Chem.*, **348** (1994) 572.

210 A. Padarauskas, V. Olsauakaite and V. Paliulionyte, *Anal. Chim. Acta*, **374** (1998) 159.

211 E. Simunicova, D. Kaniansky and K. Loksikova, *J. Chromatogr. A*, **665** (1994) 203.

212 Anon., *Dionex Tech. Note*, **91** (1994) 1.

213 Anon., *Dionex Tech. Note*, **35** (1994) 1.

214 W.R. Barger, R.L. Mowery and J.R. Wyatt, *J. Chromatogr. A*, **680** (1994) 659.

215 E. Dabek-Zlotorzynska and J.F. Dlouhy, *J. Chromatogr. A*, **706** (1995) 527.

216 B. Tenberken, P. Ebert, M. Hartmann, M. Kibler, A. Mainka, T. Prokop, A. Roder and K. Bächmann, *J. Chromatogr. A*, **745** (1996) 209.

217 B. Tenberken and K. Bächmann, *J. Chromatogr. A*, **755** (1996) 121.

218 X. Xiong and S.F.Y. Li, *J. Chromatogr. A*, **835** (1999) 169.

219 X. Cahours, P. Morin and M. Dreux, *J. Chromatogr. A*, **810** (1998) 209.

220 H. Sato, *J. Chromatogr.*, **465** (1989) 339.

221 K.-S. Whang, C.-W. Wang, *Electrophoresis*, **18** (1997) 241.

Chapter 2

Experimental

This section describes the instrumentation, chemicals and procedures used throughout this work, unless specified otherwise in a particular chapter.

2.1 Instrumentation

Three capillary electrophoresis instruments were used to perform separations during this study. Work described in Chapters 6 and 7 was carried out on an Agilent Technologies ^{3D}CE (Waldbron, Germany). This instrument was equipped with a deuterium lamp with a photodiode array detector. Injections were performed hydrodynamically with pressures up to 50 mbar used for various length of injection times.

A Waters Capillary Ion Analyser (Milford, MA, USA) was used for experiments involving a blue LED (λ_{max} = 476 nm, emission bandwidth at half-height 21 nm, RS 235-9900, RS Components, VIC, Australia) as the light source. This instrument was used in Chapters 3 and 6. Injections were performed hydrostatically, with a height of 10 cm being used with various length of injection times.

An Applied Biosystems 270A-HT (Perkin-Elmer, San Jose, CA, USA) interfaced to Turbochrom chromatography software (Perkin-Elmer) was also used for work in Chapters 3 and 5. This instrument was fitted with a deuterium lamp as the light source. Hydrodynamic injections were performed with a vacuum of 5" Hg (1" Hg= 3386.38 Pa) being applied for 0.6 s.

The use of other instruments for linearity evaluation is detailed in Chapter 4.

Fused silica capillaries (Polymicro Technologies Inc., Phoenix, AZ, USA) of 50 and 75 μm inner diameter, 375 μm outer diameter of varying lengths were used in conjunction with the appropriate capillary alignment interface of each instrument. Detection windows were

prepared by burning off a small section of polyimide coating using a butane torch. The detection window was cleaned with a tissue moistened with methanol.

Spectrophotometric measurements were conducted using a Cary UV-Vis-NIR Spectrophotometer (Varian Australia Pty. Ltd.) with 1 cm pathlength quartz cells.

2.2 Reagents

Unless specified otherwise all chemicals were of analytical reagent grade and are listed in the following tables.

2.2.1 Chemicals Used as Probes

Probe	**Chemical formula**	**Supplier**
Chromium trioxide	CrO_3	Fluka
Sodium chromate (LR)	Na_2CrO_4	APS Chemicals
Naphthol yellow S (Standard Fluka quality)	$C_{10}H_4N_2Na_2O_8S$	Fluka
Tartrazine (Standard Fluka quality)	$C_{16}H_9N_4Na_3O_9S_2$	Fluka
Orange G (Standard Fluka quality)	$C_{16}H_{10}N_2Na_2O_7S_2$	Fluka
Imidazole (99%)	$C_3H_4N_2$	Aldrich
Chrysoidine (Standard Fluka quality)	$C_{12}H_{13}N_4Cl$	Fluka

2.2.2 Chemicals Used as Buffers and Complexing Agents

Chemical	**Formula**	**Supplier**
Histidine	$C_6H_9N_3O_2$	Fluka
Tris(hydroxymethyl)aminomethane	$NH_2C(CH_2OH)_3$	Aldrich
Diethanolamine	$HN(CH_2CH_2OH)_2$	Fluka
2-hydroxyisobutyric acid (98%)	$(CH_3)_2C(OH)CO_2H$	Aldrich
L-lactic acid (85+%)	$CH_3CH(OH)CO_2H$	Aldrich

2.2.3 Cationic Analytes

Analyte	**Formula**	**Supplier**
Sodium chloride	NaCl	APS Chemicals
Barium chloride	$BaCl\cdot 2H_2O$	BDH
Strontium nitrate	$Sr(NO_3)_2$	Unknown
Calcium chloride	$CaCl_2\cdot 2H_2O$	APS Chemicals
Potassium chloride	KCl	APS Chemicals
Magnesium nitrate	$Mg(NO_3)_2\cdot 6H_2O$	Unknown
Manganese chloride	$MnCl_2\cdot 4H_2O$	BDH
Chromium nitrate	$Cr(NO_3)_3\cdot 9H_2O$	Hopkin & Williams
Iron nitrate	$Fe(NO_3)_3\cdot 9H_2O$	Chem-Supply
Cobalt chloride	$CoCl_2\cdot 6H_2O$	APS Chemicals
Lithium chloride	LiCl	May and Baker
Lanthanum nitrate	$La(NO_3)_3\cdot 6H_2O$	Koch-Light
Cerium nitrate	$Ce(NO_3)_3\cdot 6H_2O$	Strem Chemicals
Praseodymium nitrate	$Pr(NO_3)_3\cdot 5H_2O$	Koch-Light
Neodymium nitrate	$Nd(NO_3)_3\cdot 6H_2O$	Koch-Light

Analyte	**Formula**	**Supplier**
Samarium nitrate	$Sm(NO_3)_3 \cdot 6H_2O$	Koch-Light
Europium nitrate	$Eu(NO_3)_3 \cdot 6H_2O$	Koch-Light
Gadolinium nitrate	$Gd(NO_3)_3 \cdot 5H_2O$	Koch-Light

2.2.4 Anionic Analytes

Analyte	**Formula**	**Supplier**
Methanesulfonic acid (LR)	CH_3SO_3H	Sigma
Ethanesulfonate, sodium salt	$CH_3CH_2SO_3Na$	Aldrich
Propanesulfonate, sodium salt	$CH_3(CH_2)_2SO_3Na$	Aldrich
Butanesulfonate, sodium salt	$CH_3(CH_2)_3SO_3Na$	Aldrich
Pentanesulfonate, sodium salt	$CH_3(CH_2)_4SO_3Na$	Sigma
Hexanesulfonate, sodium salt	$CH_3(CH_2)_5SO_3Na$	Sigma
Heptanesulfonate, sodium salt	$CH_3(CH_2)_6SO_3Na$	APS Chemicals
Octanesulfonate, sodium salt	$CH_3(CH_2)_7SO_3Na$	Sigma
Sodium bromide	NaBr	Sigma
Sodium sulfate	Na_2SO_4	Aldrich
Sodium phosphate	$Na_3PO_4 \cdot 12H_2O$	Aldrich
Potassium hydrogen phthalate	$KOOCC_6H_4COOH$	APS Chemicals
Sodium carbonate	Na_2CO_3	BDH
Sodium formate	CHOONa	APS Chemicals
Sodium acetate	CH_3COONa	APS Chemicals
Malonic acid, sodium salt (LR)	$CH_2(COONa)_2$	APS Chemicals
Sodium thiocyanate	NaSCN	Aldrich
Potassium bromate	$KBrO_3$	Aldrich
Sodium chlorate	$NaClO_3$	BDH
Tartaric acid, disodium salt	$Na_2C_4H_4O_6 \cdot 2H_2O$	BDH

Analyte	**Formula**	**Supplier**
Succinic acid, disodium salt (LR)	$(CH_2COONa)_2 \cdot 6H_2O$	BDH
Tri-sodium citrate	$Na_3C_6H_5O_7 \cdot 2H_2O$	APS Chemicals
Oxalic acid	$(COOH)_2 \cdot 2H_2O$	APS Chemicals
Sodium fluoride	NaF	Aldrich
Sodium nitrate	$NaNO_3$	APS Chemicals
Sodium perchlorate	$NaClO_4$	APS Chemicals
Sodium iodate	$NaIO_3$	Aldrich
Sodium chloride	NaCl	APS Chemicals

2.2.5 Other Chemicals

Chemical	**Formula**	**Supplier**
Sodium hydroxide	NaOH	APS Chemicals
Tetradecyltrimethylammonium hydroxide	$CH_3(CH_2)_{13}N(CH_3)_3OH$	Waters
Hydrochloric acid	HCl	BDH
Hydroxypropyl methyl cellulose		Aldrich
Poly(ethyleneimine) (50% w/w)	$(-NHCH_2CH_2-)_x$ $[N(CH_2CH_2NH_2)CH_2CH_2-]_y$	Acros
N-dodecyl-*N*,*N*-dimethylammonio-3-propanesulfonate (SB-12)	$C_{17}H_{37}NO_3S$	Fluka

2.3 Procedures

2.3.1 Preparation of Analytes and Electrolytes

Water treated with a Millipore (Bedford, MA, USA) Milli-Q system was used to prepare standard solutions and electrolytes. All electrolytes were degassed under vacuum sonication and were filtered through a 0.45 μm syringe filter (Activon Thornleigh, Australia) before use.

2.3.2 Calculations

Mobilities were calculated using the equation:

$$\mu = \frac{L_d \times L_t}{V \times t_m} \qquad (2\text{-}1)$$

where μ= mobility of analyte ($m^2 V^{-1} s^{-1}$)

L_d= length of capillary to detector (m)

L_t= total length of capillary (m)

V= voltage (V) and

t_m= migration time (seconds).

Detection limits were calculated at twice baseline noise.

Separation efficiencies were calculated based on the peak width at half-height using the equation:

$$N = \frac{5.55 \times t_m^{\,2}}{w_{1/2}^{\,2}} \qquad (2\text{-}2)$$

where N= number of theoretical plates

t_m = migration time (seconds) and

$w_{1/2}$ = peak width at half-maximum height (seconds).

Chapter 3

Indirect Photometric Detection of Anions Using Dyes as Probes and Electrolytes Buffered With an Isoelectric Ampholyte

3.1 Introduction

From Eqn. (1.14) in Chapter 1 it is clear that an effective means of increasing the sensitivity of indirect photometric detection is to increase the absorptivity of the probe. The most direct implementation of this approach has been to use dyes as probes, since these often exhibit very high molar absorptivities of the order of 10^5 L.mol^{-1} cm^{-1} in the visible spectral range. The opportunity to perform indirect detection in the visible region offers the additional potential advantage of better detection selectivity compared to indirect detection in the UV range when dealing with real samples with complex matrices since many potentially interfering sample components can be expected to show little absorbance.

Careful formulation of the electrolytes, especially in regard to the choice of buffer and any other additives and to the purity of all the used chemicals, is required. Competitive displacement occurs when an ion of the same charge as the analyte and the probe (i.e. a co-ion) is present in the background electrolyte and may be displaced by the analyte during migration in the same manner as the probe is displaced in the fundamental process of indirect detection. When the co-ion is non-absorbing, a loss of detection sensitivity will result and "system" peaks are often introduced into the electropherogram [1, 2]. Depending on the concentration of the co-ion and the relative mobilities of the probe and co-ion, such system peaks may occur at regions in an electropherogram where analytes should be detected, therefore making their detection difficult. Although from the theory of competitive displacement it is clear that purity of the probes and other chemicals used in the electrolyte is crucial, this role has not been experimentally demonstrated.

The very high molar absorptivities of typical dyes result in their use at relatively low concentrations in BGEs, usually at the sub-millimolar level. This places stringent requirements on the purity of the reagents used in order to avoid the presence of co-ionic impurities in the electrolyte and hence significant levels of competitive displacement. The introduction of co-ions should be avoided completely if at all possible or their effects should be minimised by keeping the concentration of the co-ion as small as possible, such as by purification of probes and other electrolyte components.

It should also be noted that the necessity to avoid the presence of co-ions in the electrolyte leads to particular considerations for buffering of the electrolytes. Whilst unbuffered electrolytes are sometimes used [3, 4], buffering is normally necessary to achieve optimal reproducibility and tolerance to sample matrices [5, 6]. This is normally performed by the addition of a buffering counter-ion.

An ampholyte dissolved in solution will exist in a zwitterionic form with zero overall charge and therefore will not act as a competing co-ion or increase the conductivity of an electrolyte. The buffering capacity of an ampholyte depends on how close the two pK_a values of its buffering groups are to the isoelectric point, which is the pH halfway between these two pK_a values and is the pH at which the ampholyte has zero overall charge. A major advantage of ampholytic buffers is that their very low conductivity allows them to be added to electrolytes in relatively high concentrations without increasing Joule heating effects. Hence it is not necessary that they buffer as strongly as conventional buffers. Although Doble *et al.* [7] have demonstrated the use of lysine and glutamic acid as ampholytic buffers, there are unfortunately only a few ampholytes which are effective buffers.

In this Chapter, using BGEs buffered with the ampholyte histidine, two dyes (naphthol yellow S and tartrazine) are used as probes for indirect photometric detection using a

blue LED as the light source. The necessity for high purity probes is also demonstrated. Analytical performance parameters of BGEs based on the two dyes are presented, together with examples of their use in the analysis of real samples.

3.2 Experimental

3.2.1 Instrumentation for CE

The general experimental details are given in Chapter 2.

The CE instruments used in this Chapter were an Applied Biosystems 270A-HT and a Waters Capillary Ion Analyser. The Applied Biosystems Model 270A-HT was used for detection at 223 and 258 nm. The Waters Capillary Ion Analyser was used with a blue LED light source for detection at 476 nm.

3.2.2 Procedures

Purified dyes were prepared by dissolving the dye in the minimum possible volume of boiling water and then allowing the dye to recrystallise. The recrystallised product was collected by filtration over a Buchner funnel. Each dye was recrystallised twice to obtain satisfactory purity. The hot naphthol yellow S solution was gravity filtered through filter paper to remove a small amount of insoluble material during the first recrystallisation. The purified dyes were dried in a vacuum desiccator. Determination of anionic impurities was performed by CE using a chromate electrolyte [6]. In brief, a fused silica capillary, an electrolyte consisting of 5 mM chromate buffered at pH 9.2 with diethanolamine and 0.5 mM tetradecyltrimethylammonium bromide (TTAB) and indirect detection at 254 nm were used to separate and quantify the inorganic anions using a standard addition method.

3.3 Results and Discussion

3.3.1 Choice of Probes and Buffer

A number of features must be taken into account in the choice of the dyes to be used as probes. The molecular structure of the dye would determine important parameters such as its solubility, mobility and spectral properties. Firstly and most importantly, the expected mobility could be estimated on the basis of the number of negatively charged functional groups and the approximate size of the molecule. It was estimated that at least two anionic groups would be required for a typical dye probe having molecular weight of less than 1000 in order to produce a medium to high mobility for the dye. Secondly, it is desirable that the dye is soluble in water and does not adsorb onto the capillary wall. Solubility data on most dyes can be found in the literature [8]. The structure of the molecule was used as a guide to its potential adsorption properties and dyes having one or more basic group were excluded on the premise that they could exhibit interactions with silanols of the fused silica wall. Based on the above considerations naphthol yellow S and tartrazine were chosen and their mobility and molar absorbances are shown in Table 3-1. See Figures 3-1 and 3-2 for structures of tartrazine and naphthol yellow S respectively.

Table 3-1 Absorptivities and electrophoretic mobilities of dyes used in this study.

Dye	**Absorption maxima (nm) and corresponding molar ($L.mol^{-1}\ cm^{-1}$)**	**Mobility ($x10^{-9}\ m^2 V^{-1} s^{-1}$)**
Naphthol yellow S	223 (23,125) 428 (17,000)	-46.4
Tartrazine	258 (21,350) 426 (21,600)	-45.4

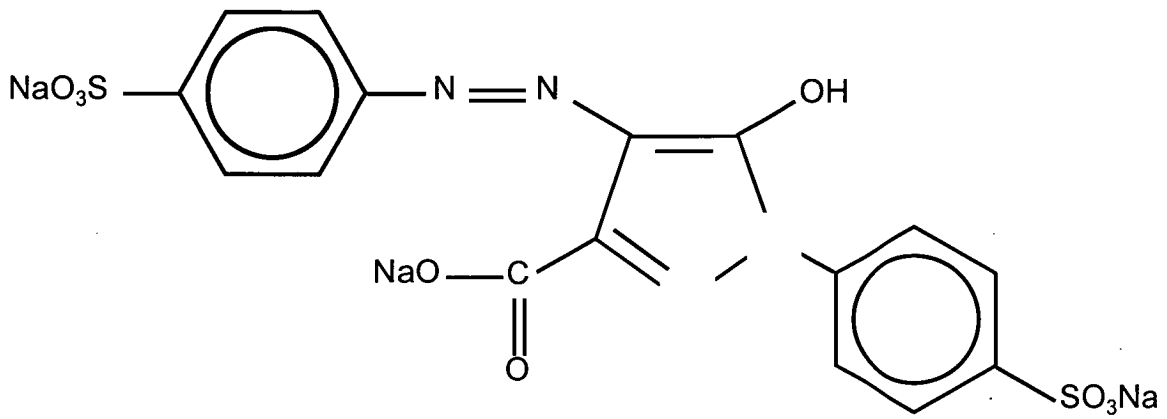

Figure 3-1 Tartrazine

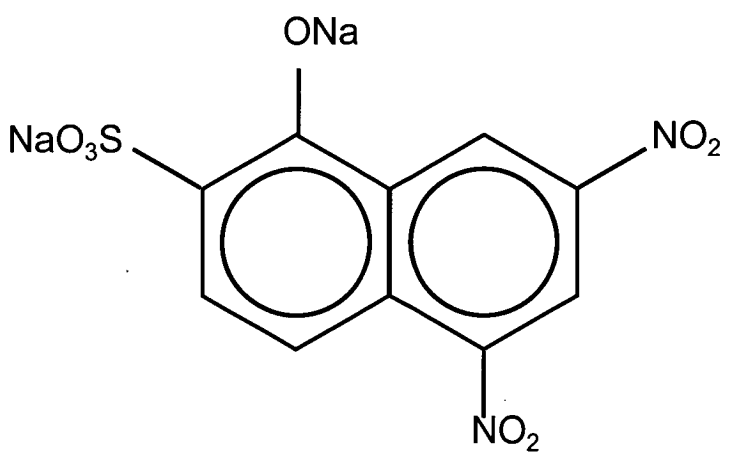

Figure 3-2 Naphthol yellow S

To avoid competitive displacement effects, isoelectric buffers were to be used and the major considerations in their choice were the p*I* (which determines the pH at which buffering occurred) and the buffering capacity. Unless anions of weak acids are to be analysed, a BGE pH in the neutral region is desirable as alkaline electrolytes will absorb carbon dioxide producing carbonate which will then act as a competing co-ion. For an ampholyte to exhibit an appreciable buffering capacity, the pK_a values should be approximately within 1 unit either side of the p*I*. Few ampholytes meet this requirement, and hence while many ampholytes exist, relatively few can be used as buffers. Although the buffering capacity of histidine is not as high as those of two other readily available isoelectric buffers lysine (p*I* 9.7) and glutamic acid (p*I* 3.2), histidine was chosen primarily because its p*I* value of 7.7 allows it to be used at desirable pH values of the BGE.

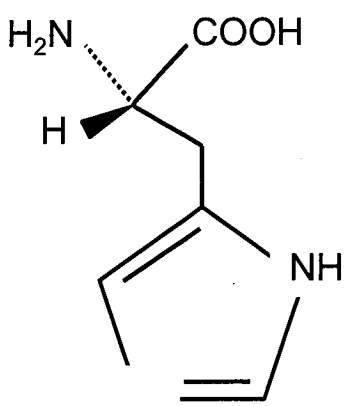

Figure 3-3 Histidine

3.3.2 Effects of Co-Ionic Impurities

Commercially available dyes are rarely very pure. In order to determine whether purification of the probes to reduce the levels of co-ionic impurities was required, a simple test was conducted. A BGE consisting of the dye in question as a probe was prepared (no buffering was used to avoid possible impurities from the buffer) and used for the separation of a standard mixture of anions (Figure 3-4(a)). The system peak that can be seen in the middle of the electropherogram in Figure 3-4(a) obtained using the unpurified dye and the inverted or distorted peaks before the system peak are typical indicators of the presence of co-ionic impurities [1, 2]. For comparison, a BGE containing the same probe after purification was tested and this showed no system peaks and only positive peaks for all analytes, including the highly mobile anions (Figure 3-4 (b)). The same behaviour was observed for both tartrazine and naphthol yellow S. It is clear that the system peak and distorted or negative peaks of analytes were caused by anionic impurities present in the probe. This is illustrated further by the results of determinations of anionic impurities in the probes (see Table 3-2) and showed that purification of the dyes was essential for their use as probes for indirect photometric detection. These results also implied that purity of buffers or any other reagents used in the electrolytes was also essential. However, purification of histidine was not necessary as it was obtained commercially in high purity.

Table 3-2 Co-ionic impurities (% molar) present in probes before and after purification

Probe	**Impurity**	**Before (%) ***	**After (%) ***
Naphthol yellow S	chloride	15.0	0.2
	sulfate	28.2	0.1
	carbonate	2.5	0.5
Tartrazine	chloride	53.6	0.3
	carbonate	5.0	2.5

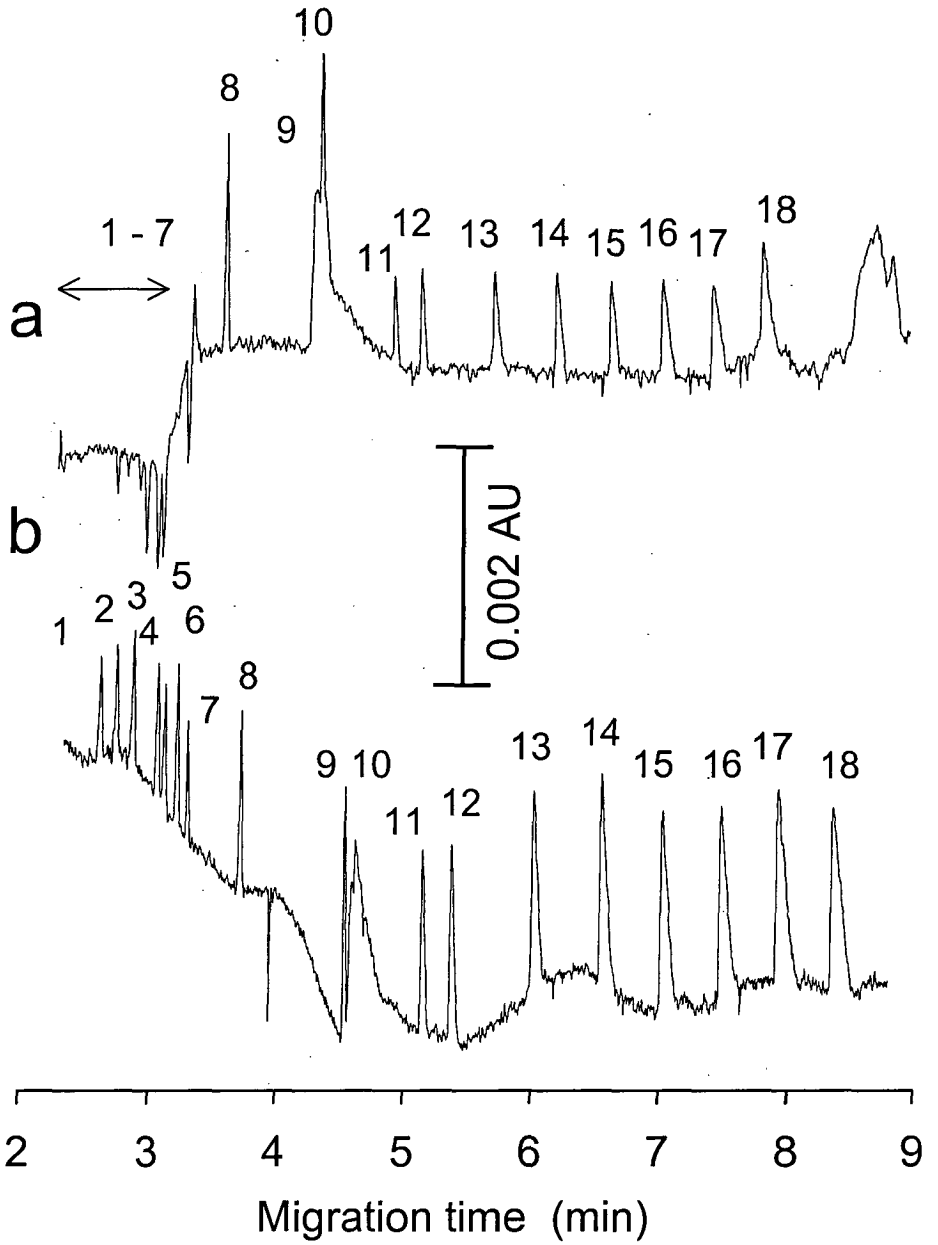

Figure 3-4 Electropherogram of a 10 μM standard anion mixture using an unpurified (a) and a purified (b) dye as probe. Peak identification: 1= chloride, 2= nitrate, 3= sulfate, 4= chlorate, 5= malonate, 6= tartrate, 7= formate, 8= phthalate, 9= methanesulfonate, 10= carbonate, 11= iodate, 12= ethanesulfonate, 13= propanesulfonate, 14= butanesulfonate, 15= pentanesulfonate, 16= hexanesulfonate, 17= heptanesulfonate, 18= octanesulfonate. Conditions- capillary: fused silica, 75 μm ID, length 0.72 m, 0.50 m to detector; electrolyte: (a) 0.50 mM unpurified naphthol yellow S, 0.05% (w/v) HPMC, pH 8.38; (b) 0.50 mM purified naphthol yellow S, 0.05% (w/v) HPMC, pH 8.42; separation voltage: -30 kV (current 3 μA at 30° C); detection: indirect photometric at 223 nm; pressure injection: 5" Hg for 0.6 s.

3.3.3 EOF Suppression

Separations of inorganic and other highly mobile anions are typically run co-electroosmotically with reversed EOF [9]. When using organic dyes as probes, the reversal of EOF using a cationic EOF modifier such as TTAB or hexamethonium bromide was not possible as a precipitate formed between the dye and the modifier. Other EOF modifiers were also not effective. For high and medium mobility anions, suppression of EOF instead of its reversal can be used to achieve reasonable run times. The EOF of BGEs buffered with histidine could be suppressed significantly by the addition of 0.05% (w/v) hydroxypropyl methyl cellulose (HPMC) [10]. It should be noted that the suppression of EOF by the addition of a neutral, uncharged polymer has not found much use with indirect photometric detection. A rare example is the work of Shamsi *et al.* [11] who used diethylenetriamine to suppress EOF in order to increase migration times and provide better resolution. Using a positive polarity at the injection end, the water peak used as the EOF marker appeared at about 5 min for the unsuppressed histidine buffered BGE, whereas the addition of HPMC caused the EOF peak to occur at about 45 min, corresponding to a residual EOF of about $+4.4 \times 10^{-9}$ $m^2 V^{-1} s^{-1}$. This large reduction in EOF allowed a wider mobility range of anions to be detected and also markedly decreased the analysis time of low mobility anions. This was not possible in the previous [7] work when bromocresol green and indigotetrasulfonate were used as probes in electrolytes without EOF suppression. The HPMC had no adverse effects and therefore it was further used as an additive in 0.05% concentration in the electrolytes used in this work.

3.3.4 Analytical Performance Characteristics

The final electrolytes containing either naphthol yellow S or tartrazine at 0.5 mM, 10 mM histidine and 0.05% HPMC (Table 3-3) were studied and compared on the basis of analyte effective mobilities, peak shapes, separation selectivity, detection limits and separation efficiency. The BGE consisting of naphthol yellow S–histidine was further investigated in terms of linearity and reproducibility and the use of a blue LED as a light source was also examined. Separation of a standard mixture of 18 common anions using a naphthol yellow S-histidine BGE is shown in Figure 3-5. This electrolyte was also used for the analysis of real samples. A separation of a standard mixture of 20 common anions using the tartrazine–histidine BGE is shown in Figure 3-6.

The effective mobility of each analyte was determined for both BGEs and values are given in Table 3-4. The migration order was comparable for both electrolytes, although minor selectivity changes were observed and so some anions with very similar mobilities showed differing migration orders. It is to be expected that analytes with mobilities which match that of the probe will show the most symmetrical peaks and the highest efficiencies.

Table 3-3 BGE composition

BGE	[tartrazine] (mM)	[naphthol yellow S] (mM)	[histidine] (mM)	pH	EOF (x10^{-9} m^2V^{-1} s^{-1})	Current (μA)
1	0.5	0	10	7.7	4.6	2
2	0	0.5	10	7.7	4.7	2

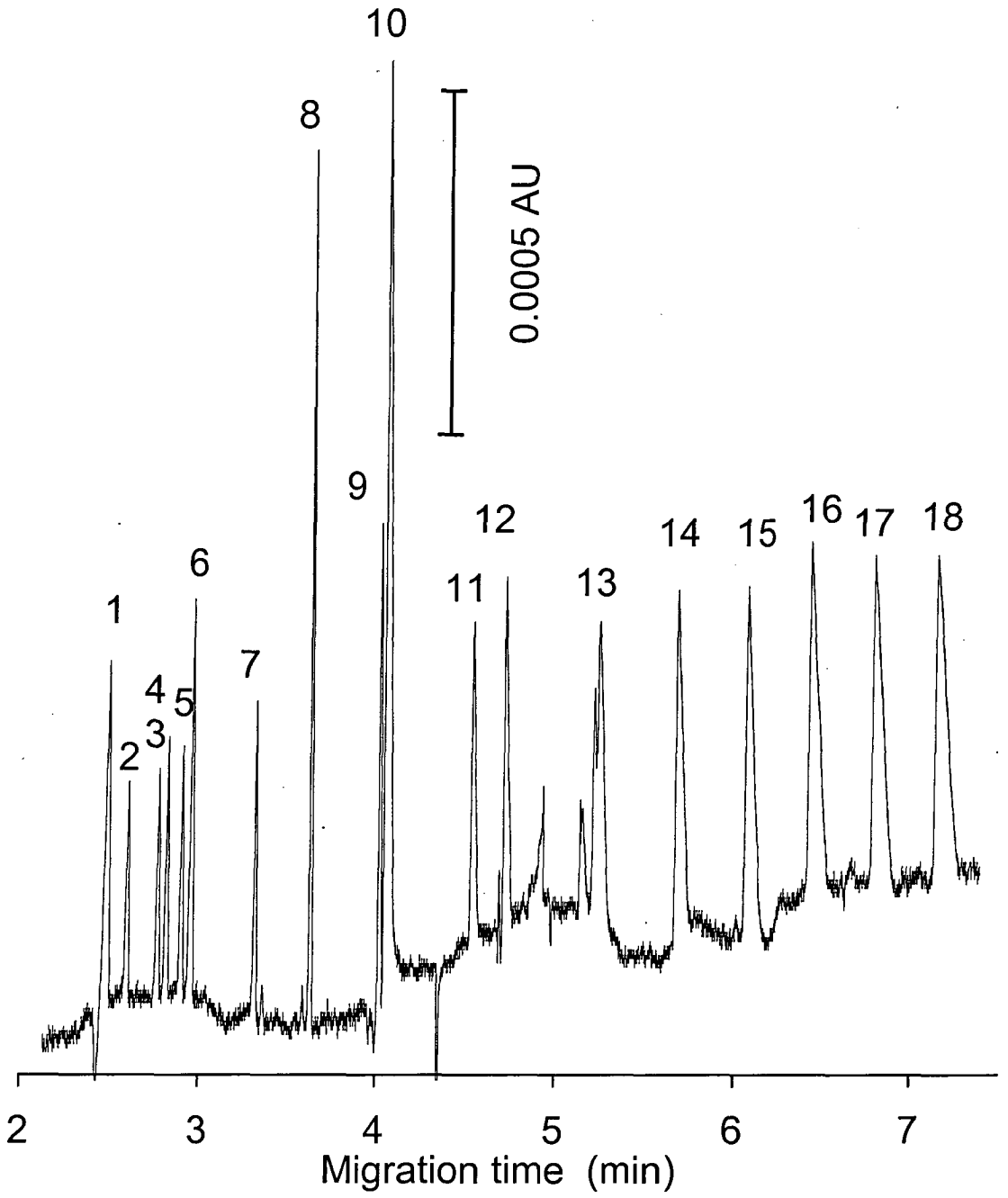

Figure 3-5 Electropherogram of 10 μM standard anion mixture under optimal BGE conditions using an LED as detector. Peak identification: 1= chloride, 2= nitrate, 3= sulfate, 4= chlorate, 5= malonate, 6= tartrate, 7= formate, 8= phosphate, 9= methanesulfonate, 10= carbonate, 11= iodate, 12= ethanesulfonate, 13= propanesulfonate, 14= butanesulfonate, 15= pentanesulfonate, 16= hexanesulfonate, 17= heptanesulfonate, 18= octanesulfonate. Conditions- capillary: fused silica, 75 μm ID, length 0.60 m, 0.52 m to detector; electrolyte: 0.50 mM purified naphthol yellow S, 10.0 mM histidine, 0.05% HPMC, pH 7.7; separation voltage: -30 kV (current 3 μA at 30°C); detection: indirect photometric at 476 nm (LED); hydrostatic injection: 10 cm for 20 s.

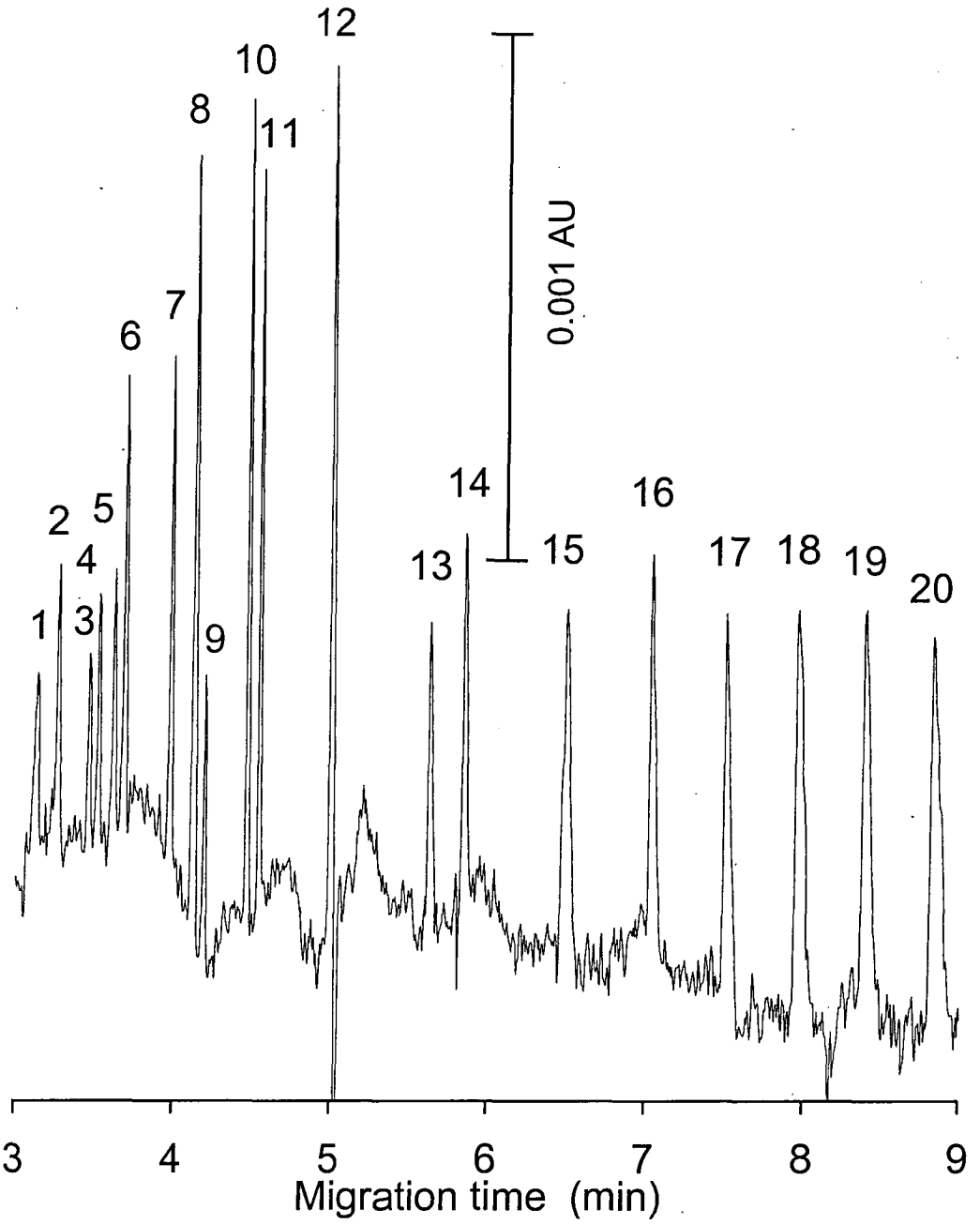

Figure 3-6 Electropherogram of 5 μM standard anion mixture under optimal BGE conditions using a deuterium lamp as detector. Peak identification: 1= chloride, 2= nitrate, 3= perchlorate, 4= thiocyanate, 5= chlorate, 6= malonate, 7= tartrate, 8= bromate, 9= formate, 10= phosphate, 11= phthalate, 12= methanesulfonate, 13= iodate, 14= ethanesulfonate, 15= propanesulfonate, 16= butanesulfonate, 17= pentanesulfonate, 18= hexanesulfonate, 19= heptanesulfonate, 20= octanesulfonate. Conditions- capillary: fused silica, 75 μm ID, length 0.72 m, 0.50 m to detector; electrolyte: 0.50 mM purified tartrazine, 10.0 mM histidine, 0.05% HPMC, pH 7.7; separation voltage: -30 kV (current 2 μA at 30°C); detection: indirect photometric at 258 nm; pressure injection: 5" Hg for 0.6 s.

The separation efficiencies for each analyte and BGE, calculated as the number of theoretical plates, are given in Table 3-4, which shows that efficiencies varied over the range 36,000 to almost 300,000 theoretical plates. It is important to note that good peak shapes were produced for a wide range of anions using the two probes.

Detection limits of each anion for each electrolyte are given in Table 3-4. All detection limits were sub-μM when a deuterium lamp was used except for succinate in the naphthol yellow S-histidine BGE. The best detection limits occurred for anions of medium mobility, which is expected since the probes also have medium mobility. When comparing the observed detection limits to other values reported in literature, the following comments can be made. First, the sub-μM detection limits found are an order of magnitude lower than the reported generalised detection limits of indirect photometric detection (10^{-4}-10^{-5} mol L^{-1}) [9]; second, the detection limits achieved when using the deuterium lamp are better than those reported by Doble *et al.* [7] using another dye (potassium indigotetrasulfonate) as a probe and glutamic acid as the buffer; and third it should be noted that for the detection in the visible range using an LED, the detection sensitivity was only about half of the likely optimum and consequently the achieved detection limits were higher than optimal. The optimum results would be achieved if LEDs with the same emission maximum as the probes were used. The absorption maxima of the dyes (426 nm and 428 nm, see Table 3-1) were about 50 nm lower than the emission maximum (476 nm) of the blue LED used. Detection using the deuterium lamp at the absorption maximum of the dye did not bring about better signal-to-noise ratios because of considerably higher noise levels. It is well documented that LEDs are low noise light sources and this can be used to advantage for photometric detection in CE [12]. An improvement in limits of detection by a factor of approx. two could be expected if a LED having an appropriate wavelength of maximum emission was to be used.

Table 3-4 BGE Performance

Analyte	Mobility ($x10^{-9}$ $m^2 V^{-1} s^{-1}$)		Efficiency (10^3 plates)		LOD, D_2 lamp 223 nm		LOD, LED 476 nm	Reproducibility (% RSD)	
	BGE 1	BGE 2	BGE 1	BGE 2	BGE 1	BGE 2	BGE 2	BGE 2	
					Conc (μM)	Conc (μM)	Conc (μM)	Migration time	Area / time
chloride	-70.1	-66.7	37	41	0.8	0.5	1.2	0.1	2.4
carbonate	-45.0	-43.4	219	78	N/A	0.3	0.4	0.9	5.8
sulfate	-69.7	-64.9	NA	125	N/A	0.5	1.6	0.2	5.9
nitrate	-68.9	-65.9	85	65	0.6	0.6	2.0	0.2	6.0
phosphate	-49.4	-47.4	168	94	0.2	0.4	0.4	0.2	5.2
tartrate	-55.0	-52.7	142	87	0.3	0.3	1.0	0.2	7.8
malonate	-60.1	-58.2	177	74	0.3	0.3	1.7	0.2	4.7
formate	-52.8	-51.0	234	78	0.5	0.5	1.2	N/A	N/A
succinate	-52.2	-49.0	N/A	144	N/A	1.3	N/A	0.4	5.3
bromate	-53.2	-50.4	112	96	0.2	0.5	N/A	0.2	5.3
thiocyanate	-61.5	-57.8	298	N/A	0.6	N/A	1.1	NA	NA
chlorate	-60.9	-58.4	139	47	0.5	0.6	1.5	0.2	5.7
perchlorate	-63.2	-60.3	277	N/A	0.7	N/A	N/A	N/A	N/A
phthalate	-49.3	-47.2	N/A	96	0.2	0.3	N/A	N/A	N/A
iodate	-39.4	-40.2	54	143	0.4	0.5	1.2	0.3	5.1
methanesulfonate	-43.5	-44.3	129	123	0.1	0.4	0.7	0.3	3.2
ethanesulfonate	-37.3	-38.0	114	29	0.3	0.5	1.0	0.4	5.4
propanesulfonate	-33.7	-34.3	131	70	0.4	0.7	1.2	0.4	5.1
butanesulfonate	-31.2	-31.7	85	78	0.4	0.3	1.1	0.4	3.5
pentanesulfonate	-29.3	-29.7	105	80	0.4	0.5	1.0	0.4	4.9
hexanesulfonate	-27.7	-28.1	53	71	0.4	0.5	1.1	0.5	7.9
heptanesulfonate	-26.3	-26.6	145	41	0.3	0.6	1.1	0.5	4.8
octanesulfonate	-25.0	-25.3	172	56	0.4	0.6	1.2	0.5	4.3

N/A= not evaluated

BGE 2 (see Table 3-3), containing naphthol yellow S and histidine, was investigated for detection linearity and reproducibility. Chlorate, bromate, iodate, pentanesulfonate and octanesulfonate were chosen as the analyte anions to be studied since they cover a wide mobility range. A standard mixture of these anions was injected at varying concentrations in the range 5–500 μM and the detector response (area divided by migration time) was plotted against concentration to determine the linearity range. Linearity ($r^2 = 0.9965$-0.9995) was observed over the entire concentration range examined. Reproducibility was determined using a standard anion mixture (20 μM each analyte) injected ten times consecutively and a summary of the results is given in Table 3-4. Although the %RSD values increased with increasing migration times, the migration time reproducibilities (generally <0.5% except for carbonate) can be considered as good for a CE method. The reproducibilities for normalised peak areas (%RSD 2.4-7.9%) were somewhat worse but still acceptable for a CE method.

3.3.5 Analysis of Real Samples

A series of real samples was analysed in order to demonstrate the analytical potential of this technique. It should be pointed out that the use of buffered electrolytes is vital if the method is to be extended to a wide range of real samples. An excellent demonstration of the potential of the method is the analysis of tap water (Figure 3-7), where an undiluted sample produced significant peaks and showed that the developed method could be used for trace analyses which hitherto have not been possible with less sensitive indirect photometric detection methods for CE.

The naphthol yellow S-histidine BGE was used to quantify known anions in carbonated mineral water, still mineral water and beer (Figure 3-8), using standard addition. Of the two anions present in the carbonated mineral water in appreciable concentrations, the experimentally determined concentration of chloride of 221.1 mg/L agreed closely with typical analysis values of 220 mg/L reported on the label. Good reproducibilities of migration times and normalised peak areas were observed with RSD values typically <0.6% and <4%, respectively.

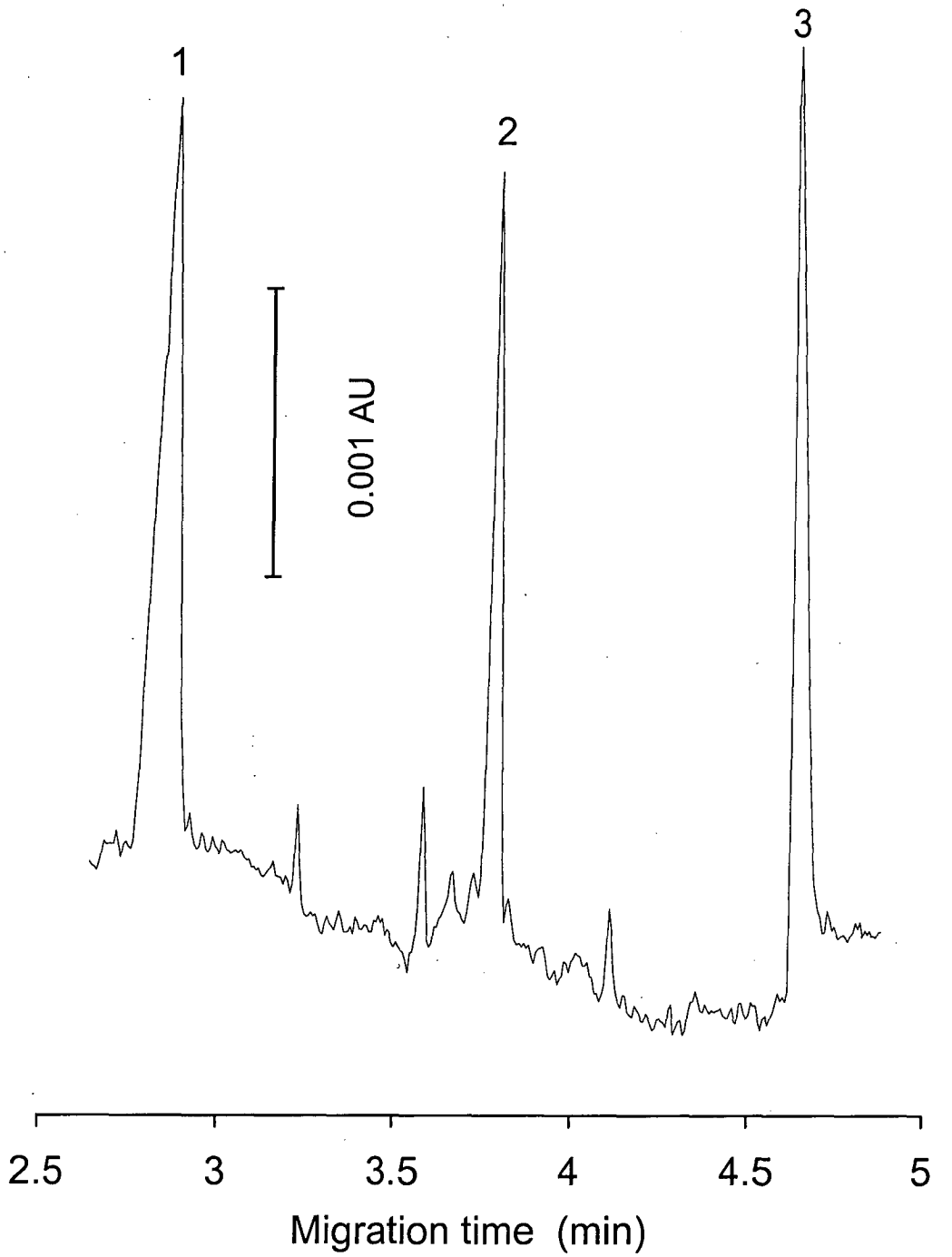

Figure 3-7 Electropherogram of tap water. Peak identification: 1= chloride, 2= fluoride, 3= phosphate. Conditions- electrolyte: 0.50 mM purified naphthol yellow S, 10.0 mM histidine, 0.05% HPMC, pH 7.7. All other conditions as given in Figure 3-4.

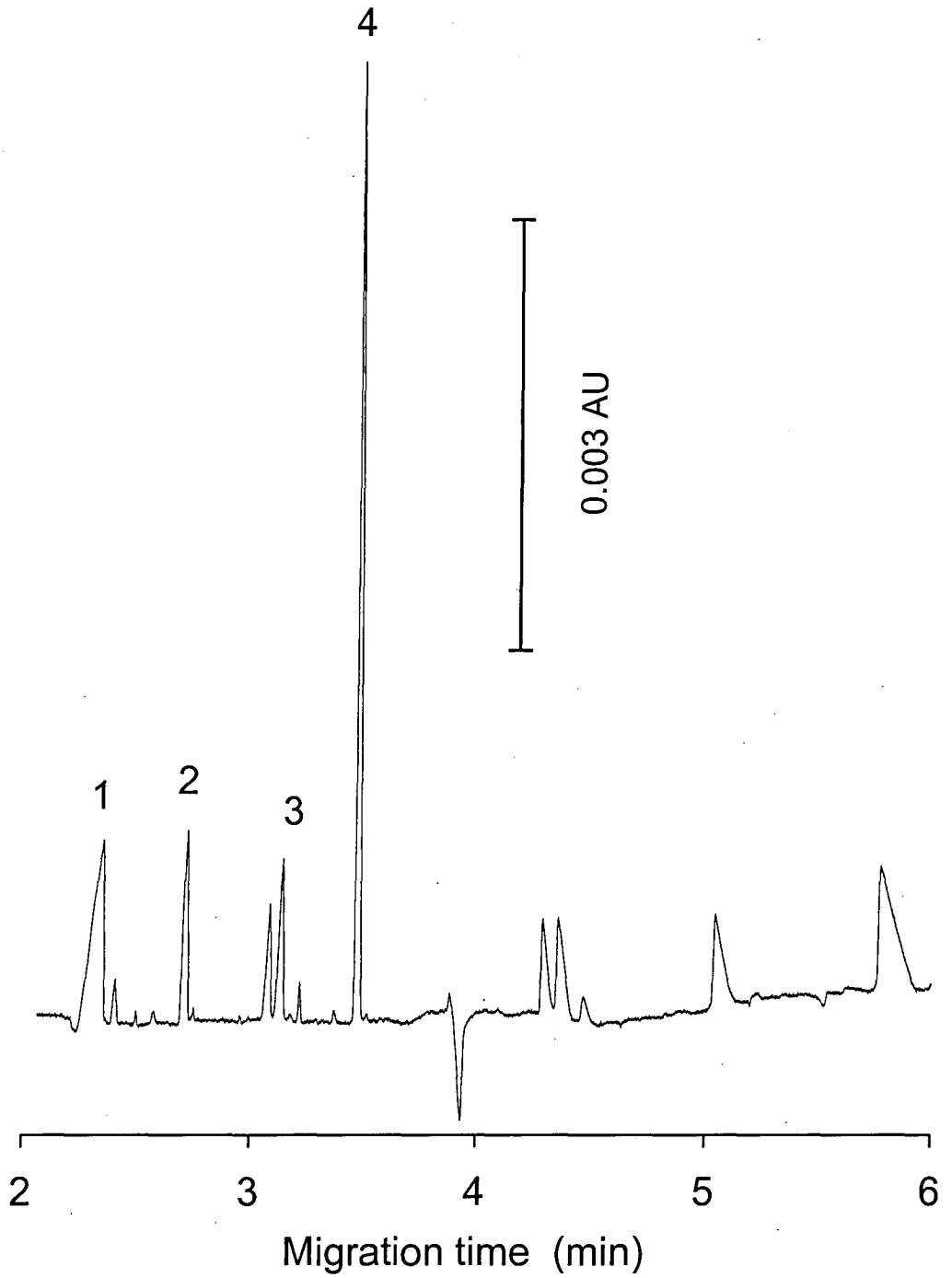

Figure 3-8 Electropherogram of 10% beer solution. Peak identification: 1= chloride, 2= tartrate, 3= formate, 4= phosphate. Other conditions as given in Figure 3-5.

3.4 Conclusions

New probes suitable for indirect photometric detection can be identified when a systematic approach taking into account their desirable properties is applied. Purification of probes and other electrolyte constituents is often necessary as a high level of purity of all BGE components with regard to co-ionic impurities is critical for optimal performance of indirect detection, especially when using a highly absorbing probe at low concentration in the BGE. Naphthol yellow S and tartrazine used as probes in electrolytes buffered with the isoelectric buffer histidine and with HPMC as an additive for EOF suppression provided LODs in the sub- μM range, which are approximately an order of magnitude lower than those achieved with most of the indirect photometric detection probes used previously.

LEDs as light sources have the potential to provide a further improvement in the LODs due to their typically lower noise levels, but to maximise this improvement, the emission maximum of the LED should match the absorption maximum of the probe.

Considerably more work is needed to explore the analytical potential of the approach outlined in this work, especially when probe concentration in the electrolyte becomes sufficiently low that tolerance to sample ionic strength is reduced and less sample stacking occurs. The full advantages of detection in the visible region for real samples with complex matrixes have also yet to be realised

3.5 References

1 P.A. Doble and P.R. Haddad, *Anal. Chem.*, **71** (1998) 15.

2 M. Macka, P.R. Haddad, P. Gebauer and P. Bocek, *Electrophoresis*, **18** (1997) 1998.

3 Y.J. Xue and E.S. Yeung, *Anal. Chem.*, **65** (1993) 2923.

4 H. Siren, A. Maattanen and M.L. Riekola, *J. Chromatogr. A*, **767** (1997) 293.

5 M. Macka, P. Andersson and P.R. Haddad, *Anal. Chem.*, **70** (1998) 743.

6 P. Doble, M. Macka, P. Andersson and P.R. Haddad, *Anal. Commun.*, **34** (1997) 351.

7 P. Doble, M. Macka and P.R. Haddad, *J. Chromatogr. A*, **804** (1998) 327.

8 E. Gurr, *Synthetic Dyes in Biology, Medicine, and Chemistry*, Academic Press, New York 1971.

9 P. Doble and P.R. Haddad, *J. Chromatogr. A*, **834** (1998) 189.

10 G. Schomburg, in: Khaledi (Ed.), *High Performance Capillary Electrophoresis*, John Wiley & Sons, New York 1998, pp. 481-523.

11 S.A. Shamsi, R.M. Weathers and N.D. Danielson, *J. Chromatogr. A*, **737** (1996) 315.

12 M. Macka, P. Andersson and P.R. Haddad, *Electrophoresis*, **17** (1996) 1898.

Chapter 4

Method for Evaluation of Linearity and Effective Pathlength of On-Capillary Photometric Detectors in Capillary Electrophoresis

4.1 Introduction

In contrast with electrolytes used for direct detection, where the separation current is the sole limiting factor which determines the upper electrolyte concentration limit, the background absorbance of the electrolyte becomes an additional limiting factor of the probe concentration in indirect detection with highly absorbing probes. For reliable quantitative results, the background absorbance must remain within the linear range of the detector. Hence there is a clear need to know the detector linearity and as most manufacturers do not give reliable data, it has to be determined experimentally.

A number of approaches to determine detector linearity are possible [1-4]. However, it has been shown [1] that the best method of evaluating the linearity is by carefully measuring the response (absorbance) caused by a series of known probe concentrations so that the sensitivity (response/concentration) can be calculated. A plot of sensitivity *versus* concentration can then be constructed to show when the detector linearity limit is reached, usually by determining the concentration at which the sensitivity falls below its maximum value by a defined amount (such as a 5% decline from maximum sensitivity). This approach shows more clearly when the detector linearity is exceeded than by estimating when a simple plot of absorbance *versus* concentration begins to deviate from a straight line [5]. Importantly, the plot of sensitivity *versus* absorbance is strictly an instrumental characteristic which should be independent of the absorptivity of the probe, thereby eliminating any need for further linearity measurements for different probes. Such plots can also offer useful comparisons on detector performance in different instruments by providing information on sensitivity and linearity between various detectors and instruments and an estimate of effective pathlength can also be

calculated. A comparison of the detection sensitivity achieved with various probes can also be gained by this technique.

Unlike in spectrophotometry using rectangular cells and collimated light where all pathlengths are equal, in cells possessing a variety of possible individual pathlengths, such as a cylindrical cell in on-capillary detection in CE, an effective pathlength is defined as the single pathlength of a hypothetical rectangular cell which would yield the same absorbance as that measured through the illuminated part of the cylindrical cell [4]. Effective pathlength is dependent on the geometry of the light beam incident on the capillary window. The effective pathlength would equal the capillary inner diameter if only the centre of the capillary would be illuminated and the ray of a collimated beam could travel through the full length of the inner diameter of the capillary. For beams further away from the central axis, the distance travelled through the capillary will be shorter and finally approach zero for a ray travelling through the fused silica capillary but outside the inner channel of the capillary.

Consider the situation as illustrated in Figure 4-1 . A ray of light which passes exactly through the centre of the capillary (R_1) will have a pathlength equal to the ID of the capillary. A ray of light which passes through the capillary slightly off-centre (R_2) will have a pathlength slightly less than the capillary ID. The pathlength will become progressively shorter as the ray of light passes through the capillary further off-centre (R_3). Depending on the optics design, it is also possible for non-parallel light beams to pass through the capillary (R_4). The individual pathlengths will combine to produce an effective pathlength, which ideally would be equal to but in reality will be always less than the capillary ID. Depending on the width of the aperture defining the illuminated part of the capillary, all those individual pathlengths will combine to produce the final effective pathlength. In reality, the effective pathlength will be always smaller than the inner capillary diameter.

Bruin *et al.* [4] presented a theoretical model for calculation of the effective pathlength, which may be useful for approximate estimations. However, this model is based on parallel light beams passing through the cylindrical capillary and this model is therefore not applicable to detectors used in practice. Therefore, it is desirable to have an experimental method for the determination of effective pathlength. Macka *et al.* [1] fitted curves to experimentally measured sensitivity plots and derived the effective pathlength and the level of stray light from the fitted curves. Whilst this method would be optimal for detectors exhibiting very poor linearity, it is very time consuming. Therefore it is proposed here to use a simple and fast method, based on a calculation of the effective path length for a known probe absorptivity and the measured sensitivity in the linear range of the detector.

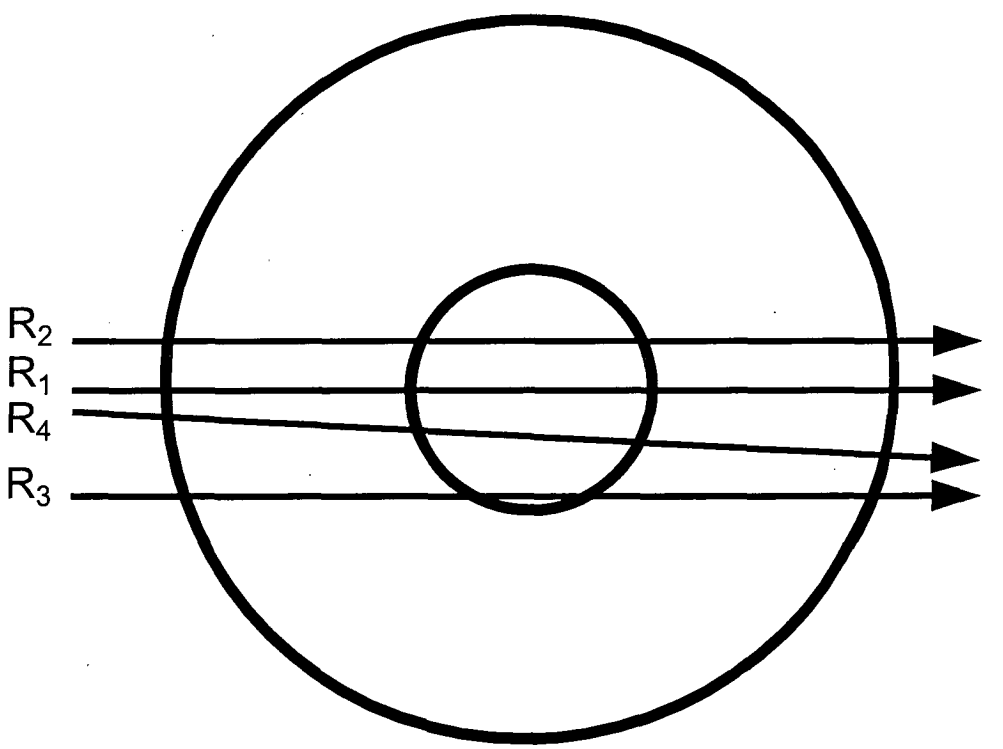

Figure 4-1 Illustration of possible pathlengths through a capillary

4.2 Experimental

4.2.1 Instrumentation

The general experimental details are given in Chapter 2.

Absorbance measurements were recorded on four different CE instruments. These were Applied Biosystems 270A-HT, Waters Capillary Ion Analyser, Agilent Technologies ^{3D}CE and P/ACE System MDQ (Beckman Instruments Inc., Fullerton, CA, USA). The Applied Biosystems 270A-HT was fitted with a deuterium lamp with variable wavelength detection. The Waters CIA was fitted with a deuterium lamp with detection at 254 nm. The Agilent Technologies ^{3D}CE was fitted with a deuterium lamp with a photodiode array detector. A blue alignment interface designed for use with 75 μm ID capillaries was used for this work. An Agilent High Sensitivity Detection Cell and Extended Light Path Capillary were also used with this instrument. The P/ACE System MDQ was used with two different detection systems, a deuterium lamp with a fixed filter at 254 nm used for UV measurements, and a 256 element diode array photodiode array detector. A 100 x 800 μm slit width aperture was used with both systems.

A new capillary for each instrument was cut to suitable length from a 60 m spool of fused silica capillary of 75 μm ID, 365 μm OD. For the High Sensitivity Detection Cell an inlet capillary of 40 cm and an outlet capillary of 8.5 cm were cut and a small portion of polyimide coating was burned from the end of both capillaries using a butane torch. The capillaries were installed and aligned into an Agilent High Sensitivity Detection Cell as recommended. The assembled cell was installed into a cassette and was inserted into the instrument. A 50 μm ID Extended Light Path Capillary with a bubble factor of 3 (optical pathlength of 150 μm) (Agilent Part # G1600-61232) was installed into a red capillary interface as recommended. The different instrumental configurations are listed in Table 4-1 and for convenience in this chapter are referred to as Instruments 1-7.

Table 4-1 Instrumental configurations

Instrument No.	Instrument brand
1	Agilent Technologies ^{3D}CE
2	Applied Biosystems 270A-HT
3	Waters CIA
4	Beckman MDQ PDA
5	Beckman MDQ UV
6	Agilent ^{3D}CE with High Sensitivity Detection Cell
7	Agilent ^{3D}CE with Extended Light Path Capillary

4.2.2 Reagents

Sodium chromate was used to prepare a series of aqueous chromate standard solutions. Tartrazine was purified as detailed in Chapter 3.2.2 and was used to prepare a series of tartrazine standards.

4.2.3 Procedures

A series of standards was prepared by serial dilution by a factor of two of a stock solution. Chromate standards were prepared in 50 mM sodium hydroxide to ensure the presence of chromate rather than dichromate. Absorbance measurements at 254 nm (chromate) or 426 nm (tartrazine) were performed by flushing the capillary with water or the desired standard solution (approx. 10 capillary volumes), then stopping the flow and measuring the absorbance under static conditions. The absorbance of each test solution was measured in triplicate. Absorbances of standard solutions were measured in order of increasing concentration to minimise possible carry-over errors.

4.3 Results and Discussion

4.3.1 Evaluation of Instruments Fitted With a 75 μm ID Capillary

Sensitivity data were calculated from the measured absorbances recorded with the five instruments fitted with a 75 μm ID capillary (Instruments 1-5, see Table 4-1) and plotted against chromate concentration, as shown in Figure 4-2. The concentration at which sensitivity declined by more than 5% was used to define the upper limit of detector linearity. From Figure 4-2 it can be seen that Instrument 1 provided the highest sensitivity and greatest linearity. Linearity (at 95% of maximum sensitivity) was maintained up to a concentration of ~80 mM, far in excess of the typical background electrolyte of 5 mM chromate used for indirect detection. An even more universal comparison of the instruments and their detector linearity can be gained by plotting sensitivity *versus* absorbance (Figure 4-3). This plot is independent of the absorptivity of the probe and the detection wavelength. Detector linearity upper limits for each instrument are recorded in Table 4-2. For Instrument 1 linearity was maintained up to 1.2 AU. It should be pointed out that the linearity limits for all instruments exceed background absorbances typically used (~0.1 AU) for indirect detection in capillary electrophoresis when using moderately absorbing probes such as chromate, the concentration of which is limited by the separation current.

Table 4-2 Detector linearity upper limits

Instrument No.	Instrument brand	Detector linearity upper limit (AU)
1	Agilent Technologies ^{3D}CE	1.2
2	Applied Biosystems 270A-HT	0.75
3	Waters CIA	0.175
4	Beckman MDQ PDA	0.55
5	Beckman MDQ UV	0.30

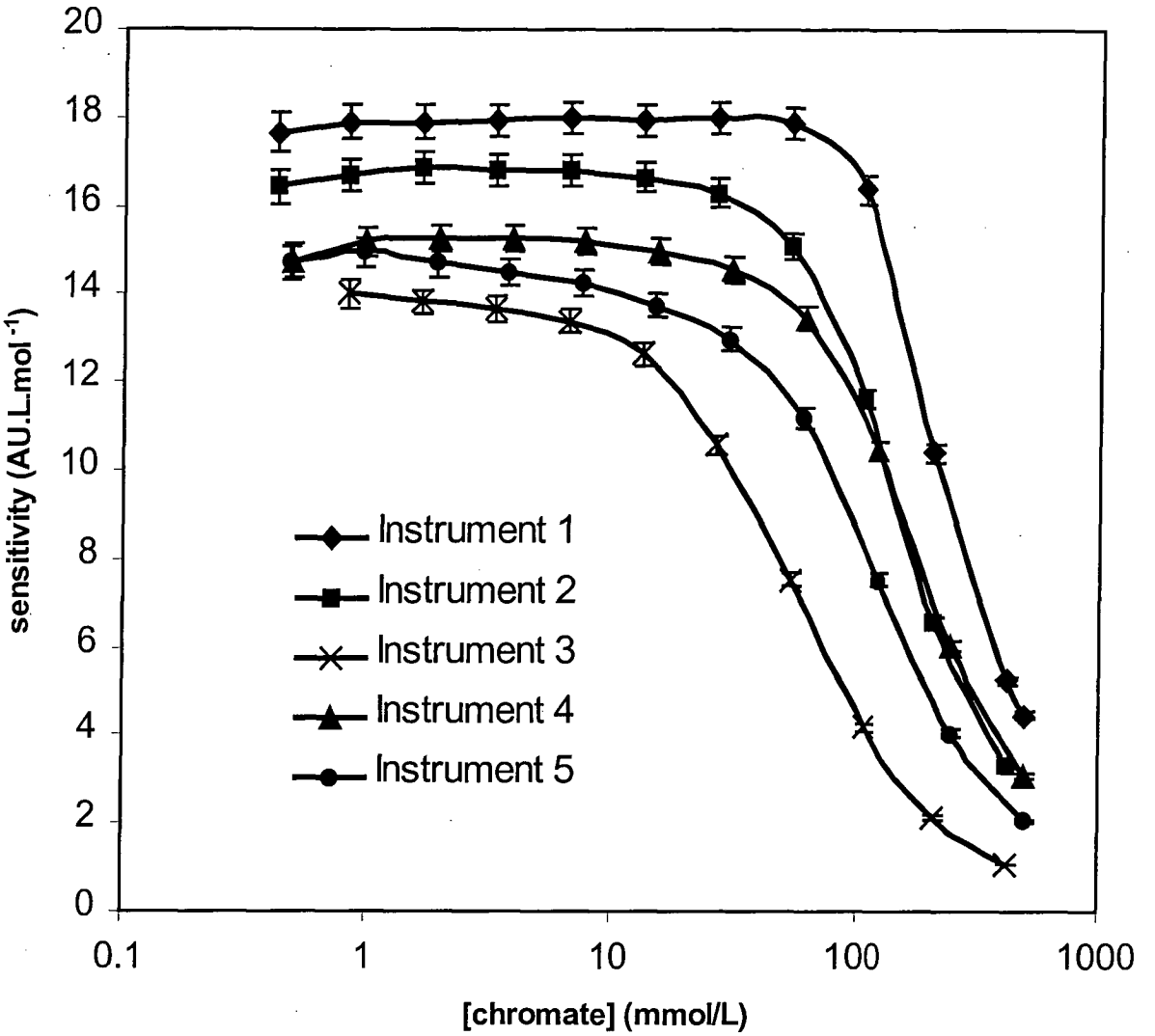

Figure 4-2 Sensitivity *versus* concentration plots for chromate at 254 nm.

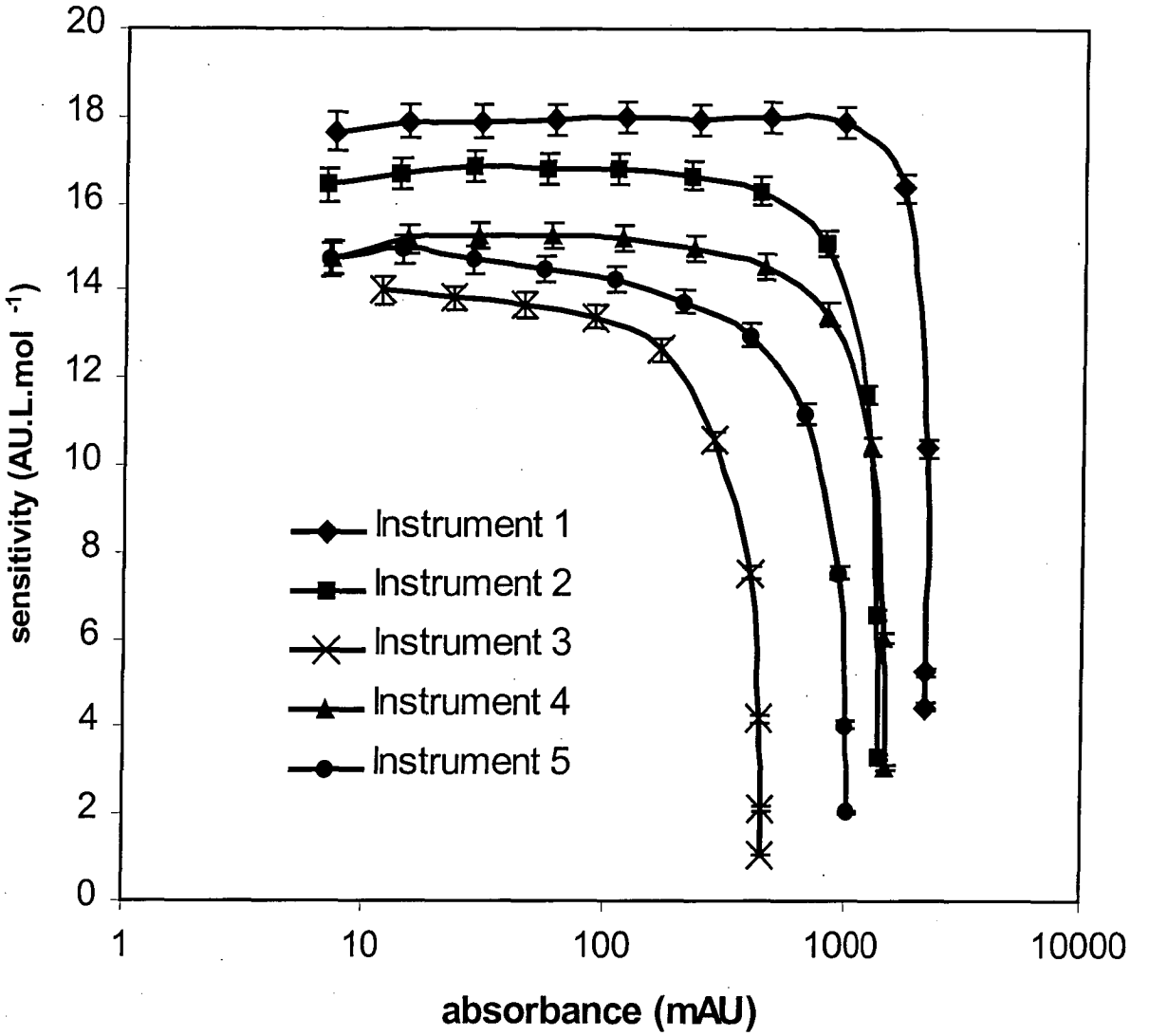

Figure 4-3 Sensitivity *versus* absorbance plots for chromate at 254 nm.

The use of highly absorbing probes, such as dyes, to improve sensitivity has been well documented [6]. Measurement of detector linearity using a highly absorbing probe such as tartrazine (ε = 21600 $L.mol^{-1}$ cm^{-1}at 426 nm, pH=8 see Chapter 3.3.1) can illustrate the increased sensitivity of such probes and also provide a guide to the concentration at which they should be present in the background electrolyte. It is desirable that the probe be present at as high a concentration as possible so that the calibration plot for analytes can be extended and also to provide significant benefits in gaining better sample stacking upon sample injection. However, this then leads to potential problems of calibration linearity if the background absorbance of the electrolyte exceeds the limit for detector linear range. A plot of sensitivity *versus* absorbance for tartrazine on Instruments 1 and 2 is shown in Figure 4-4, along with chromate data for the same instruments. This plot demonstrates two important features. First, it highlights that tartrazine is significantly more sensitive (about 7 times higher) than chromate and this translates into improved detection limits (see Chapter 3). Second, detector linearity followed the same trend as evident from the chromate data, with sensitivity decreasing at approximately the same absorbance. This shows that detector linearity was independent of the probe, which means that the detector linearity can be characterised by the measurement of just one probe. The concentration of a different probe required to produce this absorbance can then be easily determined. A tartrazine concentration of 8 and 6 mM can be used with Instruments 1 and 2, respectively, while still retaining 95% of the maximum sensitivity and remaining in the linear range of the detector.

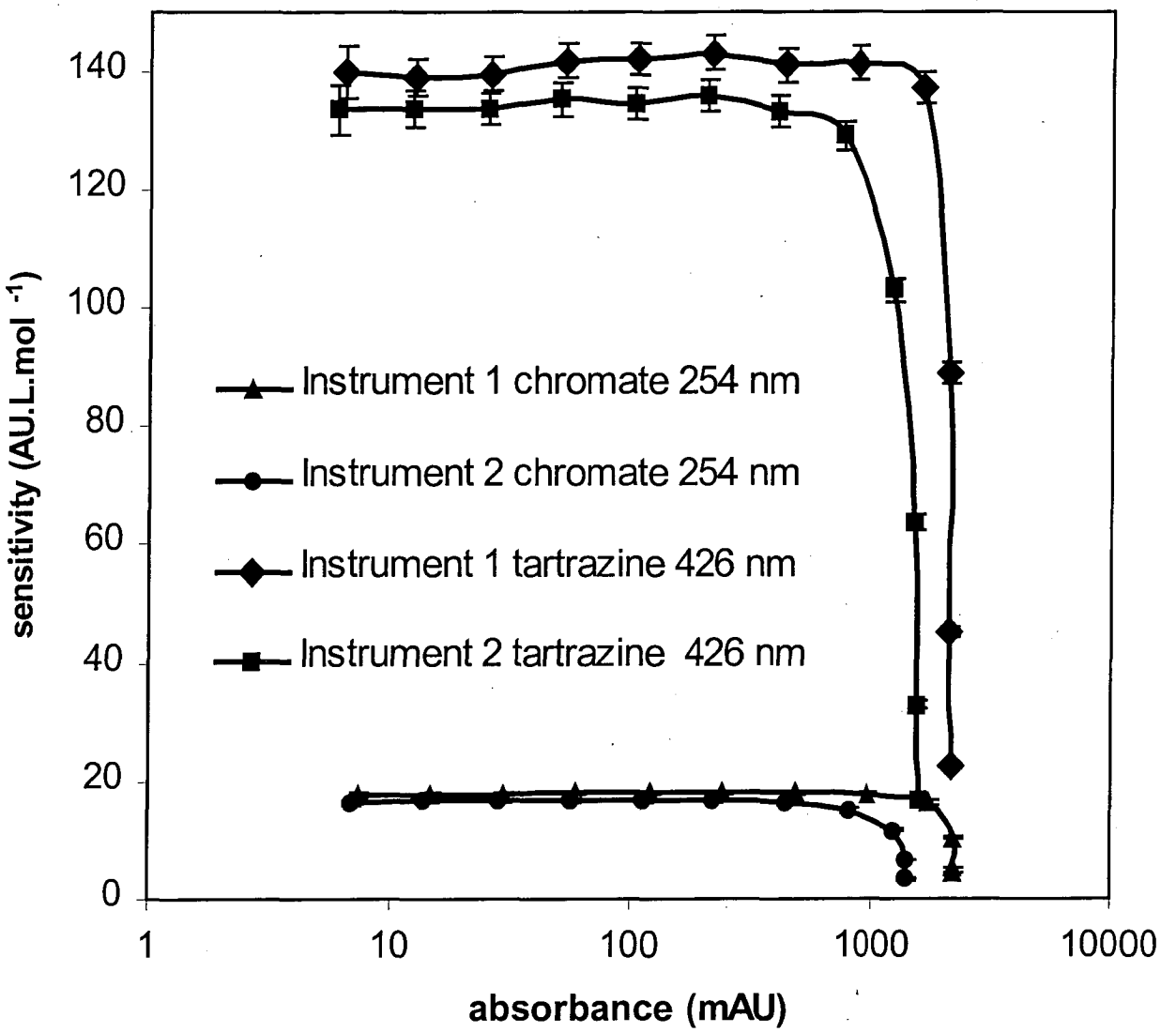

Figure 4-4 Sensitivity *versus* absorbance plots for chromate at 254 nm and tartrazine at 426 nm

Effective pathlengths were calculated by rearranging the Beer-Lambert law to give the ratio of sensitivity to probe absorptivity.

From the Beer-Lambert law:

$$A = \varepsilon c \ell \tag{4.1}$$

where A = absorbance, ε = absorptivity, c = concentration, and ℓ = pathlength,

can substitute sensitivity $\left(S = \frac{A}{c} \right)$ into (4.1) to give

$$S = \varepsilon \ell \tag{4.2}$$

Rearranging for ℓ gives

$$\ell = \frac{S}{\varepsilon} \tag{4.3}$$

which can be easily calculated from the measured sensitivity and probe absorptivity.

The sensitivity value chosen was at an absorbance of ~0.05 AU, which is well inside the linear range of all five instruments. It is vital that such a calculation is performed in the linear absorbance range to provide a true estimate of the effective pathlength. This highlights the importance of knowing the detector linearity range. Observed effective pathlengths ranged from 49.7 μm (Instrument 3) to 64.6 μm (Instrument 1) for a capillary of 75 μm ID (Table 4-3). Effective pathlength can be used to judge and compare the quality of the detector optics. Most importantly, it is well known that detection pathlength inhomogeneity, similarly to incident light wavelength inhomogeneity (polychromatic light), will result in detector non-linearity [7]. This effect will cause a departure from linearity across the whole absorbance range, also affecting the low-absorbance region, in contrast to stray light which mostly affects the high-absorbance regions [1, 7]. It is important to note that this method of measurement of effective pathlength does not need any prior knowledge of the detector geometry and

it allows a general judgment on the geometry based on the determined effective pathlength value. Finally, it should be pointed out that as different detectors used with one same capillary will produce different linearity and effective pathlength values, different capillary diameters (both ID and OD would play a role) will result in somewhat different linearity values and, of course, in different pathlength values. It can be generally anticipated that smaller capillary diameters will result in relatively poorer photometric detection.

Table 4-3 Effective pathlengths of instruments fitted with 75 μm ID capillary

Instrument No.	Instrument brand	Detector linearity upper limit (AU)	Effective pathlength (μm)
1	Agilent Technologies ^{3D}CE	1.20	64.6
2	Applied Biosystems 270A-HT	0.75	60.5
3	Waters CIA	0.175	49.7
4	Beckman MDQ PDA	0.55	54.9
5	Beckman MDQ UV	0.30	53.6

4.3.2 Evaluation of Unusually Shaped Detection Cells

Irregularly shaped cells such as bubble cells, Agilent Extended Light Path Capillaries [8] and z cells are used in capillary electrophoresis in order to increase optical pathlength and hence detection sensitivity. Significant improvements in detection limits have been reported, particularly for the analysis of biologically important substances. Mrestani and Neubert have used an Agilent High Sensitivity Detection Cell for the detection of anti-tumour chemotherapeutic agents (etoposide phosphate and methotrexate) [9]. Detection limits were improved ten-fold compared with a normal 75 μm capillary. The same authors [10] also achieved a nine-fold improvement in detection limits of thiamine in plasma, urine and saliva with the use of an Agilent High Sensitivity Detection Cell compared with a 75 μm capillary. The use of an Agilent Extended Light Path Capillary with optical pathlength 150 μm also provided enhanced sensitivity. The determination of meroprenem in biological samples using an Agilent

High Sensitivity Detection Cell has also been reported [11]. Desiderio et al. [12] have also employed an Agilent High Sensitivity Detection Cell for the determination of fluoxetine and norfluoxetine in serum and plasma samples. The use of an Agilent High Sensitivity Detection Cell and Extended Light Path Capillary resulted in a ten and three-fold improvement respectively in detection limits compared with a normal 75 μm capillary. A mixed-backbone oligonucleotide (GEM 231) has been determined in tumour and liver tissues using an Extended Light Path Capillary [13]. The authors reported a detection limit of 100 pg and a linear range of 1-1000 μg/mL. Mycophenolic acid, used as an immunosuppressant after organ transplantation, has been quantified in plasma samples [14] using a bubble cell. Doble *et al.* [15] reported only a three-fold improvement in detection limits of strong acid anions when a Z cell of 3 mm optical pathlength was used in conjunction with indirect detection, illustrating the fact that although increasing the detection pathlength brings large S/N gains in direct detection, this approach yields in only moderate increase in S/N in indirect detection, as with increasing the pathlength the noise grows significantly as well.

The Agilent High Sensitivity Detection Cell is a decoupled detection cell consisting of silica parts, which are fused together to create the detection cell [16]. A black fused silica body effectively minimises stray light. The Extended Light Path Capillary has an increased ID at the detection window in a shape of a 'bubble'. This leads to a combination of the sensitivity of a wide ID capillary without the associated increase in separation current. Detector linearity and effective pathlength of detection cells with unusual geometries, such as the Agilent High Sensitivity Detection Cell and Agilent Extended Light Path Capillary, can be easily evaluated using this approach

Sensitivity data were collected in the same fashion as for 75 μm ID capillaries using a series of chromate standards with an Agilent ^{3D} CE fitted with an Agilent High Sensitivity Detection Cell (Instrument 6) and an Extended Light Path Capillary (Instrument 7). Sensitivity for both detectors was much higher than when normal, straight walled capillaries were used. From Figure 4-5 it can be seen linearity for the

Extended Light Path Capillary (at 95% of maximum sensitivity) was maintained up to an absorbance of 1490 mAU. The High Sensitivity Detection Cell maintained 95% of maximum sensitivity up to an absorbance of 2190 mAU (Figure 4-6). Previous work has claimed an absorbance of more than 2000 mAU can be reached with less than 3% deviation from linearity [16]. This is consistent with the results found in this study.

An advantage of this approach is that an estimate of the effective pathlength of cells with unusual geometry can be made. It is interesting to calculate the effective pathlengths of irregularly shaped detection cells such as the Extended Light Path Capillary and High Sensitivity Detection Cell. The High Sensitivity Detection Cell has been claimed to have a pathlength of 1200 μm [16]. This is similar to the experimentally determined figure of 1068 μm. The Extended Light Path Capillary has a pathlength of 150 μm and an effective pathlength of 128 μm.

Table 4-4 Detector linearity limits and effective pathlengths of increased pathlength cells

Instrument No.	Instrument brand	Detector linearity upper limit (AU)	Effective pathlength (μm)
6	Agilent ^{3D}CE with High Sensitivity Detection Cell	2.19	1068
7	Agilent ^{3D}CE with Extended Light Path Capillary	1.49	128

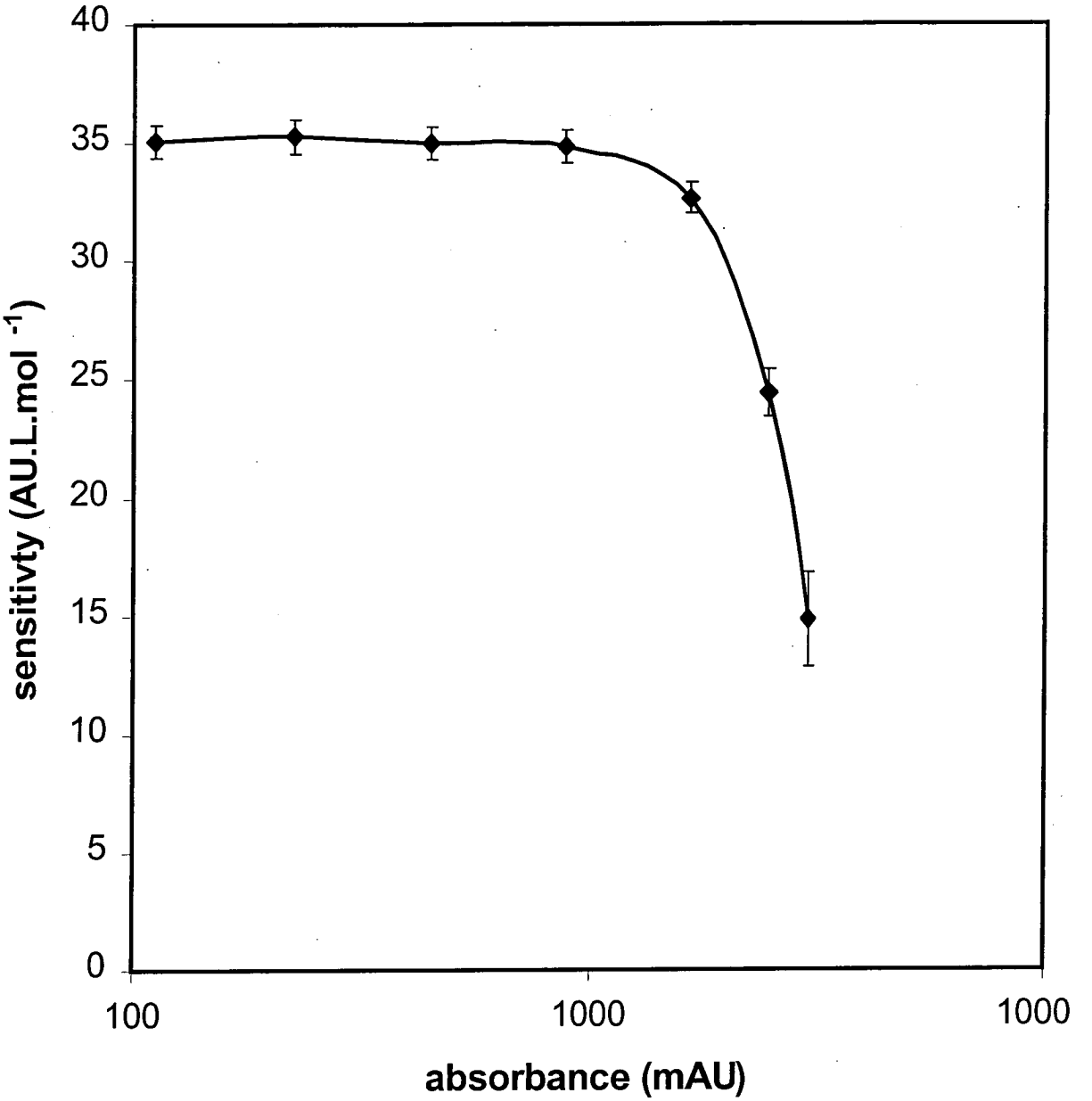

Figure 4-5 Sensitivity *versus* absorbance plot for Agilent ^{3D}CE fitted with an Extended Light Path Capillary.

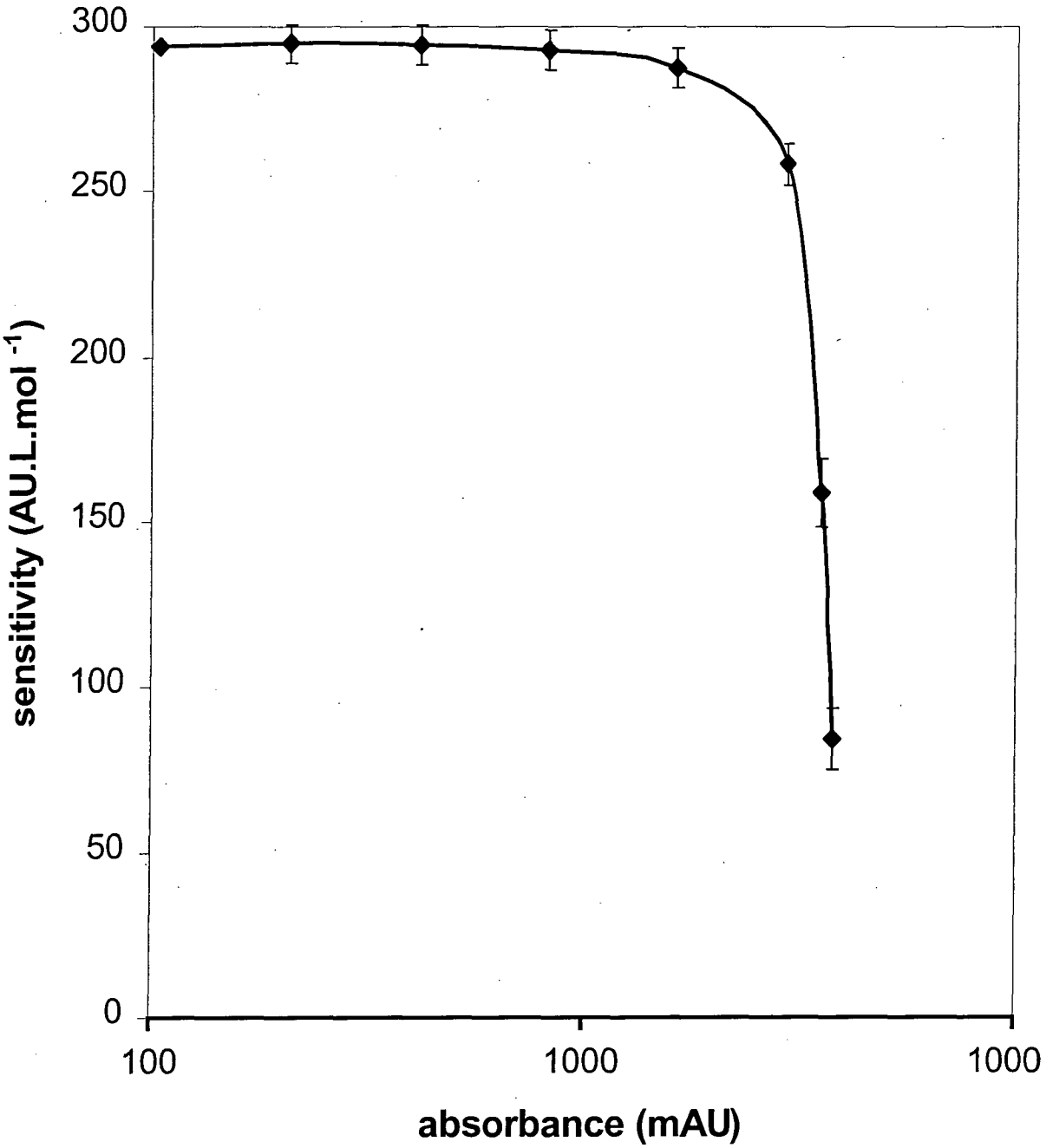

Figure 4-6 Sensitivity *versus* absorbance plot for Agilent ^{3D}CE fitted with High Sensitivity Detection Cell.

4.4 Conclusions

The evaluation of detector linearity in capillary electrophoresis instruments provides vital information regarding the upper linearity limit of the instrument, the sensitivity of probes used for indirect detection, and the maximum concentration at which a probe may be used in background electrolytes. From this work it can be clearly seen that some instruments have superior optical properties which can lead to improved results. To demonstrate this approach, unusually shaped detection cells such as the Agilent High Sensitivity Detection Cell and Extended Light Path Capillary have also been evaluated. Particularly when using highly absorbing probes that can lead to electrolytes with high background absorbance values, it is crucial to know the detector characteristics so that background electrolyte concentrations of most probes can be markedly increased whilst still working in the linear range of the detector. This is particularly important for highly absorbing probes, the concentration of which is limited by the background absorbance rather than by the separation current. Increasing the background electrolyte concentration of such a probe is essential for gaining better sample stacking. The effective pathlength is another important instrumental parameter which is determined quickly and easily from the approach described in this work. In addition, judgements can be made on the quality of detector optics of on-capillary absorbance detectors and the concentration of the probe used for indirect detection methods can be optimised.

4.5 References

1 M. Macka, P. Andersson and P.R. Haddad, *Electrophoresis*, **17** (1996) 1898.

2 Y. Walbroehl and J.W. Jorgenson, *J. Chromatogr.*, **315** (1984) 135.

3 A.E. Bruno, E. Gassmann, N. Pericle and K. Anton, *Anal. Chem.*, **61** (1989) 876.

4 G.J.M. Bruin, G. Stegeman, A.C. van Asten, X. Xu, J.C. Kraak and H. Poppe, *J. Chromatogr.*, **559** (1991) 163.

5 R. Cassidy and M. Janoski, *LC-GC*, **10** (1992) 692.

6 P. Doble, M. Macka and P.R. Haddad, *J. Chromatogr.* A, **804** (1998) 327.

7 J.D. Inge and S.R. Crouch, Spectrochemical Analysis, Prentice Hall, Englewood Cliffs, 1988, pp. 379-380.

8 D.N. Heiger, P. Kaltenbach and H-J. P. Sievert, *Electrophoresis,* **15** (1994) 1234.

9 Y. Mrestani and R. Neubert, *Electrophoresis,* **19** (1998) 3022.

10 Y. Mrestani and R. Neubert, *J. Chromatogr. A*, **871** (2000) 351.

11 Y. Mrestani, R. Neubert and F. Nagel, *J. Pharm. Biomed. Anal.*, **20** (1999) 899.

12 C. Desiderio, S. Rudaz, M.A. Raggi and S. Fanali, *Electrophoresis,* **20** (1999) 3442.

13 R. Bansal, H.X. Chen, J.L. Marshall, J. Tan, R.I. Glazer and I.W. Wainer, *J. Chromatogr. B,* **750** (2001) 129.

14 S. Unsalan, G. Hempel, J. Boos and G. Blachke, *Chromatographia,* **54** (2001) 635.

15 P. Doble, M. Macka and P.R. Haddad, *J. Chromatogr. A,* **804** (1997) 327.

16 Agilent Technologies Technical Note, Agilent Publication No. 12-5965-5984E.

Chapter 5

Optimisation of Probe Concentration in Indirect Photometric Detection in Capillary Electrophoresis Using Highly Absorbing Dyes

5.1 Introduction

It has been demonstrated [1, 2] that the simplest and most effective means of improving detection sensitivity is to increase the probe absorptivity (ε) by using a strongly absorbing probe ion, such as a dye. However, this has generally meant that the highly absorbing probe is added to the BGE in much lower concentrations than less absorbing probes in order to maintain a similar background absorbance. Low probe concentrations restrict the analyte concentration range which can be injected before destacking, dispersion and peak broadening occur. This problem cannot be overcome by the simple expedient of increasing the ionic strength of the BGE through the addition of a suitable electrolyte since this would introduce additional co-ions which would reduce the effectiveness of the indirect detection process by competition with the probe. The BGE concentration of less absorbing probes is generally limited by the conductivity of the solution and the resultant separation currents when voltages are applied. Excessive currents and subsequent Joule heating adversely affect the efficiency and sensitivity of a separation. High separation currents are unlikely to be reached when using strongly absorbing probes because the detector linearity is likely to be exceeded before maximum acceptable currents will be reached.

Examination of the literature reveals that when the detector linearity characteristics are unknown the BGE concentrations of highly absorbing probes are often set at arbitrary values of 0.1-1 mM in order to provide similar background absorbances to traditionally used indirect detection BGEs, such as 5 mM chromate. In Chapter 4, it was shown that many detectors maintain linear response (up to 95% of maximum sensitivity) at absorbances far exceeding the 0.1-0.2 AU values used regularly. This presents the possibility of increasing the probe concentrations by up to an order of magnitude, which

should lead to a combination of high sensitivity, ruggedness, greater analyte calibration linearity and improved peak shapes and stacking. Benefits such as these may make indirect photometric detection with highly absorbing probes at increased concentrations more attractive for the analysis of real samples requiring high sensitivity and the ability to handle high ionic strength matrices. However, a further practical factor which must also be considered when selecting the BGE concentration of the probe is the fact that some probes tend to adsorb onto the fused silica capillary wall, resulting in baseline fluctuations and increased noise [3, 4]. Therefore, the probe concentration may need to be carefully optimised not only with regard to background absorbance and detector linearity, but also the baseline stability and noise.

In this chapter the beneficial effects arising from the use of higher probe concentrations are investigated in cases where the probe has a high absorptivity. The dye tartrazine has been used as probe in a BGE buffered with histidine in order to eliminate extraneous co-ions and therefore to maximise detection sensitivity. The purpose of this study has been to demonstrate that careful optimisation of the probe concentration is necessary in order to improve sample stacking which in turn will lead to improved peak shapes, resolution and sensitivity over a greater range of analyte concentration range.

5.2 Experimental

5.2.1 Instrumentation

The capillary electrophoresis instrument used during this work was an Applied Biosystems 270A-HT. A voltage of +30 kV was applied during all separations, with temperature maintained at 25° C.

5.2.2 Calculations

Resolution between adjacent peaks was calculated using the following formula adapted from [5]:

$$R_{s(i,i+1)} = \left(\frac{t_{i+1} - t_i}{b_i + a_{i+1}} \right) \tag{5-1}$$

where t_{i+1} and t_i are migration times of peaks i+1 and i respectively, b_i is the distance in time from t_i to the following edge of peak i at 10% of peak height and a_{i+1} is the distance in time from t_{i+1} to the leading edge of peak i+1 at 10% of peak height. Resolution product R is given by the formula:

$$R = \prod_{i=1}^{n-1} R_{s(i,i+1)} \tag{5-2}$$

where n is the number of peaks.

5.3 Results and Discussion

5.3.1 Limitations on Probe Concentration

The maximum probe concentration for an absorbing probe is in principle limited by two factors: separation current and background absorbance of the BGE. Limiting current values are typically estimated as the value at which a plot of current *versus* BGE concentration begins to deviate from linearity. Limiting background absorbances can be determined using the approach wherein sensitivity (absorbance/probe concentration) is measured for a range of varying probe concentrations and then plotted *versus* absorbance. The absorbance at which sensitivity drops below 95% of its maximum value is defined as the detector linearity limit. It is instructive to now consider a typical detector with a linearity limit of 0.2 AU and an effective path length of 55 μm. For less absorbing probes (absorptivity < 2,000 $L.mol^{-1}\ cm^{-1}$), a concentration of 18 mM can be used before the limiting absorbance of 0.2 AU is reached. However, excessive Joule

heating (deviation from linearity in a plot of current *versus* concentration) is likely to occur before such a concentration is reached, hence the conductivity of the electrolyte determines the maximum concentration at which such a probe may be used. In contrast, a highly absorbing probe (absorptivity > 20,000 $L.mol^{-1}$ cm^{-1}) will reach the limiting background absorbance of 0.2 AU at a concentration of 1.8 mM, well before the limiting current is reached. Clearly, the maximum concentration of such a highly absorbing probe is dependent on detector linearity limitations rather than current limitations, and therefore the detector linearity limit needs to be known. From previous work (Section 4.3.1), it has been shown that the detector linearity limit for the detector used in this work (Applied Biosystems 270A-HT) is 0.75 AU, which corresponds to a tartrazine concentration of 6 mM. A plot of tartrazine concentration *versus* current at 30 kV showed linearity (R^2= 0.9997) over this concentration range, showing that current limitations were not exceeded. Hence 6 mM was set as the maximum allowable tartrazine concentration.

5.3.2 Choice of Model BGE System

The highly absorbing anionic dye tartrazine (see Figure 3-1) has been previously used as an anionic probe in Chapter 3 and also to evaluate detector linearity in Chapter 4. A BGE consisting of tartrazine and the isoelectric ampholytic buffer histidine was used as a model electrolyte during this work. It has been shown in earlier work in Chapter 3 that the reversal of electroosmotic flow (EOF) with a cationic surfactant to provide co-EOF separation of anions is not possible due to the formation of a tartrazine-surfactant precipitate when commonly used EOF modifiers such as tetradecyltrimethylammonium bromide (TTAB) and cetyltrimethylammonium bromide (CTAB) were used. To provide the fastest possible separations of anions using negative polarity at the injection end, the EOF was suppressed by the addition to the BGE of 0.05% hydroxypropyl methyl cellulose (HPMC).

Under these BGE conditions, the use of tartrazine at higher concentrations was found to present the additional problem of unstable baselines due to adsorption of tartrazine onto the capillary wall, even in the presence of HPMC. Yeung and Lucy [6] have used the

zwitterionic surfactant Rewoteric AM CAS U to minimise adsorption of cationic proteins onto the capillary wall and also to suppress EOF. In the present system, addition of 3 mM of the zwitterionic surfactant *N*-dodecyl-*N,N*-dimethylammonio-3-propanesulfonate (SB-12) (c.m.c. 3.3 mM) to the BGE provided a stable baseline for tartrazine concentrations up to 5 mM. However, the EOF was not suppressed (μ_{EOF} = $74x10^{-9}$ $m^2 V^{-1} s^{-1}$), even when the concentration of SB-12 was increased above 3 mM. Nevertheless, these BGE conditions allowed the detection of analyte anions having electrophoretic mobilities less than $-54x10^{-9}$ $m^2 V^{-1} s^{-1}$ within 10 min using a counter-EOF separation under positive voltage. Such a mobility range for analyte anions is suited ideally to the use of tartrazine as a probe as it has a similar electrophoretic mobility ($-45.4x10^{-9}$ $m^2 V^{-1} s^{-1}$) and therefore provides well-shaped peaks. Analyte anions of higher mobility could not be separated and detected using this approach, but their determination would be better suited to the use of a probe having a higher mobility than tartrazine. Hence for all further work in this study, BGEs consisted of 10 mM histidine at pH 7.7, 3 mM SB-12 zwitterionic surfactant, and the desired concentration of tartrazine.

5.3.3 Optimisation of Tartrazine Concentration

Tartrazine has absorption maxima at 258 and 426 nm, with absorptivities of 22,465 and 21,600 $L.mol^{-1}.cm^{-1}$ respectively. A series of BGEs with tartrazine concentrations ranging from 0.5 to 5 mM were prepared and baseline noise at the two absorption maxima was measured (Figure 5-1). Detection at 258 nm provided the lowest noise as a result of the intensity spectral characteristics of the deuterium lamp light source, which emits much less light at 426 nm than 258 nm. Further work was conducted with indirect detection at 258 nm.

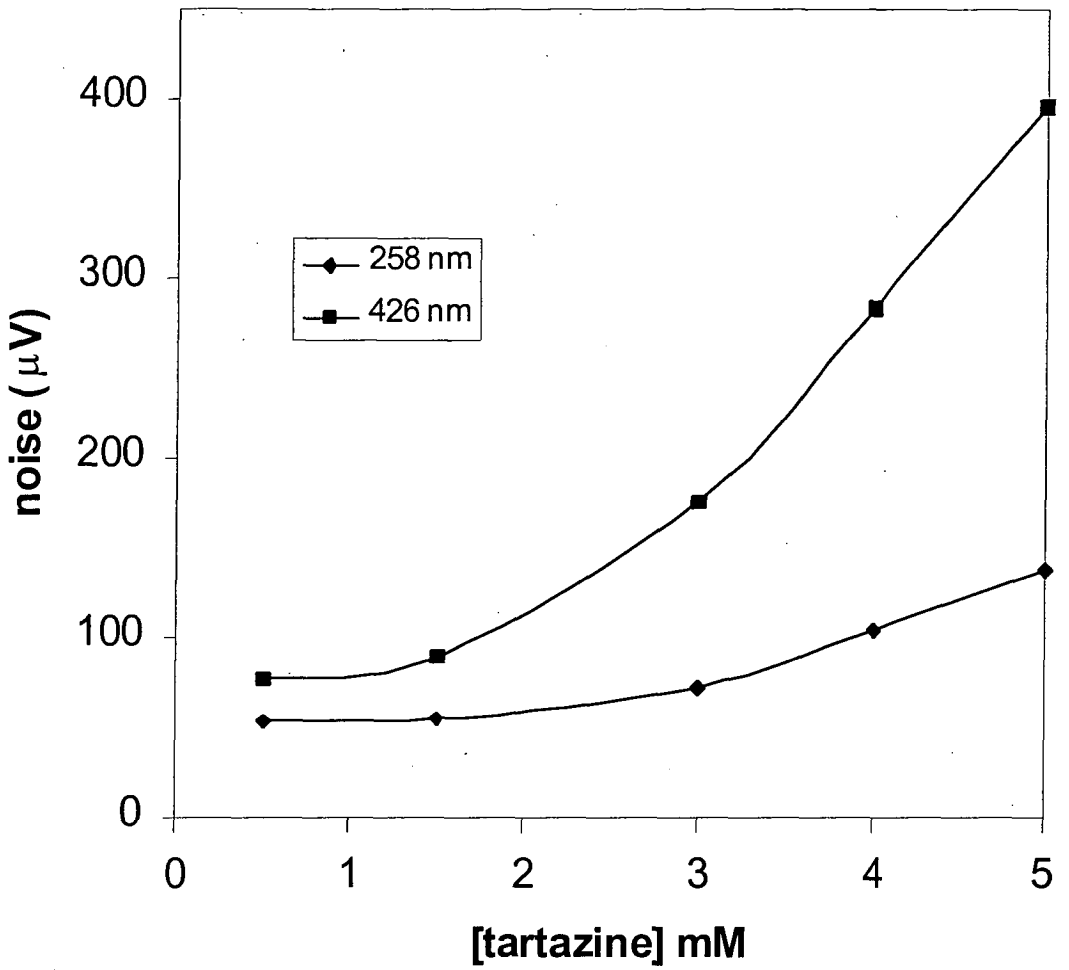

Figure 5-1 Baseline noise *versus* tartrazine concentration at 258 and 426 nm. Conditions-electrolyte: varying tartrazine concentration, 10 mM histidine, 3 mM SB-12 zwitterionic surfactant, pH 7.70, detection: 258 and 426 nm.

A standard mixture of 25 μM C_1-C_8 alkanesulfonates was used as a test sample to determine the optimal BGE concentration of tartrazine which maintained high indirect detection sensitivity whilst using the highest possible tartrazine concentration to extend the linear calibration range. Tartrazine is well suited to the analysis of low to medium mobility analytes, such as those included in the test mixture. Separations were undertaken at varying tartrazine concentration and individual peak heights and baseline noise were measured. A plot of signal to noise ratio *versus* tartrazine concentration (Figure 5-2) shows that the optimal range was 1.5-3 mM tartrazine, with any increases in peak heights at concentrations higher than this range being offset by the accompanying increase in baseline noise. An optimal tartrazine concentration of 3 mM was chosen as a compromise between achieving highest sensitivity and maintaining the probe concentration as high as practicable. This BGE gave a background absorbance of 410 mAU, which was within the detector linearity limit of the detector (Figure 5-3).

5.3.4 Comparison of 0.5 mM and 3 mM Tartrazine BGEs

A test mixture of methanesulfonate, ethanesulfonate, butanesulfonate and octanesulfonate was used to compare the responses of BGEs containing 0.5 mM and 3 mM tartrazine at various concentrations of the analytes. Samples containing 0.1-12.5 mM of each analyte were analysed using both electrolytes, with peak widths at 10% of peak height and migration times being recorded. Resolution data were calculated using Eqn.'s (5-2) and (5-3) and are plotted in Figure 5-4. The initial resolution product was 8 (approx $R_s = 2$ for each adjacent peak pair) for very dilute samples, but this value decreased rapidly for more concentrated samples when the 0.5 mM tartrazine BGE was used. This BGE could tolerate a mixture concentration of only 0.5 mM before peak shapes deteriorated and resolution was decreased. On the other hand, the 3 mM tartrazine BGE permitted a mixture concentration of 3 mM to be used without any deleterious effects on resolution. Moreover, this BGE showed much less marked loss of resolution for higher sample concentrations than did the 0.5 mM tartrazine BGE. An excellent example is the analysis of a 5mM solution as shown in Figure 5-6 . All peaks are clearly resolved with the use of the 3 mM BGE and peak heights are significantly larger. In general, peaks at higher analyte concentrations were approximately twice as high with the 3 mM BGE compared to the 0.5 mM BGE.

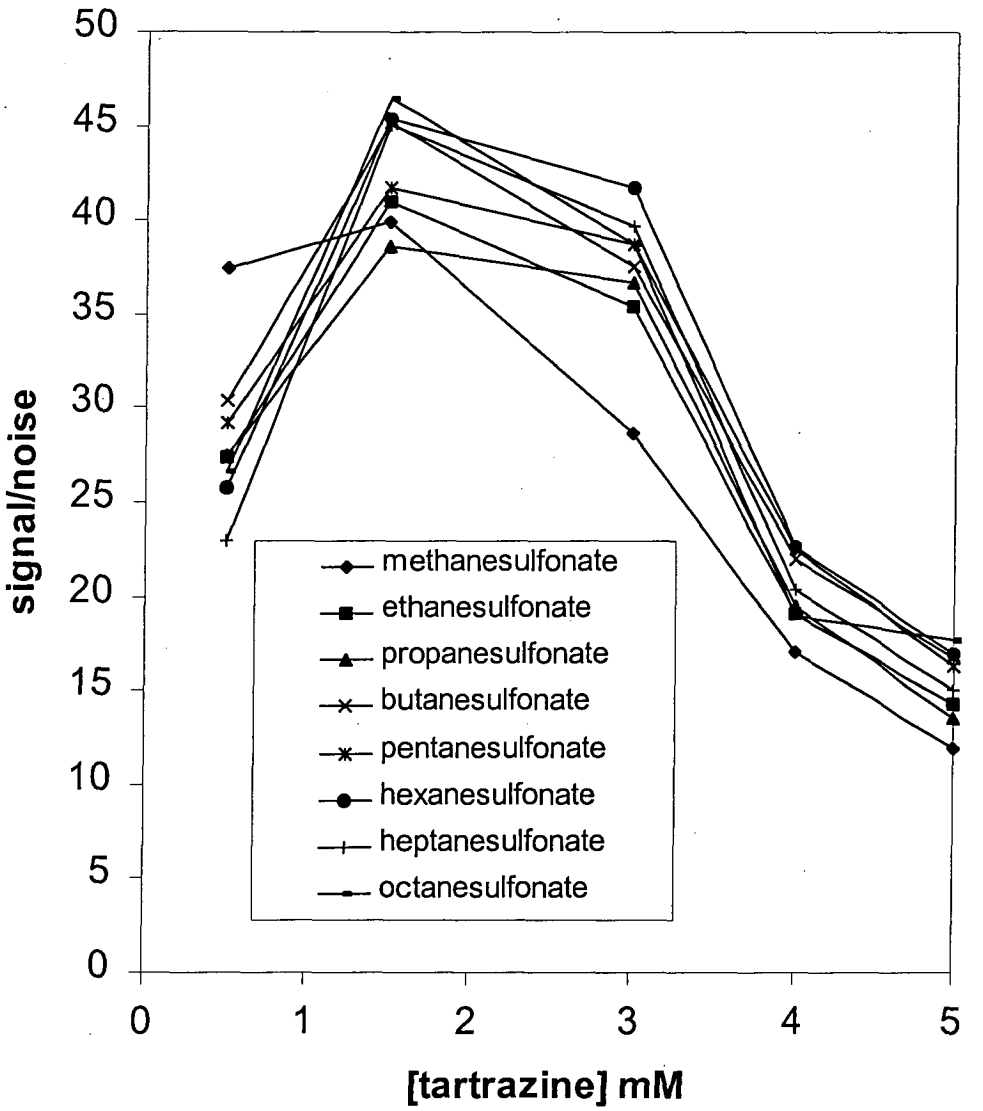

Figure 5-2 Plot of signal to noise ratio *versus* tartrazine concentration for C_1-C_8 alkanesulfonate mixture. Conditions – sample: 25 μM each of C_1-C_8 alkanesulfonates, electrolyte: varying tartrazine concentration, 10 mM histidine, 3 mM SB-12 zwitterionic surfactant, pH 7.70, voltage: 30 kV, injection: 0.6 s at 5" Hg, temperature 25° C, detection: indirect photometry at 258 nm.

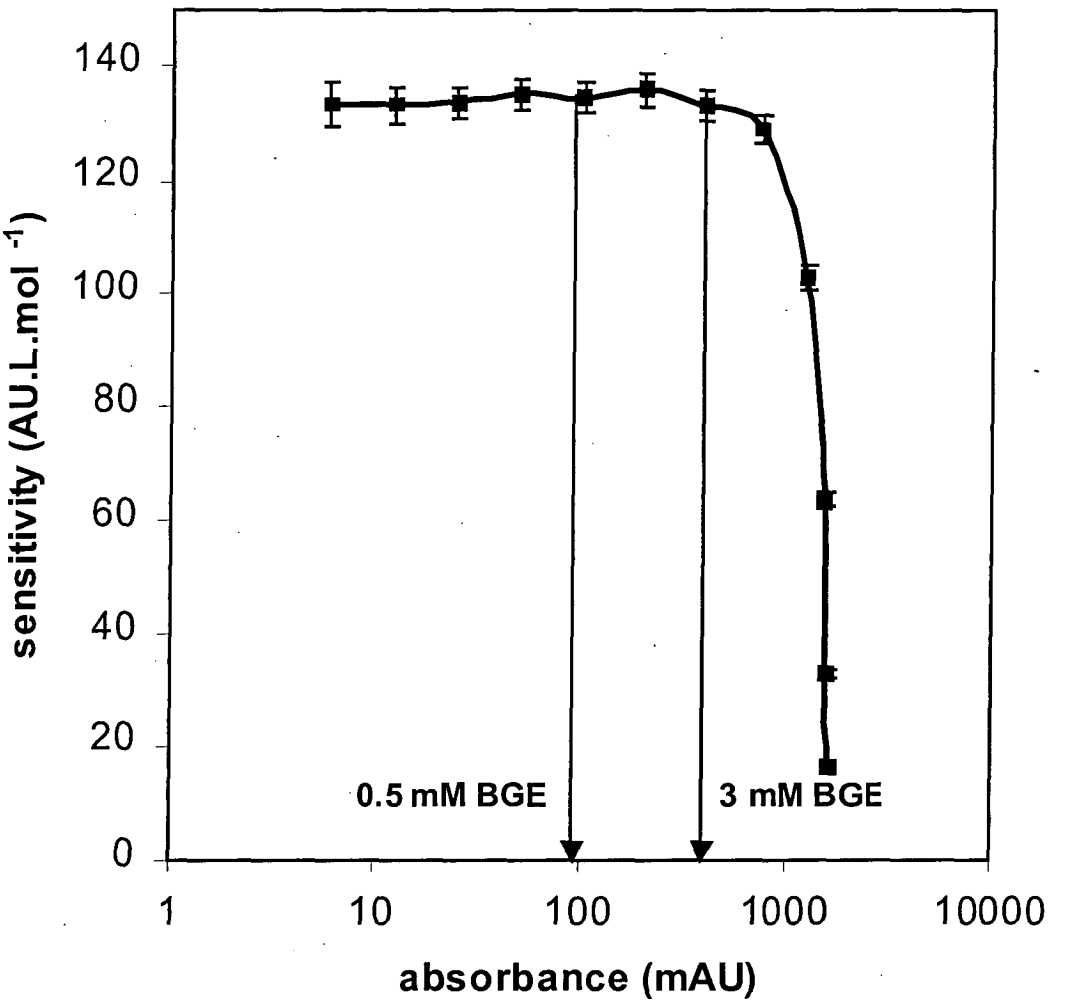

Figure 5-3 Sensitivity *versus* absorbance plot for tartrazine with Applied Biosystems 270A-HT CE instrument.

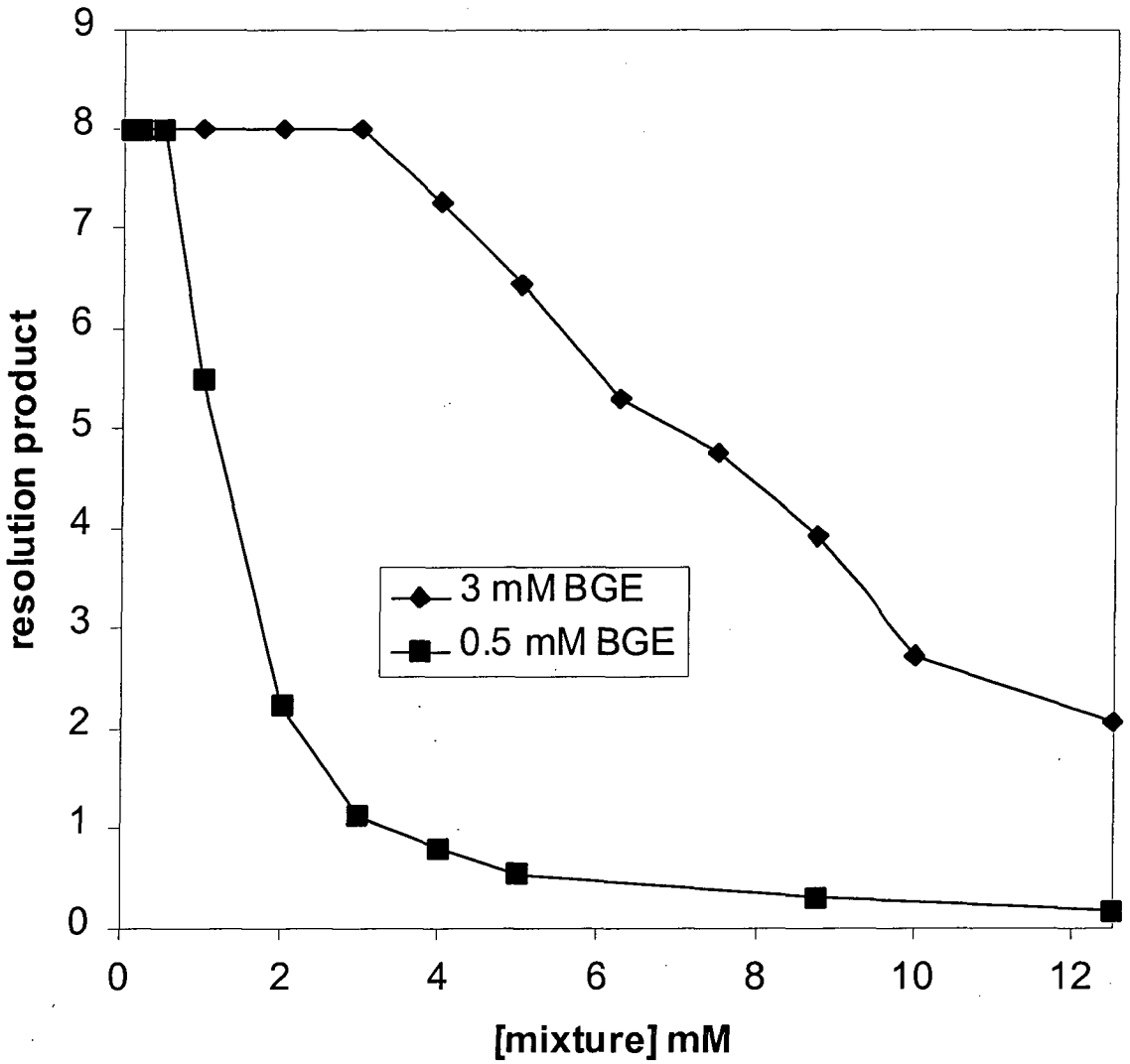

Figure 5-4 Resolution product obtained at various concentrations each of a mixture of methanesulfonate, ethanesulfonate, butanesulfonate and octanesulfonate, using 0.5 and 3 mM tartrazine electrolytes.

Calibration linearity also extended over a much larger range for the more concentrated BGE, although in practice the loss of resolution between adjacent peaks was a more serious problem since this occurred at lower sample concentrations.

Figure 5-5 demonstrates that increasing the probe concentration in the BGE did not adversely affect sensitivity at low analyte concentrations. Here, a 10 μM mixture of aliphatic sulfonic acids was injected and it can be seen that peak heights were slightly greater for the 3 mM tartrazine BGE due to improved stacking effects, but the baseline noise was slightly elevated so that the two BGEs gave very similar sensitivity. Detection limits are provided in Table 5-1. The 0.5 mM BGE gave a slightly higher EOF, resulting in a shorter run time. The important conclusion was that the increased probe concentration BGE provided excellent sensitivity at low analyte concentrations.

Table 5-1 Detection limits (μM) obtained with 3 mM and 0.5 mM tartrazine electrolytes.

Solute	0.5 mM tartrazine BGE	3 mM tartrazine BGE
Octanesulfonate	0.79	0.63
Heptanesulfonate	0.77	0.81
Hexanesulfonate	0.80	0.74
Pentanesulfonate	0.71	0.77
Butanesulfonate	0.79	0.84
Propanesulfonate	0.73	0.77
Ethanesulfonate	0.89	0.89
Methanesulfonate	0.73	0.95

Reproducibility measurements were also carried out with the 0.5 and 3 mM tartrazine BGEs. A 25 μM mixture of aliphatic sulfonic acids was injected for 20 consecutive runs without replacement or addition of electrolyte. Peak heights, areas and migration times were recorded and percent relative standard deviation were calculated (Table 5-2). Once again, the 3 mM BGE performed comparably with the 0.5 mM BGE, although peak heights were significantly more reproducible with the 3 mM BGE. The marginally poorer reproducibility of migration times for the 3 mM BGE can be explained by the longer migration times resulting from lower EOF of the BGE.

Table 5-2 Reproducibility data with 3 mM and 0.5 mM tartrazine electrolytes. Calculations from 20 successive runs.

Solute	Migration time RSD (%)		Peak area RSD (%)		Peak height RSD (%)	
	0.5 mM BGE	3 mM BGE	0.5 mM BGE	3 mM BGE	0.5 mM BGE	3 mM BGE
Octanesulfonate	0.43	0.86	6.28	5.02	5.99	1.43
Heptanesulfonate	0.34	0.79	6.09	4.66	4.16	1.76
Hexanesulfonate	0.37	0.88	5.43	4.08	4.86	1.94
Pentanesulfonate	0.36	0.80	5.81	3.92	4.37	1.89
Butanesulfonate	0.34	0.83	4.94	4.89	2.94	1.36
Propanesulfonate	0.34	1.08	3.71	3.14	3.43	1.13
Ethanesulfonate	0.33	1.40	4.92	4.80	2.79	1.31
Methanesulfonate	0.35	1.52	3.14	4.02	2.22	1.44

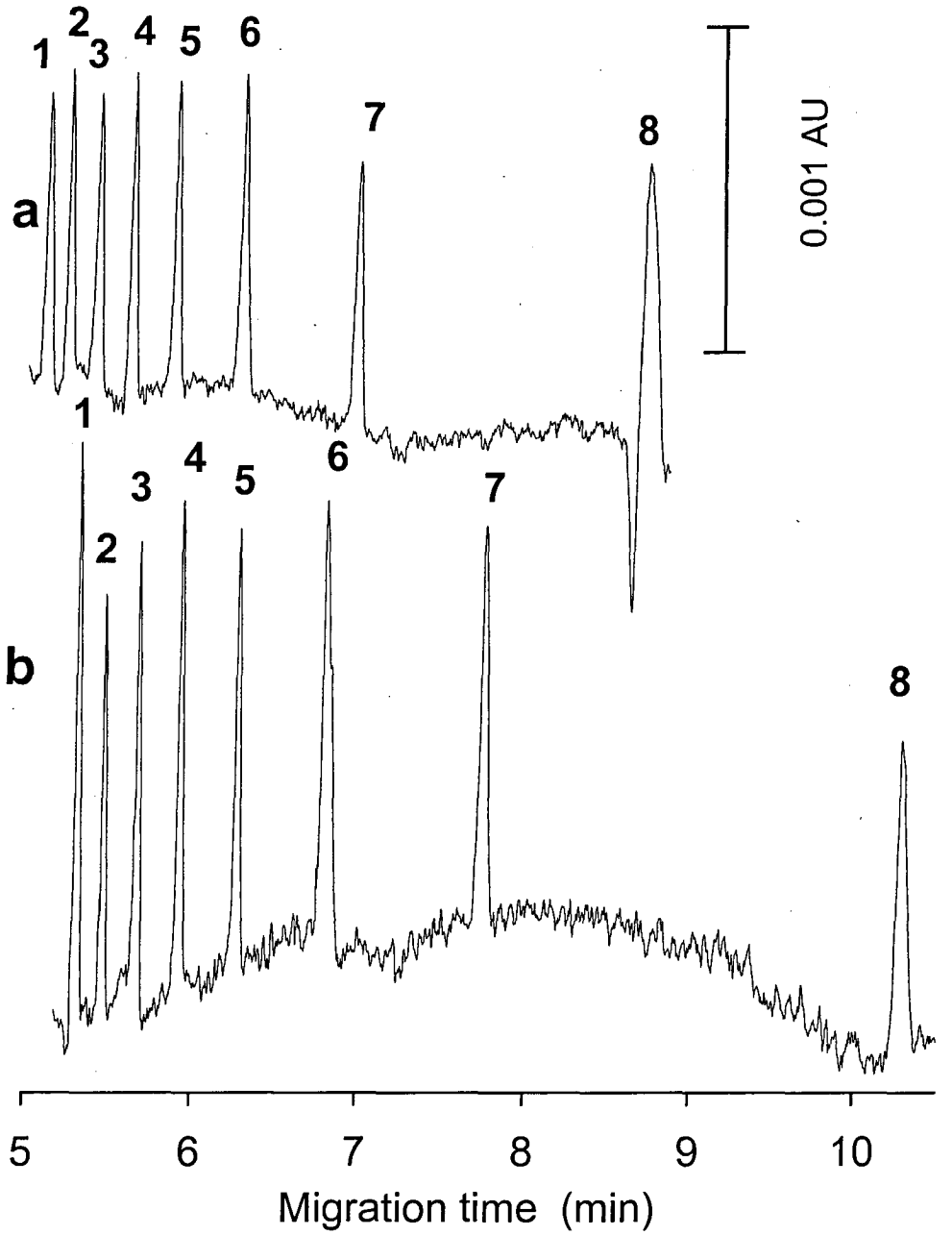

Figure 5-5 Electropherograms of C_1-C_8 alkanesulfonates (10 μM of each analyte) obtained with (a) 3 mM tartrazine and (b) 0.5 mM tartrazine electrolytes. Peak identification: 1= octanesulfonate, 2= heptanesulfonate, 3= hexanesulfonate, 4= pentanesulfonate, 5= butanesulfonate, 6= propanesulfonate, 7= ethanesulfonate, 8= methanesulfonate. Conditions- capillary: fused silica, 75 μm ID, length 0.72 m, 0.50 m to detector; electrolyte: (a) 3 mM tartrazine or (b) 0.5 mM tartrazine, 10.0 mM histidine, 3 mM SB-12 zwitterionic surfactant, pH 7.70; separation voltage: +30 kV, detection: indirect photometric at 258 nm; pressure injection: 0.6 s at 5" Hg, temperature: 25° C.

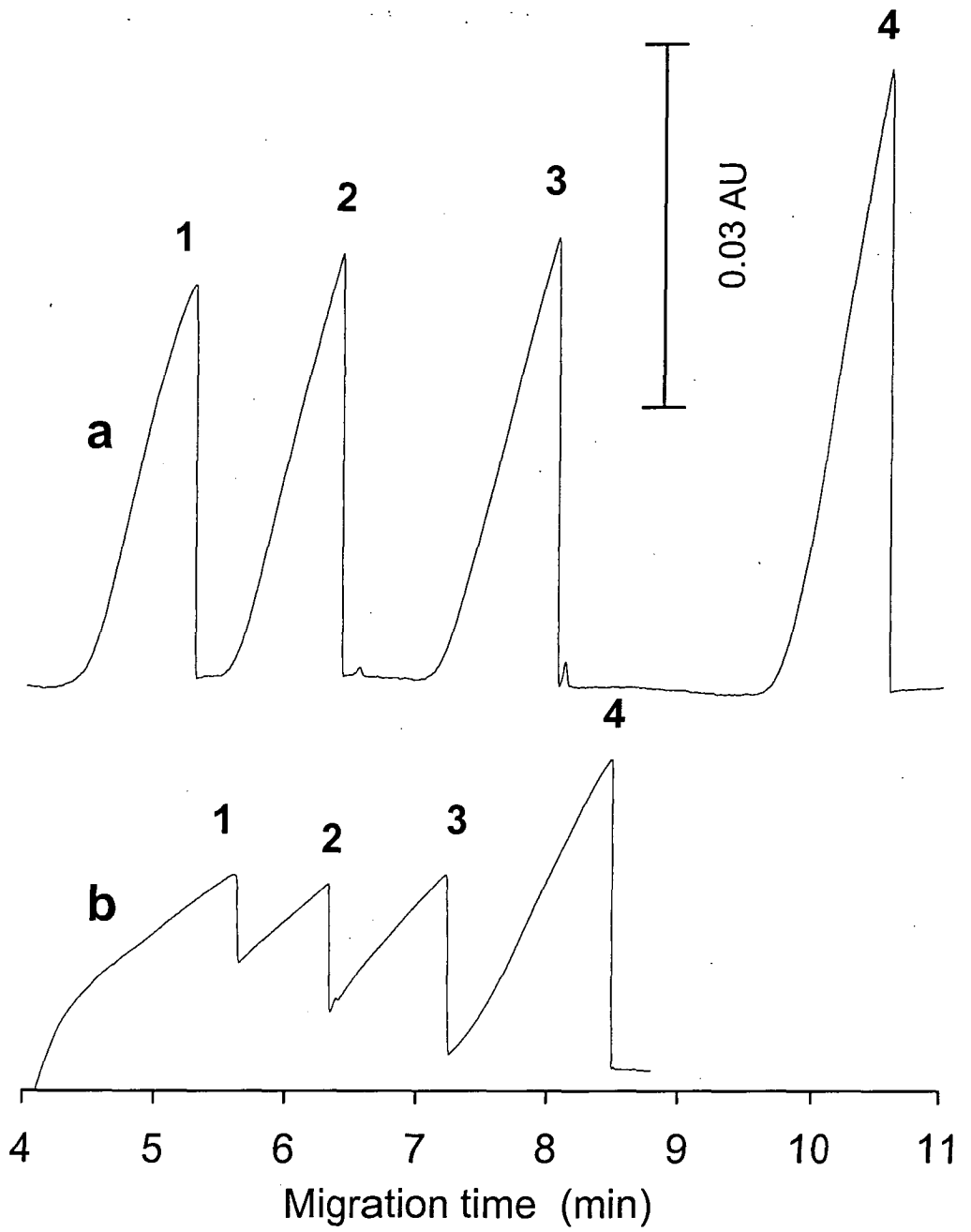

Figure 5-6 Electropherograms of 5 mM mix obtained with (a) 3 mM tartrazine and (b) 0.5 mM tartrazine electrolytes. Peak identification: 1= octanesulfonate, 2= butanesulfonate, 3= ethanesulfonate, 4= methanesulfonate. Conditions as in Figure 5-5.

5.4 Conclusions

In order to maximise stacking and limit electromigration dispersion in electrolytes for indirect photometric detection in CE, the highest possible probe concentration should be used. However, when highly absorbing probes are used to increase detection sensitivity (e.g. probe with absorptivities higher than approx. 2,000 $L.mol^{-1}.cm^{-1}$) the probe concentration must be optimised carefully with respect to two factors: (i) the background absorbance of the electrolyte, which should not exceed the linear range of the detector, and (ii) possible adsorption of the probe on the capillary wall resulting in unstable baseline and increased baseline noise. It is therefore essential that the linearity characteristics of the detector are known before this optimisation can proceed (see Chapter 4).

Using the dye tartrazine as a model highly absorbing probe and a zwitterionic surfactant to suppress the adsorption of the probe onto the capillary wall, studies have been undertaken on the separation of a range of aliphatic sulfonic acids in a counter-EOF mode. It has been demonstrated that after careful optimisation the probe concentration could be increased approximately 6 fold over levels used previously. This has resulted in improved peak shapes and resolution whilst retaining the benefits of highly absorbing probes at low concentrations, in particular highly sensitive detection.

The optimised method is suitable for the separation of low-to-medium mobility anions in the counter-EOF mode. Use of a different surface-active additive capable of suppressing both the EOF and the adsorption of the probe is needed to permit the determination of high mobility anions. The obvious advantages of more highly concentrated BGEs, such as improved stacking, peak shapes, sensitivity and increased working range, highlight the viability of this approach for the potential analysis of real samples containing matrix ions of high ionic strength.

5.5 References

1 F. Foret, S. Fanali, L. Ossicini and P. Bocek, *J. Chromatogr.*, **470** (1989) 299.

2 P. Doble, M. Macka and P.R. Haddad, *J. Chromatogr. A,* **804** (1998) 327.

3 T. Fuchigami and T. Imasaka , *Anal. Chim. Acta.*, **291** (1994) 183.

4 M. Macka, P. Andersson and P.R. Haddad, *Electrophoresis,* **17** (1996) 1898.

5 S.J. Lopez-Grio, G. Vivo-Truyols, J.J. Baeza-Baeza, J.R. Torres-Lapasio and M.C. Garcia-Alvarez-Coque, *Anal. Chim. Acta*, **433** (2001) 187. \

6 K.K.-C. Yeung and C.A. Lucy, *Anal. Chem.*, **69** (1997) 3435.

Chapter 6

Sensitive Indirect Photometric Detection of Inorganic and Small Organic Anions by Capillary Electrophoresis Using Orange G as a Probe Ion

6.1 Introduction

There has been a tendency to use highly absorbing probes at concentrations of around an order of magnitude less than more weakly absorbing probes in order to maintain similar background absorbances without due consideration of the reasons behind this. Excessive separation currents and Joule heating can be avoided by the use of a low conductivity buffer, such as an isoelectric ampholyte [1]. The major restriction on probe concentration then becomes the background absorbance. Investigation of detector linearity performed in Chapter 4 has shown that many detectors in commercially available instruments maintain a linear response far in excess of values previously suspected. This opportunity has not been exploited until recently in Chapter 5, where the concentration of the highly absorbing probe ion tartrazine was increased from 0.5 to 3 mM whilst remaining inside the upper detector linearity limit of the instrument. Through careful manipulation of the electrolyte, attendant problems due to the increased probe concentration, such as adsorption to capillary walls, degraded baselines and increased baseline noise, were minimised. The addition of a zwitterionic surfactant minimised adsorption of tartrazine onto the fused silica capillary wall, providing a flat baseline. Increased stacking effects due to a higher electrolyte concentration resulted in increased peak heights which more than compensated for rises in baseline noise. Detection sensitivity was maintained and the increase in probe concentration allowed improved resolution of analytes with narrower peaks and improved separation efficiencies. The linear response of analytes was also extended over a greater concentration range. The one disadvantage to this approach was that the addition of the zwitterionic surfactant resulted in a relatively high cathodic EOF, meaning that only anions of mobility less than -54×10^{-9} $m^2 V^{-1} s^{-1}$ could be detected within 10 min. Detection of faster anions was thus not practical and this restriction limited the potential applications of the system. Another problem observed was that a slight deterioration in

baseline stability occurred at probe concentrations exceeding 3 mM due to adsorption of the dye at the capillary wall. The background absorbance of 410 mAU was well inside the upper limit for the instrument used.

The use of a suitable dye with regard to its mobility and absorptivity at even higher concentrations in a suitable instrument could lead to similar sensitivity as previously but with improved method performance parameters in terms of ruggedness, reproducibility, linear response range and resolution. If the EOF of the electrolyte could be controlled in such a way to allow the separation and detection of a wider mobility range of analytes, the potential could exist for the analysis of real samples. Such a system would combine the best features of the sensitivity of highly absorbing probes (normally used at low probe concentration) and the ruggedness of less absorbing probes (used at concentrations from 5-10 mM).

In this chapter a highly absorbing probe, Orange G, buffered with the ampholyte histidine is employed at concentrations far exceeding those conventionally used. An innovative approach using a combination of a semipermanently coated capillary, a neutral polymer as an additive in the BGE, reduced inner diameter capillary and the application of pressure during the run has been successfully employed to achieve highly sensitive detection of anions having a wide range of mobilities. The associated benefits from the increased probe concentration are also discussed.

6.2 Experimental

6.2.1 Instrumentation

The general experimental details are given in Chapter 2.

The capillary electrophoresis instrument used during the majority of this work was an Agilent Technologies ^{3D}CE. A voltage of -30 kV was applied during all separations,

with temperature maintained at 25°C. A Waters Capillary Ion Analyser was used for experiments involving a blue LED (λ_{max} = 476 nm) as the light source.

The ion-chromatograph used in this work was a Dionex DX-500 (Sunnyvale, CA, USA) system consisting of a GP50 gradient pump, EG40 eluent generator, AS50 autosampler with thermal compartment, CD20 conductivity detector and AD20 ultra-violet/visible (UV/VIS) absorbance detector. A pump flow rate of 1.5 mL min^{-1} and column oven temperature of 35°C were used throughout. For UV detection a wavelength of 215 nm was used. The analytical column used was a Dionex AS-11 anion-exchange column fitted with a AG-11 guard column. Conductivity detection was used with suppression provided by a Dionex ASRS-Ultra self-regenerating anion suppressor. All chromatographic data were collected using Dionex PeakNet software version 5.1. A 25 µL injection loop was used throughout.

The ion chromatographic gradient elution system, optimised for the anions of interest in the air filter samples, used hydroxide ions produced by the EG40 module, with a flow rate of 1.5 mL min^{-1}. The gradient program was 0.5mM OH^- from 0-5 min, 0.5-2mM OH^- at 5-10 min, maintained at 2mM from 10-15 min, then 2-35mM from 15-24 min, 35-0.5mM at 25-26 min, then column re-equilibration at 0.5mM OH^- from 26-32 min.

6.2.2 Procedures

Orange G was purified by recrystallisation from a 3:1 solution of ethanol-water [2]. Two successive recrystallisations were performed to ensure adequate purity. Determination of anionic impurities was performed by CE using a chromate electrolyte. In brief, a fused silica capillary, an electrolyte consisting of 5 mM chromate buffered at pH 8 with Tris(hydroxymethyl)aminomethane and 0.5 mM tetradecyltrimethylammonium hydroxide (TTAOH) and indirect detection at 254 nm were used to separate and quantify inorganic anion impurities using a standard addition method. Purity of the dye after successive recrystallisations was found to be 99% compared with an initial purity of 80%.

Fused silica capillaries were coated with poly(ethylenimine) by flushing with 1 M sodium hydroxide for 30 min, water for 30 min followed by a 4% poly(ethylenimine) solution for 1 h which was left to stand in the capillary for 30 min. The capillary was finally flushed with water for 30 min before use.

All background electrolytes were buffered by the addition of 10.0 mM histidine at its isoelectric point. The use of the ampholytic isoelectric buffer resulted in an electrolyte pH of 7.7. No pH adjustments were required.

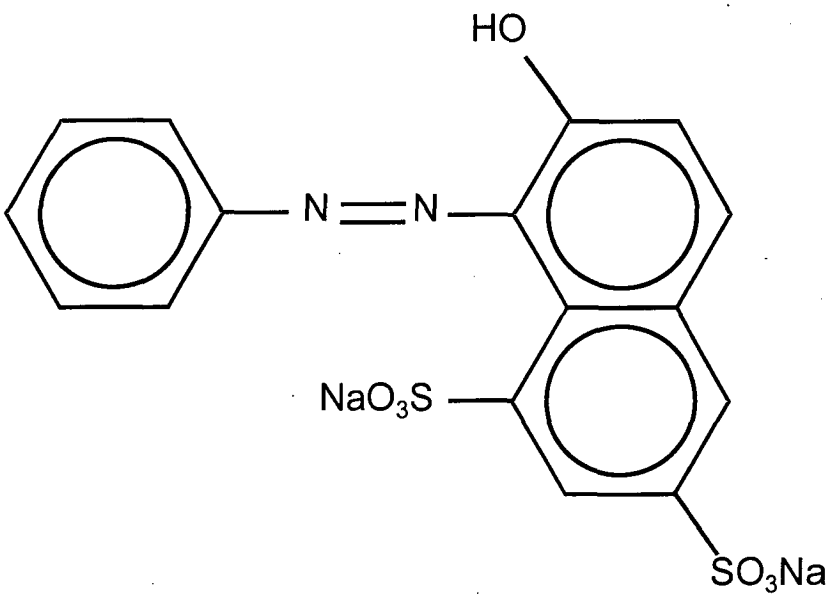

Figure 6-1 Orange G

6.3 Results and Discussion

6.3.1 Detector Linearity Restrictions

It has been established previously in Chapter 4 that the maximum background absorbance which can be reached without a loss of detection linearity with an Agilent Technologies ^{3D} CE and a 75 μm capillary is 1200 mAU. Orange G has two absorption maxima at 248 and 478 nm exhibiting absorptivities of 24,345 and 19,511 $L.mol^{-1}$ cm^{-1}, respectively. Orange G also provided an additional benefit over the previously used dyes tartrazine and naphthol yellow S as it has an absorption maximum which coincided with the maximum emission wavelength of a blue LED. The use of a deuterium lamp light source requires detection at 248 nm in order to achieve higher signal to noise ratios. By preparing and flushing an Orange G solution of known concentration, the concentration equivalent to this upper linearity detection limit was calculated and found to be 7.6 mM. Hence in this case the maximum possible Orange G concentration commensurate with remaining below the BGE absorbance value at which detector linearity was lost was 7.6 mM.

6.3.2 Modification of EOF

There are three main options which can be used to allow the separation and detection of a wide mobility range of anions. The first, and preferred, option is to reverse the EOF and to utilise a co-EOF separation with a negative voltage so that all analyte anions are transported past the detection window. This is typically achieved by the addition of a cationic surfactant, such as cetyltrimethylammonium or tetradecyltrimethylammonium bromide to the BGE, which dynamically coats the capillary wall, imparting a net positive charge to the capillary surface [3, 4]. However, this technique is not possible when anionic dyes are used as probes since they tend to form precipitates with commonly used cationic surfactants. Even at very low concentrations Orange G formed such precipitates, which could not be solubilised with various organic solvents. The second option is to use a counter-EOF separation with a large, positive EOF and a positive separation polarity voltage. Provided the magnitude of the EOF exceeds the

magnitude of the electrophoretic mobility of the anions, all anions will be detected. This approach has been used in Chapter 5 with the anionic dye tartrazine through the addition of a zwitterionic surfactant to increase the magnitude of the EOF to allow the counter-EOF separation of short chain alkane sulfonic acids. The drawback was that anions of mobility exceeding -54×10^{-9} $m^2 V^{-1} s^{-1}$ could not be detected within 10 min. The third approach, and that chosen for this current work, is to perform a counter-EOF separation with a negative separation voltage. This requires the EOF to be suppressed to as low a value as possible.

Another drawback to the use of dyes as probes, particularly at high concentrations, is the occurrence of baseline disturbances. This often appears as irreproducible baseline drift. The desired CE system was therefore one in which the EOF was suppressed and there was a minimal baseline disturbance during the run. These goals could be achieved using suitable BGE additives and by modifying the capillary surface. An initial range of BGE additives, such as hexamethonium bromide, zwitterionic surfactants and zwitterionic additives, neutral polymers, and non-ionic surfactants (Brij 35, Tween), failed to improve the baseline quality and/or suppress the EOF. Coating of capillaries with PEI did provide a slightly reversed EOF at low Orange G concentrations but at concentrations exceeding 1 mM, the EOF was once again in the positive direction. As the dye concentration was increased, the EOF gradually increased in magnitude to about $+20 \times 10^{-9}$ $m^2 V^{-1} s^{-1}$ at Orange G concentrations exceeding 3 mM. This system would be unsatisfactory in providing detection for analytes of the widest possible mobility range. Coating of capillaries with poly(diallyldimethylammonium chloride) (PDDAC), polybrene and PDDAC/dextran sulfate did not provide any improvements in terms of EOF and baselines. The use of HPMC in Chapter 4 to suppress EOF in electrolytes containing low concentrations of anionic dyes suggested that this reagent might be of use in suppressing EOF further. In fact, the addition of 0.05% HPMC to electrolytes used with a PEI coated capillary significantly suppressed the EOF (even at concentrations of 8 mM Orange G) to less than $+5 \times 10^{-9}$ $m^2 V^{-1} s^{-1}$. This suppressed EOF would allow anions of virtually all mobilities to be separated and detected with cathodic polarity at injection end without excessive run times. All further work was

therefore performed on PEI coated capillaries with the addition of 0.05% HPMC to the BGE.

6.3.3 Improvement of Baseline Stability

The combination of PEI coated capillaries and addition of HPMC to the BGE was effective in suppressing EOF and allowing the detection of fast anions. However the quality of the baselines was unsatisfactory. Other additives and coatings failed to improve this situation. The use of voltage gradients and ramping also had no impact. One interesting observation noted during previous work in Chapter 4 when measuring absorbances of dye solutions was that perfectly flat baselines occurred when the solutions were flushed through the capillary under pressure, even at dye concentrations exceeding 50 mM. The Agilent ^{3D}CE instrument had the capacity to allow the application of pressure ranging from -50 to 50 mbar (respective to injection end) during a run. A pressure of 50 mbar with a 75 μm ID capillary of 48 cm length provided a hydrodynamic flow linear velocity of 0.204 cm/s, causing a sample plug to reach the detector window in 3.3 min. The application of 50 mbar pressure during separation with an applied voltage did in fact provide a flat baseline which was far superior to any obtained previously. However, as expected, the pressure-driven flow caused a serious deterioration in separation efficiency in the 75 μm ID capillary. The same pressure conditions applied to a 50 μm capillary produced drastically different results. A slower plug velocity of 0.09 cm/s occurred, with the sample plug reaching the detector in 7.37 min, well after any anions of interest. Baseline stability was still much improved but somewhat surprisingly, separation efficiency and resolution were also quite acceptable and were only marginally lower compared to those obtained without pressure (see Figure 6-2). Therefore this combination of PEI coatings, HPMC additive and application of slight overpressure at the injection end during separations was used for all further work since it provided fast separations with stable baselines.

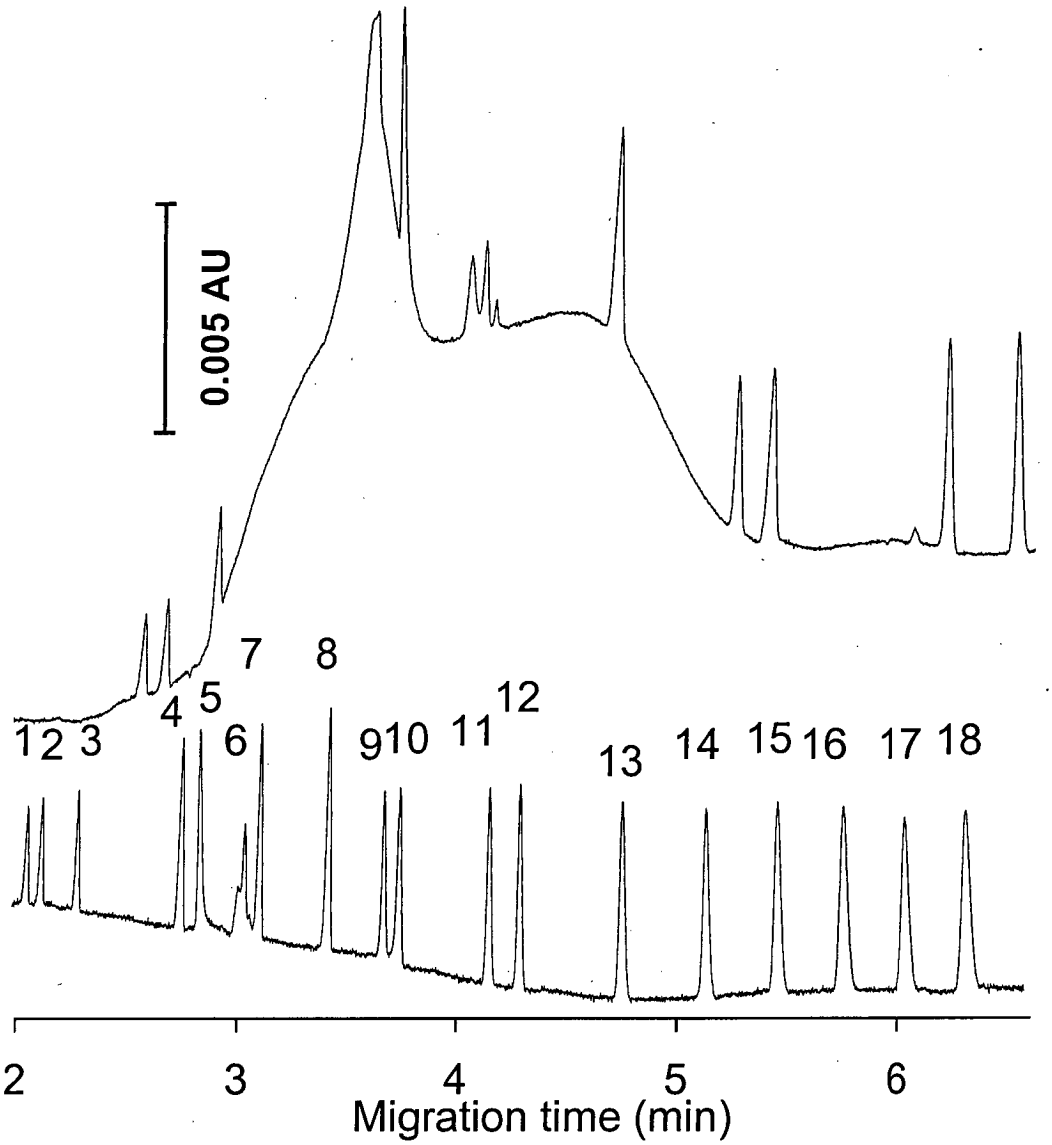

Figure 6-2 Electropherogram of 25 μM anion mixture (a) without and (b) with application of 25 mbar pressure. Peak identification: 1= bromide, 2= chloride, 3= nitrate, 4= malonate, 5= citrate, 6= fluoride, 7= succinate, 8= phthalate, 9= methanesulfonate, 10= carbonate, 11= iodate, 12= ethanesulfonate, 13= propanesulfonate, 14= butanesulfonate, 15= pentanesulfonate, 16= hexanesulfonate, 17= heptanesulfonate, 18= octanesulfonate. Conditions- capillary: PEI coated fused silica, 50 μm ID, length 0.645 m, 0.56 m to detector; electrolyte: 5 mM Orange G, 10.0 mM histidine, 0.05% HPMC; separation voltage: -30 kV (current 6 μA at 25° C); separation pressure: (a) 0 mbar, (b) 25 mbar, detection: indirect photometric at 248 nm; pressure injection: 50 mbar for 10 s.

6.3.4 Optimisation of Separation Pressure

A 3 mM Orange G, 10.0 mM histidine, 0.05% HPMC, pH 7.70 model BGE was chosen in order to determine the optimum separation pressure with regard to baseline stability, detection sensitivity and separation efficiency. A test solution containing bromide, chloride, nitrate, malonate, citrate, fluoride, succinate, phthalate, methanesulfonate, carbonate, iodate, ethanesulfonate, propanesulfonate, butanesulfonate, pentanesulfonate, hexanesulfonate, heptanesulfonate and octanesulfonate was separated using inlet pressures of 0, 10, 20, 30, 40 and 50 mbar. Pressure gradients were also investigated with various initial and final pressures and time periods. These gradients offered no advantages over the application of a constant pressure. As expected peak heights decreased steadily as the applied pressure increased (see Figure 6-3). A similar trend regarding separation efficiency also occurred (see Figure 6-4). However the baseline quality improved as pressure was increased. A minimum pressure of 25 mbar was required to provide a flat, stable baseline. This resulted in a linear flow velocity of 0.045 cm/s, which would cause a sample plug to pass the detector in 14.75 min. Some detection sensitivity and separation efficiency must be sacrificed in order to provide a satisfactory baseline. A separation pressure of 25 mbar was used for all further work.

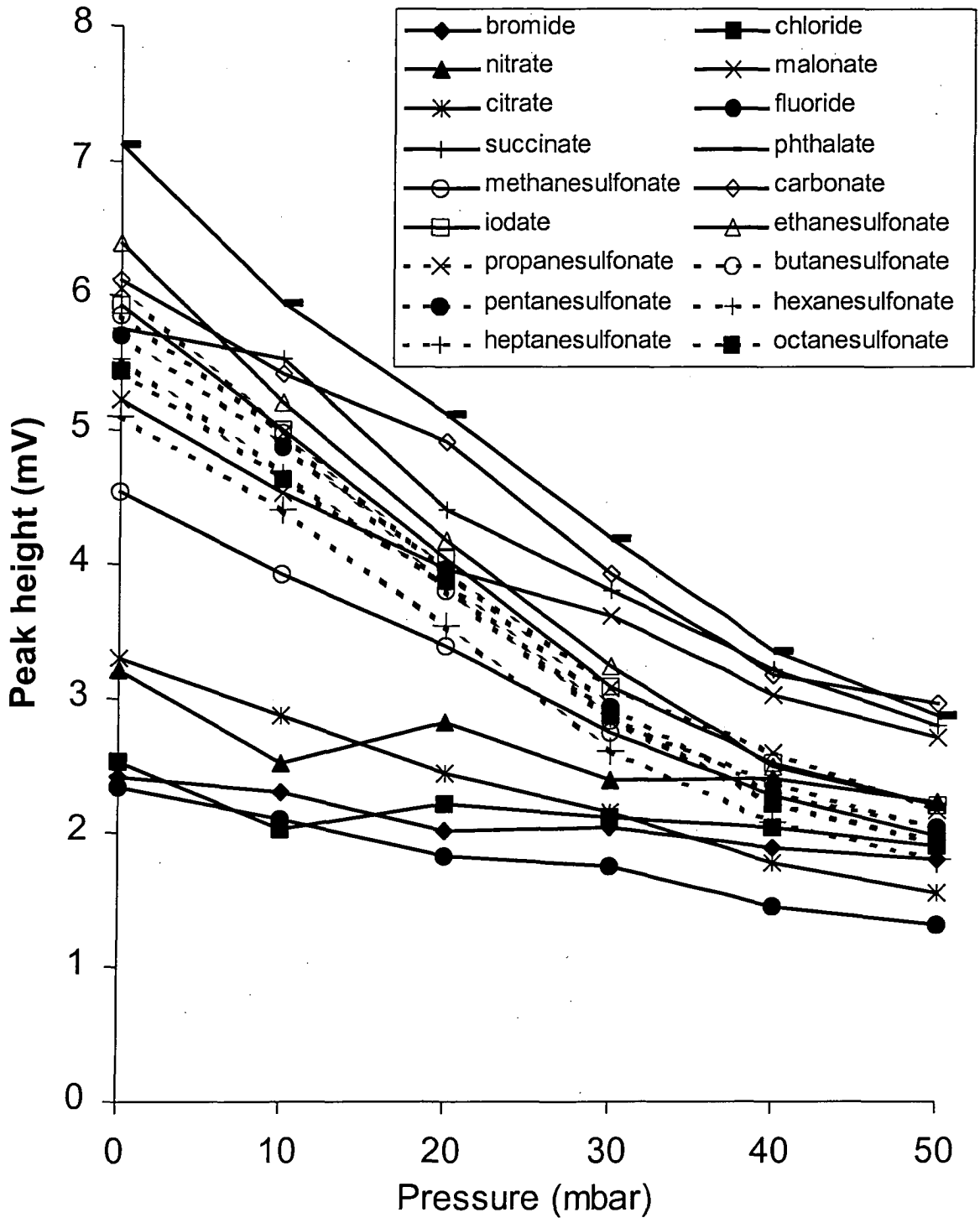

Figure 6-3 Plot of peak height *versus* separation pressure for 25 μM anion mixture. Conditions – sample: 25 μM of each anion, electrolyte: 3 mM Orange G, 10.0 mM histidine, 0.05% HPMC, pH 7.70, varying separation pressures. All other conditions as shown in Figure 6-2.

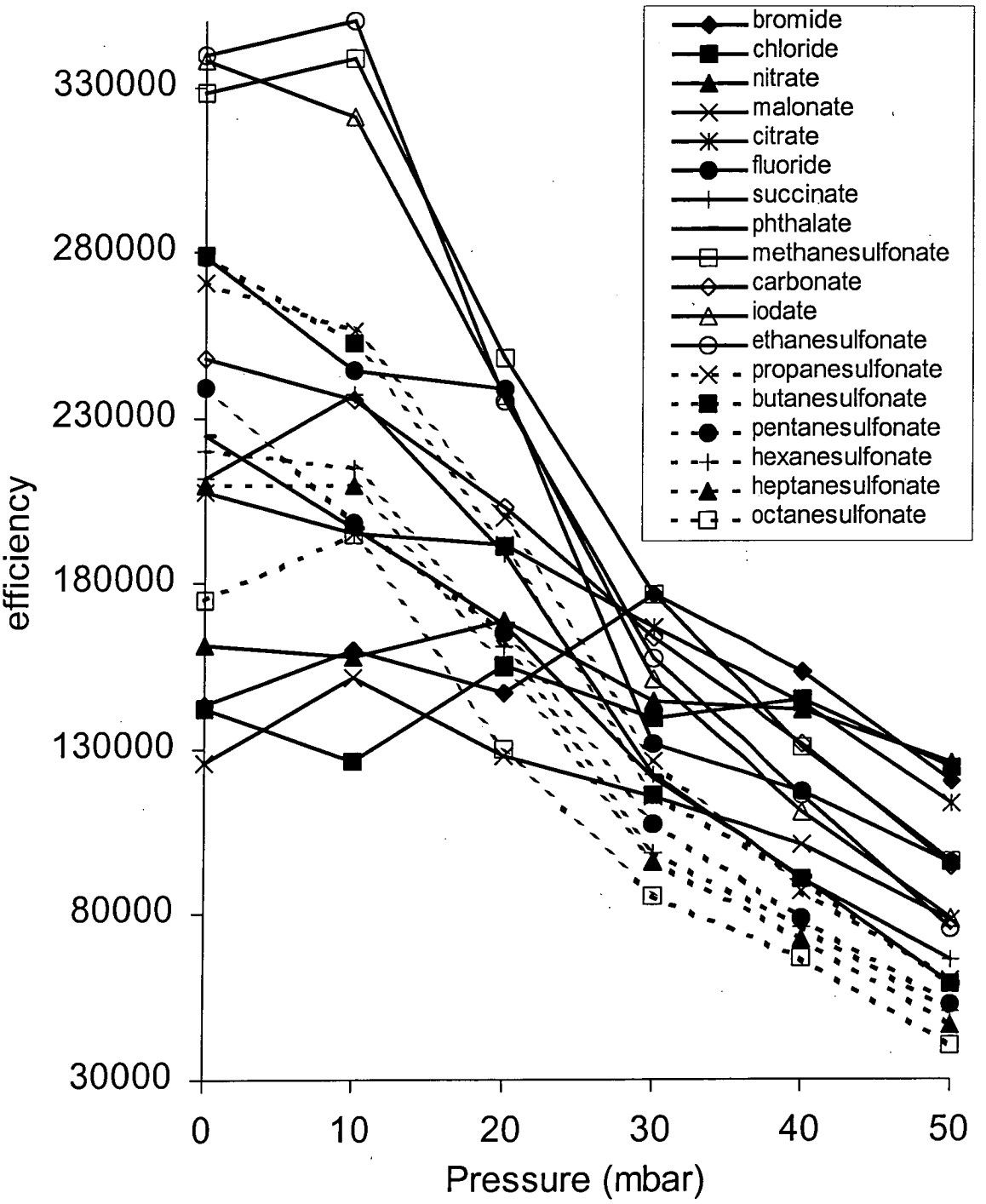

Figure 6-4 Plot of separation efficiency (number of theoretical plates) *versus* applied pressure. Conditions as in Figure 6-3.

6.3.5 Optimisation of Probe Concentration

Detector linearity limits are specific to instrumental and capillary conditions. A series of Orange G solutions were prepared and flushed through a 50 μm capillary and the resultant absorbances were measured. A plot of sensitivity *versus* absorbance was constructed and used to determine that the detector linearity upper limit of the Agilent ^{3D}CE fitted with a 50 μm capillary was 785 mAU, which corresponded to an Orange G concentration of 7.5 mM. A series of electrolytes containing varying Orange G concentrations ranging from 1-7 mM with fixed values of 10.0 mM histidine, 0.05 % HPMC, pH 7.70 were prepared for evaluation. A test solution containing 25 μM of bromide, chloride, sulfate, nitrate, oxalate, malonate, formate, citrate, succinate, methanesulfonic acid, acetate, ethanesulfonate, propanesulfonate, butanesulfonate, pentanesulfonate, hexanesulfonate, heptanesulfonate and octanesulfonate was prepared to examine each BGE for signal to noise ratio, separation efficiency and baseline stability. All separations of the test solution were performed with the application of 25 mbar pressure. Two general trends were noted. First, peak heights increased as probe concentration was increased. However, concomitant increases in baseline noise at higher probe concentrations resulted in an optimum signal to noise ratio being generally obtained at a probe concentration of around 4 mM for most analytes. Gains in peak heights at probe concentrations exceeding this value were offset by the accompanying rise in baseline noise (see Figure 6-5). Second, separation efficiencies (expressed as numbers of theoretical plates) were increased as the probe concentration was increased (see Figure 6-6). BGEs containing Orange G concentrations below 3 mM gave incomplete separation of the analytes and broadened peaks, resulting in co-migration of chloride and sulfate and succinate and citrate. Anions that were not resolved were injected individually in order to collect peak data necessary for further calculations. Increased Orange G concentrations allowed improved resolution of mixtures with sharper, better shaped peaks. Based on these observations, an optimum concentration of 4 mM Orange G was chosen as this was the highest concentration which retained maximum sensitivity.

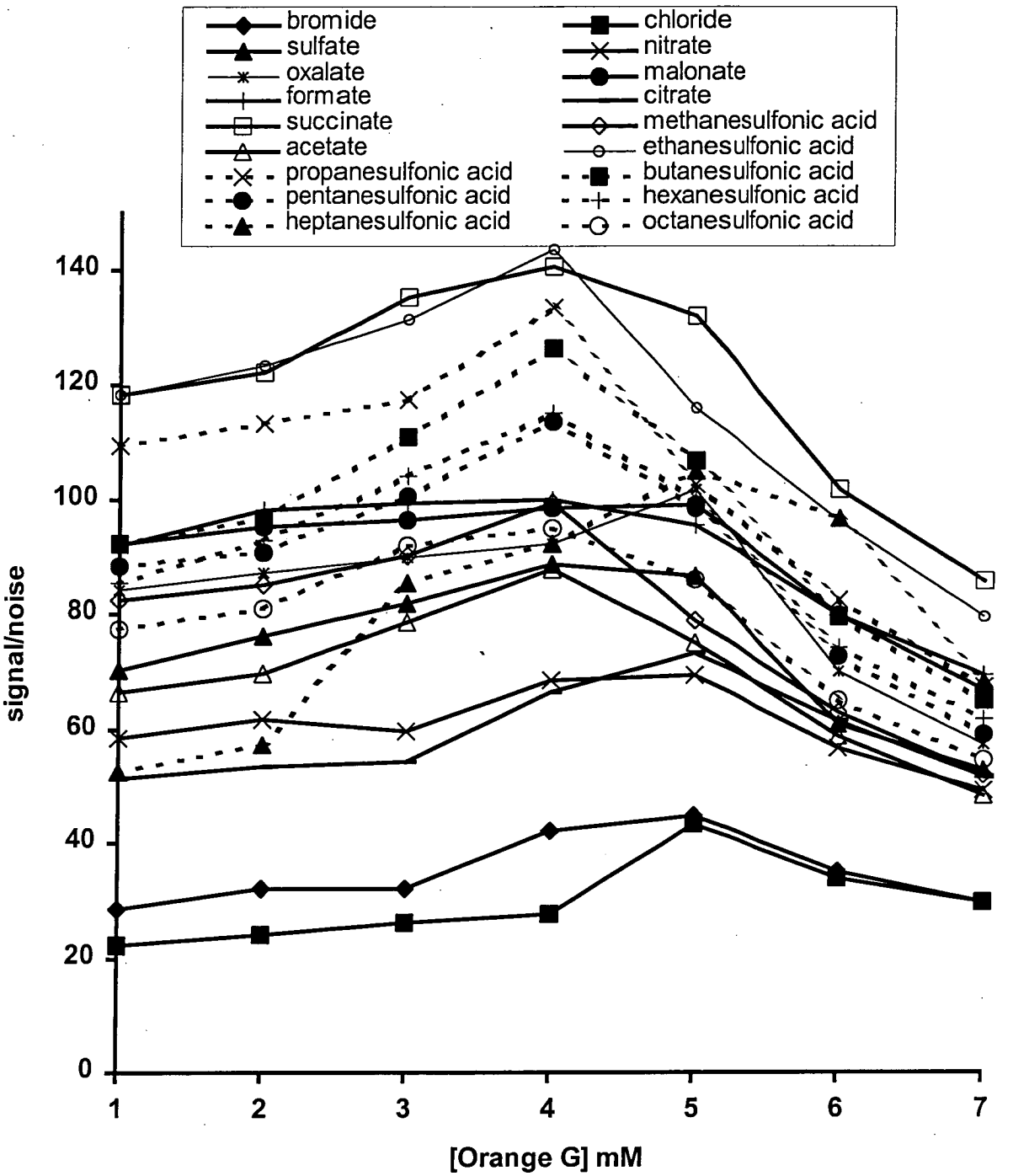

Figure 6-5 Plot of signal to noise ratio *versus* Orange G concentration for 25 μM anion mixture. Conditions – sample: 25 μM of each anion, electrolyte: varying Orange G concentration, 10.0 mM histidine, 0.05% HPMC, pH 7.70, separation pressure 25 mbar. All other conditions as in Figure 6-2.

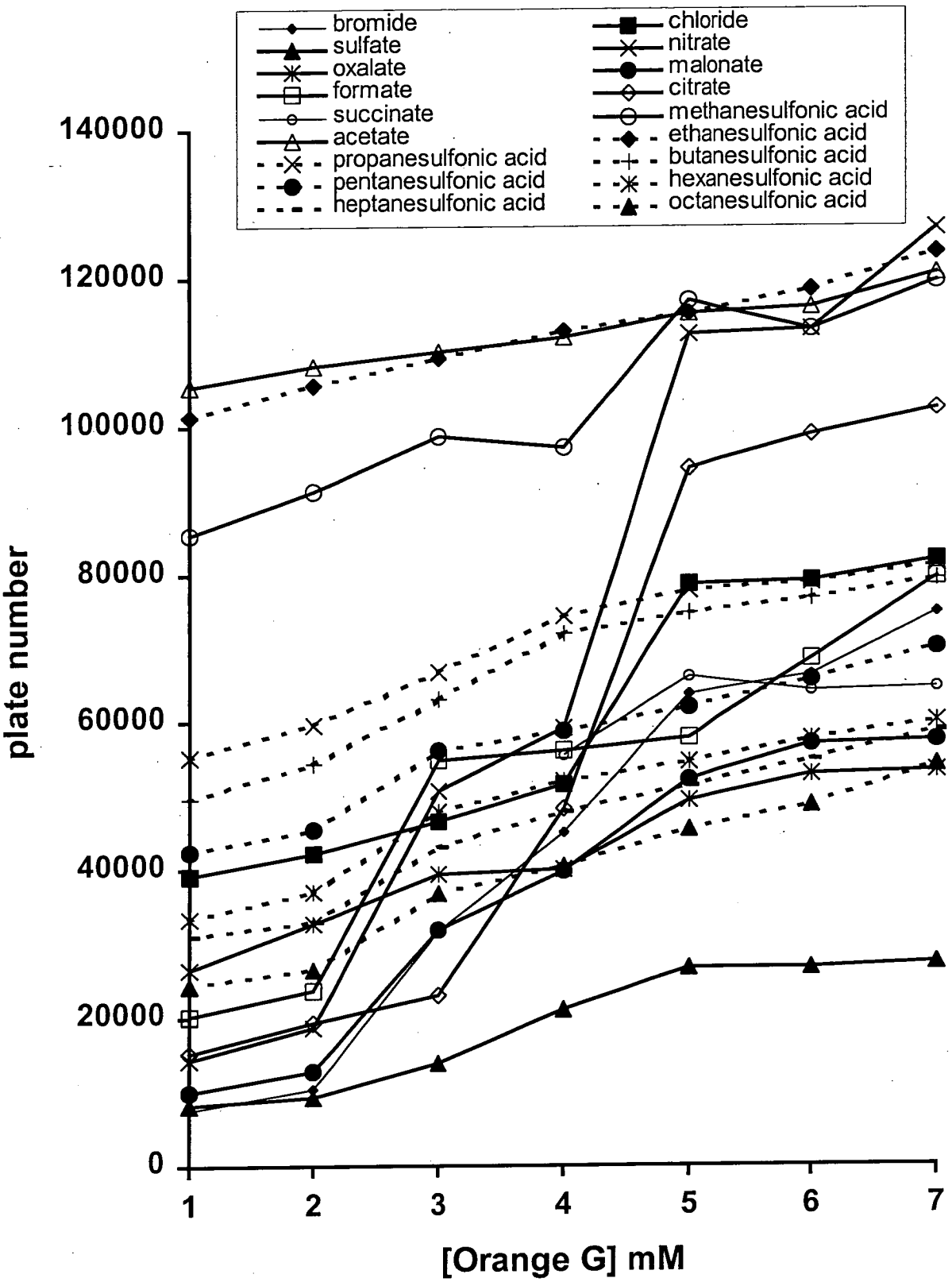

Figure 6-6 Plot of separation efficiency (number of theoretical plates) *versus* Orange G concentration. Conditions- length 0.485 m, 0.400 m to detector, all other conditions as in Figure 6-5.

6.3.6 Electrolyte Performance

Performance characteristics of the optimised electrolyte were determined. A BGE containing 4 mM Orange G, 10.0 mM histidine, 0.05% HPMC, at pH 7.70 was used in a PEI-coated 50 μm ID capillary with a pressure of 25 mbar applied during the run. A 2.5 μM standard solution of the test analytes was injected to determine detection limits and plate numbers (Table 6-1). Detection limits ranging from 0.216-0.912 μM were observed and are highly acceptable when compared to typically reported values of ~ 1 μM with the use of indirect photometric detection. Importantly, the increased probe concentration resulted in sharp peaks, leading to the very high separation efficiencies achieved. These compare very favourably with typical efficiencies in CE. A 50 μM solution of the test analytes was injected 30 times consecutively with the same electrolyte in order to measure the reproducibility of migration times, corrected peak areas and peak heights. Relative standard deviations (RSD) were calculated (see Table 6-2). Minimal changes in migration times, peak areas and peak heights occurred during 30 consecutive runs (see Figure 6-7). Proper buffering of the electrolyte with histidine caused pH changes to be minimised, which also contributed to the high reproducibility. It has also been observed that increased probe concentrations led to improved peak reproducibility in Chapter 5 and the results achieved here support this observation. The reproducibility of this electrolyte over a large number of runs without replenishment or replacement is better than previously reported values for the use of indirect detection.

Table 6-1 Detection limits (μM) and separation efficiencies (number of theoretical plates, N) obtained with 4 mM Orange G electrolyte. Conditions- sample: 2.5 μM of each analyte, BGE: 4 mM Orange G, 10.0 mM histidine, 0.05% HPMC, pH 7.70, voltage: -30 kV, injection: 20 s at 50 mbar, capillary 0.56 x 0.645 m 50 μm PEI coated, temperature: 25° C, detection: indirect photometry at 248 nm.

Anion	LOD (μM)	Efficiency (N)
Bromide	0.49	296,960
Chloride	0.35	290,730
Nitrate	0.32	277,960
Malonate	0.22	244,380
Citrate	0.37	161,330
Fluoride	0.67	154,980
Formate	0.91	194,450
Succinate	0.77	297,040
Phthalate	0.26	219,910
Methanesulfonate	0.35	244,160
Carbonate	0.30	226,770
Iodate	0.30	231,790
Ethanesulfonate	0.30	220,890
Propanesulfonate	0.27	142,270
Butanesulfonate	0.31	212,680
Pentanesulfonate	0.30	166,520
Hexanesulfonate	0.32	140,570
Heptanesulfonate	0.33	148,200
Octanesulfonate	0.33	128,910

Table 6-2 Reproducibility data (percentage Relative Standard Deviation, %RSD) obtained with 4 mM Orange G BGE. Calculations made from 30 successive runs. Conditions- sample: 50 μM of each analyte, BGE: 4 mM Orange G, 10.0 mM histidine, 0.05% HPMC, pH 7.70, voltage: -30 kV, injection: 10 sec at 50 mbar, temperature 25° C, detection: indirect photometry at 248 nm.

% RSD	migration time	corrected peak area	peak height
Bromide	0.80	2.69	5.06
Chloride	0.79	3.18	3.78
Sulfate	0.77	1.75	4.83
Nitrate	0.75	1.88	5.12
Oxalate	0.72	2.08	4.99
Malonate	0.58	1.27	3.96
Formate	0.53	3.36	4.83
Citrate	0.52	2.34	1.92
Succinate	0.44	2.20	3.06
Methanesulfonate	0.32	2.04	1.91
Acetate	0.23	1.95	1.61
Ethanesulfonate	0.19	1.61	1.46
Propanesulfonate	0.14	1.58	1.03
Butanesulfonate	0.17	1.75	1.09
Pentanesulfonate	0.22	1.75	1.01
Hexanesulfonate	0.28	1.74	1.04
Heptanesulfonate	0.33	1.63	0.88
Octanesulfonate	0.38	1.68	0.98

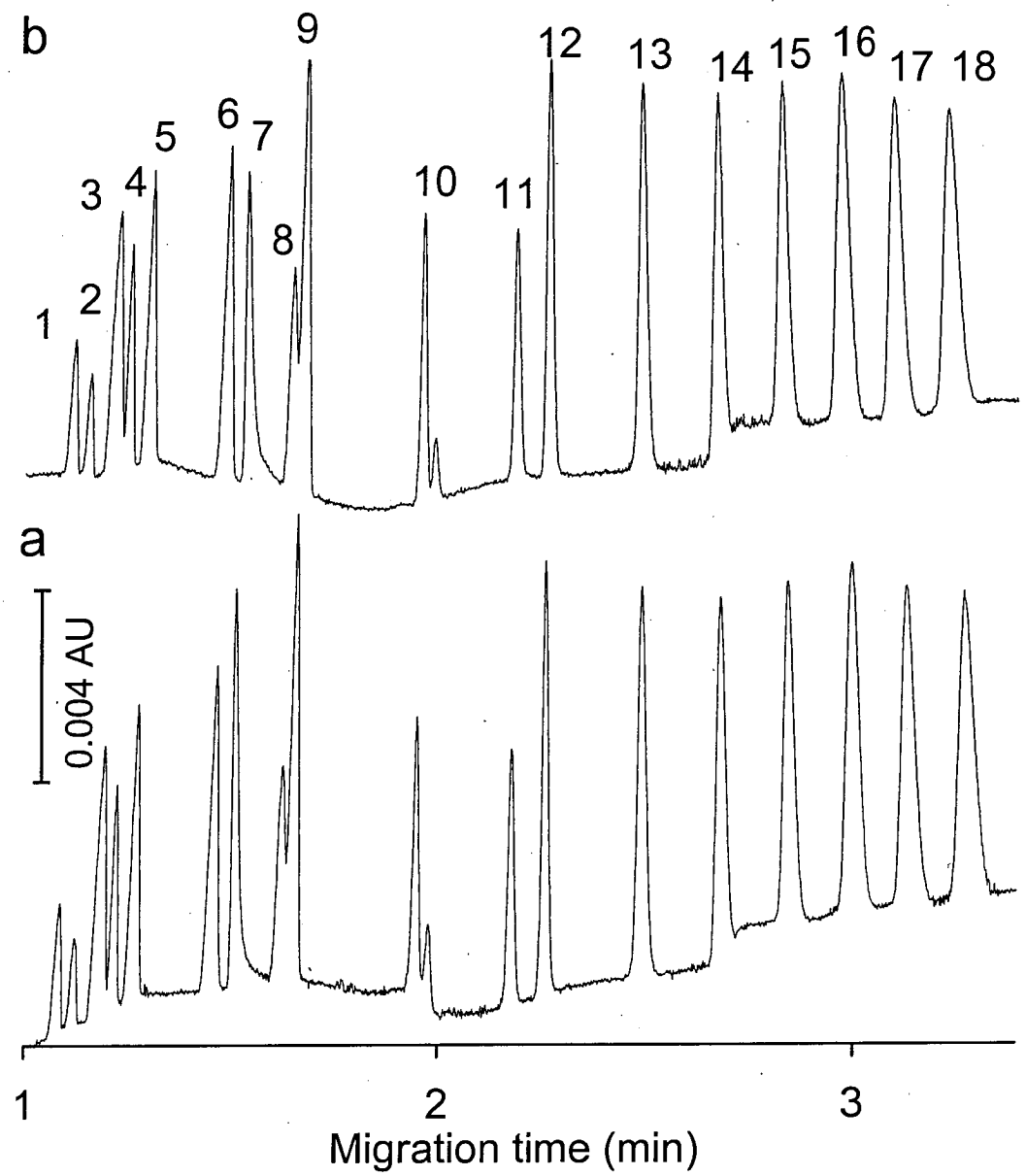

Figure 6-7 Electropherogram of 50 μM anion mixture after (a) 1 and (b) 30 runs without electrolyte replacement or replenishment. Peak identification: 1= bromide, 2= chloride, 3= sulfate, 4= nitrate, 5= oxalate, 6= malonate, 7= formate, 8= citrate, 9= succinate, 10= methanesulfonate, 11= acetate, 12= ethanesulfonate, 13= propanesulfonate, 14= butanesulfonate, 15= pentanesulfonate, 16= hexanesulfonate, 17= heptanesulfonate, 18= octanesulfonate. Conditions- electrolyte: 4 mM Orange G, 10.0 mM histidine, 0.05% HPMC; separation pressure: 25 mbar. All other conditions as in Figure 6-2.

Orange G has an absorption maximum at 478 nm which is very close to the emission wavelength of a blue LED (476 nm). The use of LEDs as highly effective light sources, particularly in the visible region of the spectrum, [5] is a viable alternative to traditional light sources such as deuterium, mercury and zinc lamps, especially since they exhibit very low noise levels. A Waters Quanta 4000 instrument that had been modified for use with LED light sources was fitted with a blue LED of output wavelength 476 nm. The detector linearity of this configuration was found to be maintained up to 200 mAU, which corresponded to a maximum Orange G concentration of 2 mM. The Waters instrument did not have the capability to allow the application of pressure during a run so an Orange G concentration of 0.5 mM was used to provide a satisfactory baseline. A 2 μM mixture was injected using a 75 μm PEI coated capillary (see Figure 6-8). Detection limits and separation efficiencies are listed in Table 6-3 and whilst peak heights were less than those achieved using the 4 mM Orange G electrolyte and 50 μm capillary on the Agilent instrument, the extremely low noise levels observed provided detection limits well below 1 μM. The baseline noise (~0.02 mAU) was at the limit of digital resolution of the instrument and data acquisition software. However, separation efficiencies were not optimal due to the low probe concentration used and it was not possible to achieve further sensitivity gains through increased peak heights and narrower peaks because the detector linearity and lack of application of pressure prevented the use of higher probe concentrations.

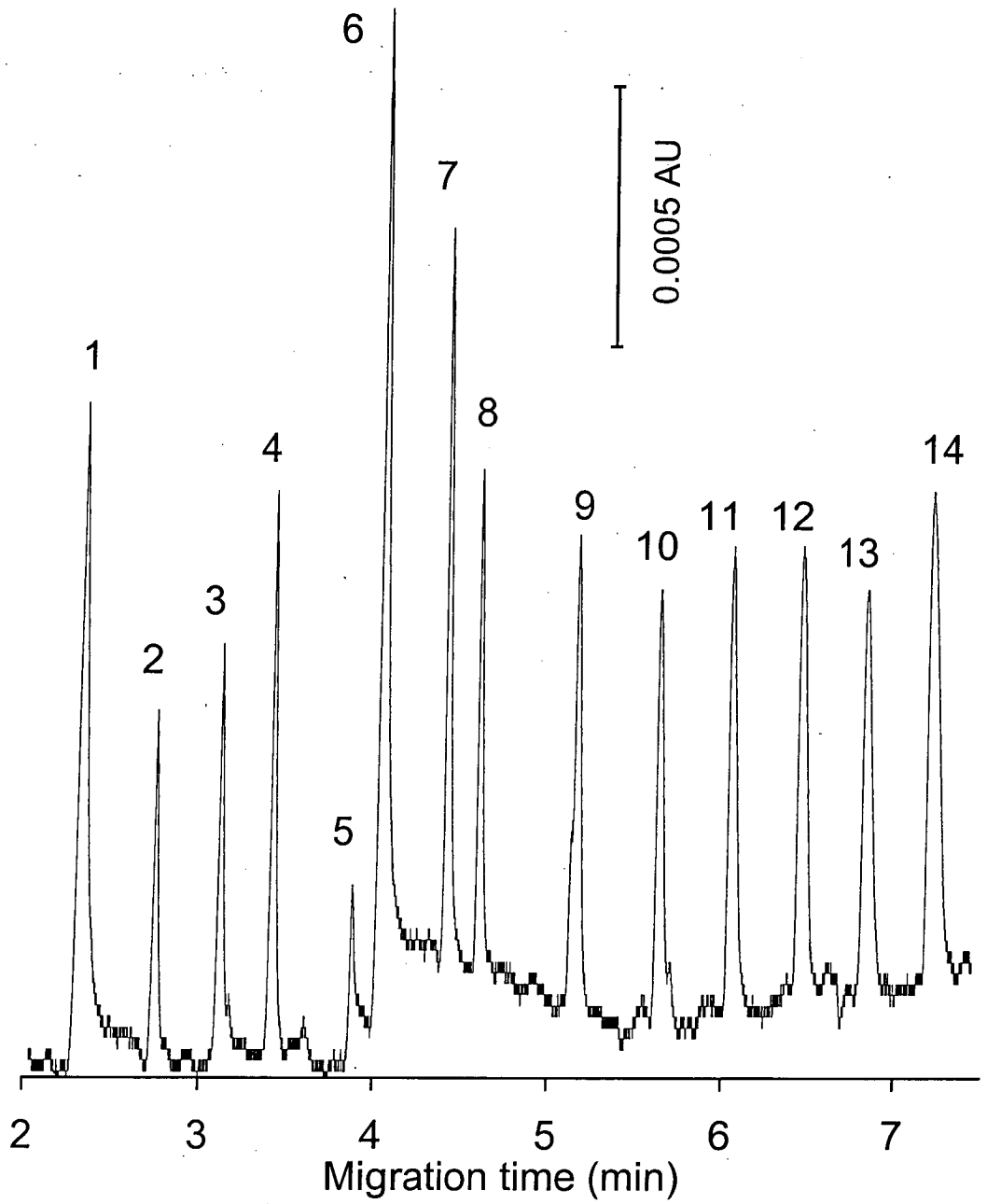

Figure 6-8 Electropherogram of 2 μM anion mixture using a blue LED light source. Peak identification: 1= chloride, 2= malonate, 3= succinate, 4= phthalate, 5= methanesulfonate, 6= carbonate, 7= iodate, 8= ethanesulfonate, 9= propanesulfonate, 10= butanesulfonate, 11= pentanesulfonate, 12= hexanesulfonate, 13= heptanesulfonate, 14= octanesulfonate. Conditions- capillary: bare fused silica, 75 μm ID, length 0.60 m, 0.52 m to detector; electrolyte: 0.5 mM Orange G, 10.0 mM histidine, 0.05% HPMC; separation voltage: -30 kV, detection: indirect photometric at 476 nm; injection: 40 s at 10 cm.

Table 6-3 Detection limits (μM) and separation efficiencies (number of theoretical plates, N) achieved with a Waters Quanta 4000 instrument and LED light source. Conditions- sample: 2 μM of each analyte, BGE: 0.5 mM Orange G, 10.0 mM histidine, 0.05% HPMC, pH 7.70, capillary: 0.52 x 0.60 m, 75 μm ID bare fused silica, voltage: -30 kV, injection: 40 sec at 10 cm, temperature 25° C, light source: blue LED, detection: indirect photometry at 476 nm.

Analyte	LOD (μM)	Efficiency (N)
Chloride	0.23	16,760
Malonate	0.42	58,690
Succinate	0.36	91,440
Phthalate	0.26	91,810
Methanesulfonate	0.83	136,200
Carbonate	0.15	87,320
Iodate	0.20	177,330
Ethanesulfonate	0.29	151,130
Propanesulfonate	0.31	108,860
Butanesulfonate	0.34	122,100
Pentanesulfonate	0.32	93,030
Hexanesulfonate	0.33	93,270
Heptanesulfonate	0.36	76,550
Octanesulfonate	0.30	61,900

6.3.7 Analysis of Air Filter Samples

The combination of high sensitivity and extended linear response range provided by this system was ideal for the analysis of samples containing analytes present in trace quantities or in matrices of higher ionic strength than normally applicable when highly absorbing probes are used. Filters used in air sampling provide such a challenge, with anions such as phosphate, methanesulfonate and oxalate being present in low concentrations and chloride, sulfate and acetate occurring at concentrations an order of magnitude greater. The analysis of air filter samples for anions is traditionally performed using ion chromatography [6-8], with relatively few uses of CE for such samples having been reported [9-13]. Dabek-Zlotorzynska *et al.* [9, 12, 13] used a pyromellitate electrolyte and indirect detection at 254 nm to determine nitrate, nitrite, chloride, oxalate and sulfate in air filter samples. Krivacsy *et al.* [10] used chromate at 254 nm to detect inorganic anions and organic acids in atmospheric aerosols. Indirect detection with 2,6-naphthalenedicarboxylic acid [14] has also been used for the determination of low molecular mass carboxylic acids in atmospheric aerosol samples. Levart *et al.* [15] detected organic acids in air samples using 2,6-pyridinecarboxylic acid as a probe at a detection wavelength of 200 nm. In general, the lack of sensitivity provided by CE in comparison with IC has been a major limitation which has restricted the use of CE for this type of analysis. Orange G is a suitable probe for the typical anions present in air samples because its electrophoretic mobility provides well shaped peaks for all of the analytes generally encountered. The effective suppression of EOF through a combination of PEI coating and HPMC added to the BGE also facilitates detection of a wide mobility range of analytes. Finally, the opportunity to use Orange G at high probe concentrations enables it to be used for analytes present at relatively high concentrations.

Calibration curves were constructed for chloride, sulfate, nitrate, oxalate, formate, acetate, phosphate, methanesulfonate and acetate. Good linearity (R^2 values exceeding 0.99) was observed over the range 1.5-200 μM. Filter samples were extracted into 6 mL of Milli-Q water and were sonicated and passed through a 0.45 μm filter prior to

analysis in triplicate using the optimised 4 mM Orange G BGE. A typical separation is shown in Figure 6-9. Peak identities were confirmed by spiking the sample with standard solutions.

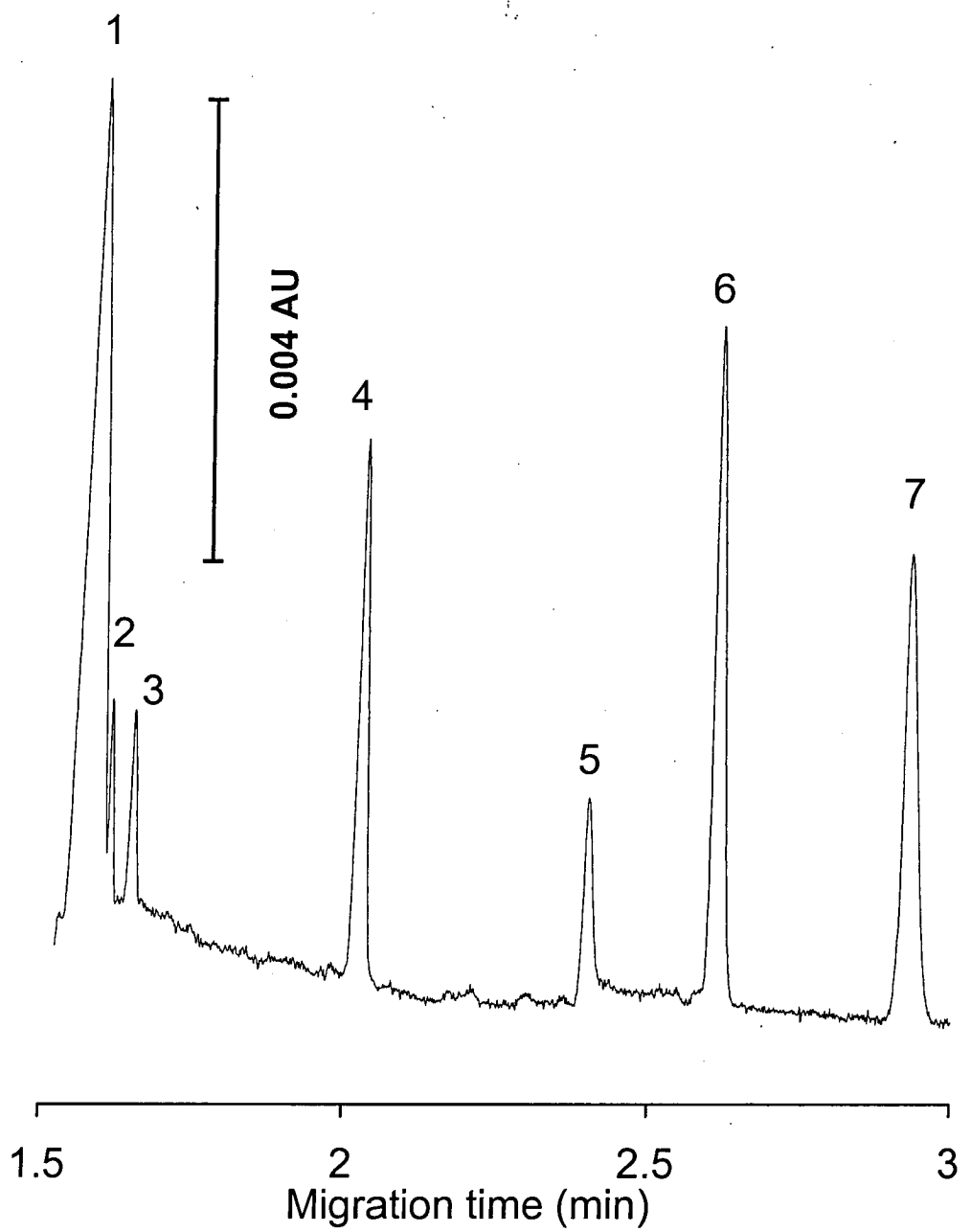

Figure 6-9 Electropherogram of a typical air filter sample extract. Peak identification: 1= sulfate, 2= nitrate, 3= oxalate, 4= formate, 5= phosphate, 6= methanesulfonate, 7= acetate. Conditions as shown in Figure 6-7

Peak areas were measured and divided by migration time to give corrected peak areas. The same samples and standards were analysed simultaneously by IC for direct comparison, again in triplicate, and calibration plots exhibiting R^2 values of >0.999 were observed. Values obtained for filter samples using IC and CE are listed in Table 6-4, from which it can be seen that agreement between the two techniques was generally good. Discrepancies in the CE and IC values for sulfate and chloride were due to overlapping of this peak pair at high concentrations in the CE method. The anomalous result for methanesulfonate by IC in sample 2 was due to this ion being eluted near the void volume and thereby being subject to peak integration errors and overlap from the high concentration of acetate present in this sample. With CE, samples were diluted where necessary to achieve separation or to remain inside the calibration range. The major advantage of the CE method was the much shorter run time of 4 min, compared to the IC run time of around 30 min including column equilibration. Additionally, the use of a dye as probe gave greater sensitivity than existing CE methods for these analytes.

Table 6-4 Determined values (μM) of anions in extracts from four air filter samples by CE and IC, with corresponding percentage differences (%) between the results given by each technique. See Experimental for details.

Analyte	1			2			3			4		
	CE	IC	%	CE	IC	%	CE	IC	%	CE	IC	%
Acetate	23.4	29.8	-21.5	81.4	79.7	2.1	57.4	61.9	-7.8	271.5	258.2	4.9
Formate	31.6	30.1	5.0	1.01	0.74	27	27.9	28.4	-1.8	0.61	0.72	-18
MSA				7.55	2.06	72	22.1	22.1	0	7.53	7.85	-4.2
Chloride		1.98		65.2	70.9	-8.7	2416	2346	2.9	147.6	187.5	27
Nitrate	6.04	5.34	13.1	9.46	8.9	5.9	31.8	33.6	-5.7	22.8	22.7	0.4
Sulfate	72.5	73.8	-1.8	100.4	99.6	0.8	256.8	216.4	15.7	92.4	105.1	-13.7
Phosphate	-	2.16		6.64	6.05	8.9	4.26	4.24	0.5	4.58	6.11	-33.4
Oxalate	3.98	4.05	-1.7	4.95	4.73	4.4	10.0	11.4	-14	7.97	7.13	10.5

6.4 Conclusions

For the use of dyes as probes to be successful, it was necessary to overcome two significant problems. First, the EOF needed to be manipulated to allow the maximum possible mobility range of analytes to be detected. This was achieved in this work through a combination of coated capillaries and the addition of a neutral polymer to the BGE. EOF was reduced to a negligible value which allows virtually all analytes anions to reach the detection window due solely to their electrophoretic mobility. This was an improvement over previously published work using dyes. Second, the degradation in quality of baselines due to increased probe concentration needed to be reduced or eliminated. A novel and somewhat counter intuitive measure provided an excellent solution. The use of pressure driven flow is normally shunned by users of CE due to loss of separation efficiency. However, the application of a relatively small amount of pressure (25 mbar) at the injection point (resulting in a hydrodynamic flow of about 0.045 cm/s) concurrently with the application of the separation voltage was demonstrated here to give remarkable improvements in the baseline stability. Loss of separation efficiency due to the hydrodynamic flow was significant when a 75 μm capillary was used, but was minimal for a 50 μm capillary. Although this was an unorthodox approach when increases in detection sensitivity were being sought, the combination of a reduced inner diameter capillary and the application of pressure provided a surprisingly sensitive technique which also had the capacity to handle samples of relatively high ionic strength greater. These benefits were utilised in the determination of trace anions in air filters extracts in which the analytes were present at concentrations an order of magnitude lower than the matrix ions. Comparisons of the analysis of samples by CE with an IC method showed acceptable agreement between the two methods, but the CE method offered much shorter run times and higher sample throughput. This is the first demonstration of the use of highly absorbing dyes as probes in the analysis of real samples. The areas remaining open to improvement include the use of a suitable LED light source with decreased baseline noise levels and hence improved signal to noise ratios. If an instrument could be modified to allow such a light source and also offer the ability to apply pressure during separation, a potent

combination of increased peak heights and reduced baseline noise could lead to further significant improvements in detection sensitivity for indirect photometric detection.

6.5 References

1 P. Doble, M. Macka and P.R. Haddad, *J. Chromatogr. A,* **804** (1998) 327.

2 W.L.F. Armarego and D.D. Perrin, *Purification of Laboratory Chemicals* , Oxford, London, 4th Edition 1996.

3 W. Buchberger and P.R. Haddad, *J. Chromatogr.,* **608** (1992) 59.

4 X. Huang, J.A. Luckey, M.J. Gordon and R.N. Zare, *Anal. Chem.,* **61** (1989) 766.

5 M. Macka, P. Andersson and P.R. Haddad, *Electrophoresis,* **17** (1996) 1898.

6 C. Perrino, M. Concetta, T. Sciano and I. Allegrini, *J. Chromatogr. A,* **846** (1999) 269.

7 S.J. Lue, T. Wu, H. Hsu and C. Huang, *J. Chromatogr. A,* **804** (1998) 273.

8 D. Krochmal and A. Kalina, *Atmos. Environ.,* **31** (1997) 3473.

9 E. Dabek-Zlotorzynska, M. Piechowski, F. Liu, S. Kennedy and J.F. Dlouhy, *J. Chromatogr. A,* **770** (1997) 349.

10 Z. Krivacsy, A. Molnar, E. Tarjanyi, A. Gelencser, G. Kiss and J. Hlavay, *J. Chromatogr. A,* **781** (1997) 223.

11 E. Meszaros, T. Marcza, A. Gelencser, J. Hlavay, G. Kiss, Z. Krivacsy, A. Molnar and K. Polyak, *J. Aersol Sci.,* **28** (1997) 1163.

12 E. Dabek-Zlotorzynska and J.F. Dlouhy, *J. Chromatogr. A,* **671** (1994) 389.

13 E. Dabek-Zlotorzynska, J.F. Dlouhy, N. Houle, M. Piechowski and S. Ritchie, *J. Chromatogr. A*, **706** (1995) 469.

14 E. Dabek-Zlotorzynska, M. Piechowski, M. McGrath and E.P.C. Lai, *J. Chromatogr. A*, **910** (2001) 331.

15 A. Levart, M. Gucek, B. Pihlar and M. Veber, *Chromatographia Supplement*, **51** (2000) 321.

Chapter 7

Highly Sensitive Indirect Photometric Detection of Cations by Capillary Electrophoresis Using the Cationic Dye Chrysoidine

7.1 Introduction

It has been clearly shown [1, 2] that the most effective means of decreasing limits of detection and thereby improving sensitivity is to increase the absorptivity of the probe. This approach has not yet been fully applied to the detection of cations. The analysis of metal ions in solution can be performed successfully using capillary electrophoresis provided the detection limits of the method are low enough. Capillary electrophoresis is a much less expensive technique than methods such as ICP-MS and AAS in terms of equipment and operating costs. Capillary electrophoresis also offers a high sample throughput due to short run times

Typically used cationic probes, such as imidazole, benzylamine, 4-methylbenzylamine (marketed as UV Cat 1 by Waters) and creatinine, have absorptivities of 5-10,000 $L.mol^{-1}\ cm^{-1}$ (see Tables 1.8 and 1.9 in Chapter 1). The use of cationic dyes with greater absorptivities would lead to increased peak heights when compared to traditional probes. Xue *et al.* [3] detected potassium using malachite green as a probe, but without buffering the electrolyte. Mala *et al.* [4] used methyl green for the detection of caesium, potassium, calcium, magnesium, sodium and lithium, but, tris(hydroxylaminomethane) (Tris) and acetic acid were used to provide a relatively low degree of buffering at pH 6.5, which most importantly meant that protonated cation Tris-H^+ would act as a competing co-ion. This method was adapted by Butler *et al.* [5] who substituted pyronine G in place of methyl green in order to better match the emission wavelength of an LED light source. Potassium, calcium, sodium and lithium were separated in a background electrolyte (BGE) comprising 0.15 mM pyronine G and 1 mM Tris at pH 4.0. In the rare occurrences of the use of cationic probes, they have been used at concentrations of less than 1 mM in order to remain within the linear range of the

absorbance detector. The adsorption problems that can be encountered during the use of cationic dyes were illustrated by the work of Higashijima *et al.* [6] who used methylene blue as an indirect fluorescence probe for amino acids. An alkylsilane derivatised capillary was used to reduce adsorption of the dye.

Recent work in Chapter 4 has shown that most modern CE instruments are capable of maintaining a linear response at absorbance values which are far in excess of those used commonly. The use of highly absorbing anionic dyes for detection of anions at increased probe concentrations has shown that significant improvements in peak shape, separation efficiency, resolution and increased detection sensitivity can be achieved (see Chapters 5 and 6). Associated problems such as baseline instability can be minimised by careful manipulation of the BGE composition, together with the capillary and operating conditions. In the present work, a highly absorbing dye, chrysoidine, has been used to provide very sensitive indirect photometric detection of cations. Separation of a wide range of metal ions was made possible by the addition of hydroxycarboxylic acids which acted as a complexing agent. Comparisons of this system with a method based on a traditional probe, imidazole, showed that chrysoidine provided more sensitive detection.

7.2 Experimental

7.2.1 Instrumentation

The general experimental details are given in Chapter 2.

The capillary electrophoresis instrument used during this work was an Agilent Technologies ^{3D}CE. A voltage of +30 kV was applied during all separations, with temperature maintained at 25°C.

7.2.2 Procedures

Fused silica capillaries were coated with poly(ethylenimine) by flushing with 1 M sodium hydroxide for 30 min, water for 30 min followed by a 4% poly(ethylenimine) solution for 1 h which was then left to stand in the capillary for 30 min. The capillary was finally flushed with water for 30 min before use.

Chrysoidine was purified using the following approach. A solution of 3 g of chrysoidine dissolved in 150 mL of Milli-Q water was placed in a separating funnel. Sodium hydroxide (1 M solution) was added dropwise until a colour change from red to yellow occurred. The deprotonated dye was then extracted with three successive 50 mL portions of chloroform. The organic extracts were collected and were washed with four 100 mL portions of Milli-Q water in order to back-extract inorganic salts and impurities. The organic layer was then dried over anhydrous sodium sulfate and was gravity filtered through a fluted filter paper. The solution was evaporated to dryness using rotary evaporation. The solid product was then dissolved in 100 mL of ethanol and was acidified with hydrochloric acid to regenerate the dye as the hydrochloride salt. The solution was rotary evaporated to dryness with successive 100 mL portions of ethanol to remove excess hydrochloric acid. The final product was dried at 100° C for two hours. A final yield of 1.8 g was obtained and the product was stored under nitrogen.

7.3 Results and Discussion

7.3.1 Selection of the Dye to be Used as a Probe

Chrysoidine (see Figure 7-1) was chosen for investigation as it is highly absorbing, monovalent and has a moderate mobility. All three factors were expected to result in improved sensitivity when compared with other probes used for cationic detection. Chrysoidine has an absorption maximum at 453 nm and an absorptivity at this wavelength of 23,427 $L.mol^{-1}$ cm^{-1}which is approximately five to ten times greater than

the absorptivities of commonly used probes. Increased detection sensitivity and peak heights should follow (Eqn. (1.14)). In order to obtain well shaped and symmetrical peaks the mobility of the probe should match the mobility of the analytes as closely as possible. Cationic dyes typically have mobilities significantly less than the electrophoretic mobilities of most metal ions. Accordingly, it would be beneficial to use a cationic dye with a relatively high mobility. As the vast majority of commercially available dyes are monovalent, those with lower molecular weights should offer the highest possible mobilities. The mobility of chrysoidine measured at pH 4 with an imidazole BGE was found to be +32 $m^2 V^{-1} s^{-1}$, which offers an acceptable mobility match for most metal ions. The use of a monovalent probe will also provide the highest possible transfer ratios, which should maximise detection sensitivity.

Analysis of chrysoidine (as supplied) using an imidazole-HIBA electrolyte showed that it contained a significant amount of sodium. It has been clearly demonstrated that introduction of co-ions must be avoided in indirect detection systems in Chapter 3. The dye was therefore purified using the procedure outlined in Section 7.2.2. Analysis of the purified dye by capillary electrophoresis with an imidazole-HIBA electrolyte showed that the purity was increased from 91% to 99.3% using this method, resulting in a suitable level of purity for use as an indirect detection probe for cations. The absorptivity of the purified dye was determined to be 26,733 $L.mol^{-1} cm^{-1}$ at 453 nm.

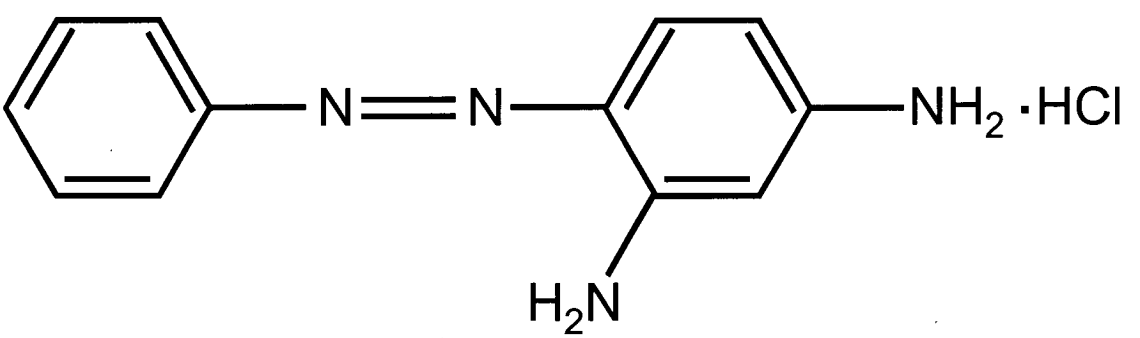

Figure 7-1 Structure of chrysoidine.

Initial investigations were made using BGEs containing only chrysoidine without the addition of a complexing agent in order to determine suitable operating conditions. It was to be not viable to perform detection at the absorption maximum of chrysoidine (453 nm) as baseline noise was far too high due to the low light intensity provided by the deuterium lamp in the visible region. A compromise wavelength of 230 nm was therefore chosen to provide the best combination of low baseline noise and chrysoidine absorptivity. The absorptivity of chrysoidine at this wavelength was only about 40% of its maximum absorptivity. An arbitrary probe concentration of 5 mM was used for initial studies and the background absorbance of BGEs containing this chrysoidine concentration was well inside the upper detector linearity limit of the particular CE instrument used (780 mAU). This moderately high dye concentration was chosen in order to decrease electromigrational dispersion, improve stacking effects and potentially to increase detection sensitivity. It has also been shown previously that dyes can be used at this concentration only if adsorption of the dye to capillary walls can be prevented or at least reduced to an acceptable level (Chapters 5 and 6). When a 5 mM chrysoidine BGE without any additives was used on an uncoated capillary, the resultant baseline was unstable and irreproducible. Baseline stability was improved markedly by coating the capillary with PEI, in a similar fashion to that detailed in Chapter 6. Addition of hydroxypropyl methyl cellulose (HPMC) to the BGE also helped to further stabilise the baseline and to suppress the electroosmotic flow (EOF). The application of a small amount of inlet pressure, together with the use of capillary of reduced ID also assisted the attainment of a stable baseline without appreciable loss of separation efficiency. Hence all further work was performed on a 50 μm PEI-coated capillary with the addition of 0.05% HPMC to the BGE and the application of a small amount of pressure to the inlet side of the capillary.

7.3.2 Separation With Addition of Complexing Agents to the BGE

The conditions described above were found to be suitable for the separation of a small number of metal ions. However, separation of mixtures of several metal ions was not possible without addition of a complexing agent. The addition of 2-hydroxyisobutyric acid (HIBA) to a 5 mM chrysoidine solution caused the pH to decrease from 4.1 to 3.

At this lowered pH the concentration of H^+ present causes competitive displacement with the probe, leading to a loss of sensitivity, especially for the high-mobility cations. Adjustment of the pH of the BGE by addition of a buffer was not possible without introduction of unwanted co-ions. Titration with anion exchange resin in the hydroxide form was investigated as a method of avoiding the addition of co-ions but the dye was found to undergo strong and irreversible adsorption onto the resin. Similarly, replacement of the dye counter-anion (chloride) for hydroxide or a weak acid complexing agent using anion-exchange was unsuccessful.

This problem was solved by modifying the dye purification process. The neutral, free-base form of the dye was isolated by evaporating the chloroform-containing dye solution (see Section 7.2.2) to dryness prior to the reformation of the dye hydrochloride. The solid product was collected, oven dried and stored under nitrogen. Analysis of the purified dye showed the absence of chloride or any other anions, suggesting that the dye was present as a free base. In this form, the dye could be titrated with a solution of a weak acid complexing agent without the pH falling below 4. The dye was therefore used with the desired complexing agent present as the dye counter-anion.

The two complexing agents chosen for use in conjunction with chrysoidine were HIBA and lactic acid. Both have been used widely in the separation of a range of metal ions [7-10]. Since the emphasis of the present study was on detection sensitivity rather than on separation selectivity, the concentrations of HIBA and lactic acid were not optimised and arbitrary concentrations at 5 mM and 10 mM, respectively, were used. These values were chosen on the basis of previous successful applications of the two complexing agents. The necessity for BGEs for indirect detection to be properly buffered without the introduction of co-ions has been well documented. In order to provide sufficient buffering, the pH of the electrolyte was adjusted to the pK_a of the complexing agent used. Hence the complexing agent provided both complexation effects to enhance separation selectivity and also the required buffering capacity.

7.3.3 Performance of the BGE

A mixture of alkaline earth, transition metals and lanthanides was chosen to investigate the performance of the BGE described above. The separation with HIBA is given in Figure 7-2 and shows that good peak shapes were obtained for analytes having a very wide mobility range, indicating that the mobilities of the complexed metal ions matched the mobility of chrysoidine. A separation of 18 cations was achieved in 4.5 min. Good peak shapes were also observed in the separation of 16 cations in less than 3.5 min using lactic acid as the complexing agent (Figure 7-3). Complexation with lactic acid did not reduce the mobilities of the analytes as markedly as did HIBA. It should be pointed out that neither the lactate nor HIBA systems were optimised with regard to the concentration of the probe and the complexing agent and it would be expected that such optimisation would lead to improved separations and better sensitivity.

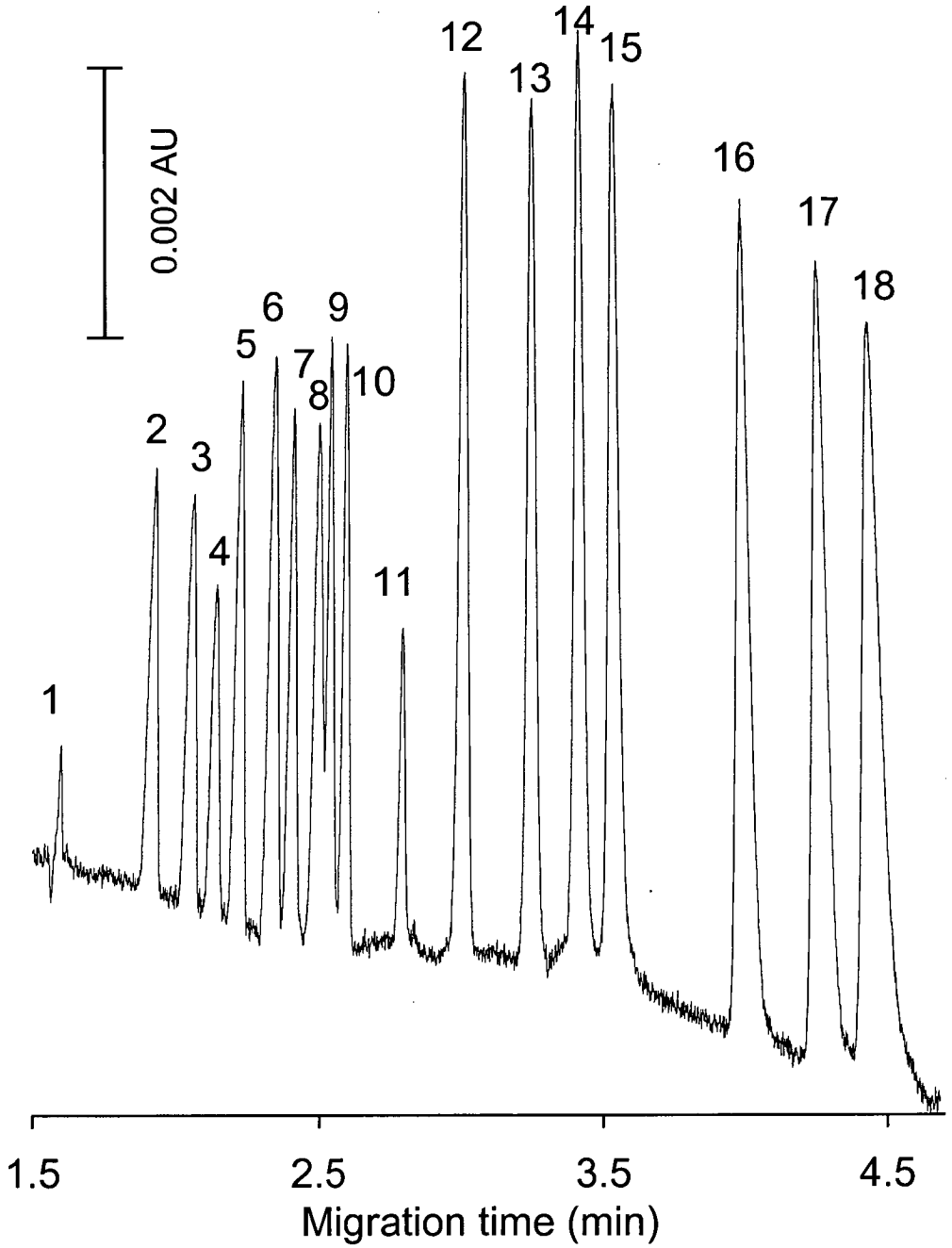

Figure 7-2 Electropherogram of 50 μM cation mixture with HIBA as complexing agent. Peak identification: 1= potassium, 2= barium, 3= strontium, 4= calcium, 5= sodium, 6= magnesium, 7= manganese, 8= chromium, 9= iron, 10 =cobalt, 11= lithium, 12= lanthanum, 13= cerium, 14= preaseodymium, 15= neodymium, 16= samarium, 17= europium, 18= gadolinium. Conditions- capillary: PEI coated fused silica, 50 μm ID, length 0.485 m, 0.40 m to detector; electrolyte: 5 mM chrysoidine, 5 mM HIBA, 0.05% HPMC, pH 4.0; separation voltage: +30 kV (current 3 μA at 25° C); separation pressure: 20 mbar; detection: indirect photometric at 230 nm; pressure injection: 50 mbar for 3 s.

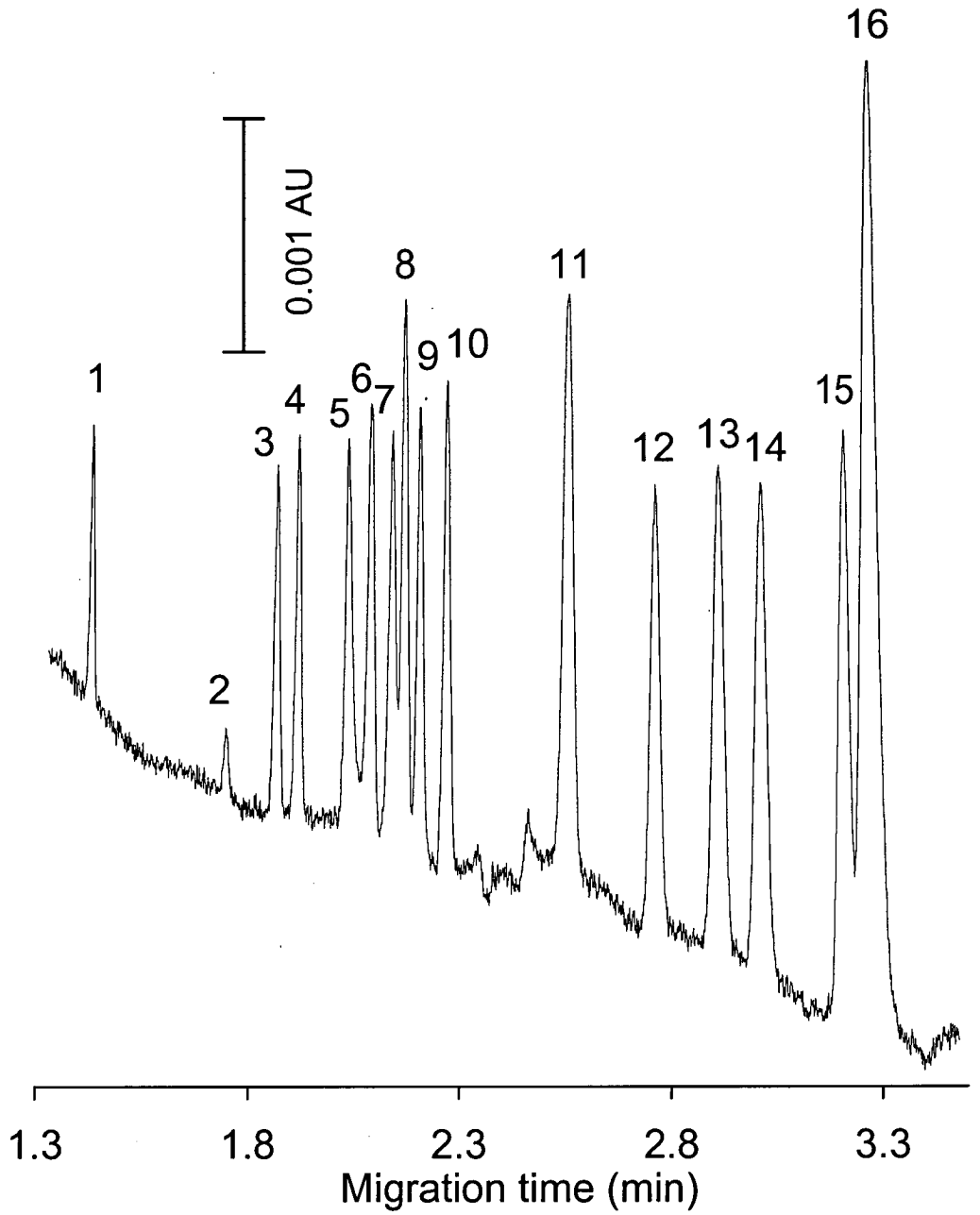

Figure 7-3 Electrophoregram of 10 μM cation mixture with lactic acid as complexing agent. Peak identification: 1= potassium, 2= barium, 3= strontium, 4= calcium, 5= sodium, 6= magnesium, 7= manganese, 8= chromium, 9= iron, 10= cobalt, 11= lanthanum, 12= cerium, 13= praseodymium, 14= neodymium, 15= samarium, 16= europium. Conditions- electrolyte: 5.0 mM chrysoidine, 10.0 mM lactic acid, 0.05% HPMC, pH 3.8; voltage: +30 kV (current 6 mA at 25° C); separation pressure: 20 mbar, injection: 50 mbar for 8 s. All other conditions as in Figure 7-2.

Detection limits and separation efficiencies were calculated from an injection of a 2 μM mixture (Figure 7-4 and Figure 7-5) and are recorded in Table 7-1. For comparison purposes, the same 2 μM mixture was analysed using a previously reported optimised 5.0 mM imidazole, 6.75 mM HIBA electrolyte and is included for comparison purposes in Figure 7-4 and Figure 7-5. Peak heights with chrysoidine are larger than those obtained with imidazole, especially significant considering the fact that a 75 μm ID capillary was used with imidazole compared to a 50 μm ID capillary with chrysoidine. Injection volumes in all three cases were the same. Significantly, peak heights and shapes for low mobility analytes were very poor when the relatively high mobility imidazole probe was used. On the other hand, peak shapes were consistently good for all analytes when chrysoidine was used as a probe. Detection limits when HIBA or lactate was used were in the range 0.22-0.61 μM and 0.12-1.43 μM, respectively. This sensitivity is remarkable considering that chrysoidine does not have an absorption maximum compatible with the use of a deuterium lamp light source. The use of a more suitable light source, such as an appropriate LED, could be expected to lead to even lower detection limits. Better signal to noise ratios may also result from careful optimisation of the probe concentration. Regardless of these restrictions, the detection limits achieved here are superior to most other previously reported values obtained using hydrodynamic injection without any sample preconcentration.

Separation efficiencies were acceptable, with values ranging from 72,170-164,210 for HIBA and 40,300-100,530 for lactic acid. Increased efficiencies were observed for electrolytes containing HIBA because of a better correlation between the mobilities of the metal-ligand complexes and that of chrysoidine. Increasing the chrysoidine concentration in order to improve stacking effects could further increase the separation efficiencies of both systems.

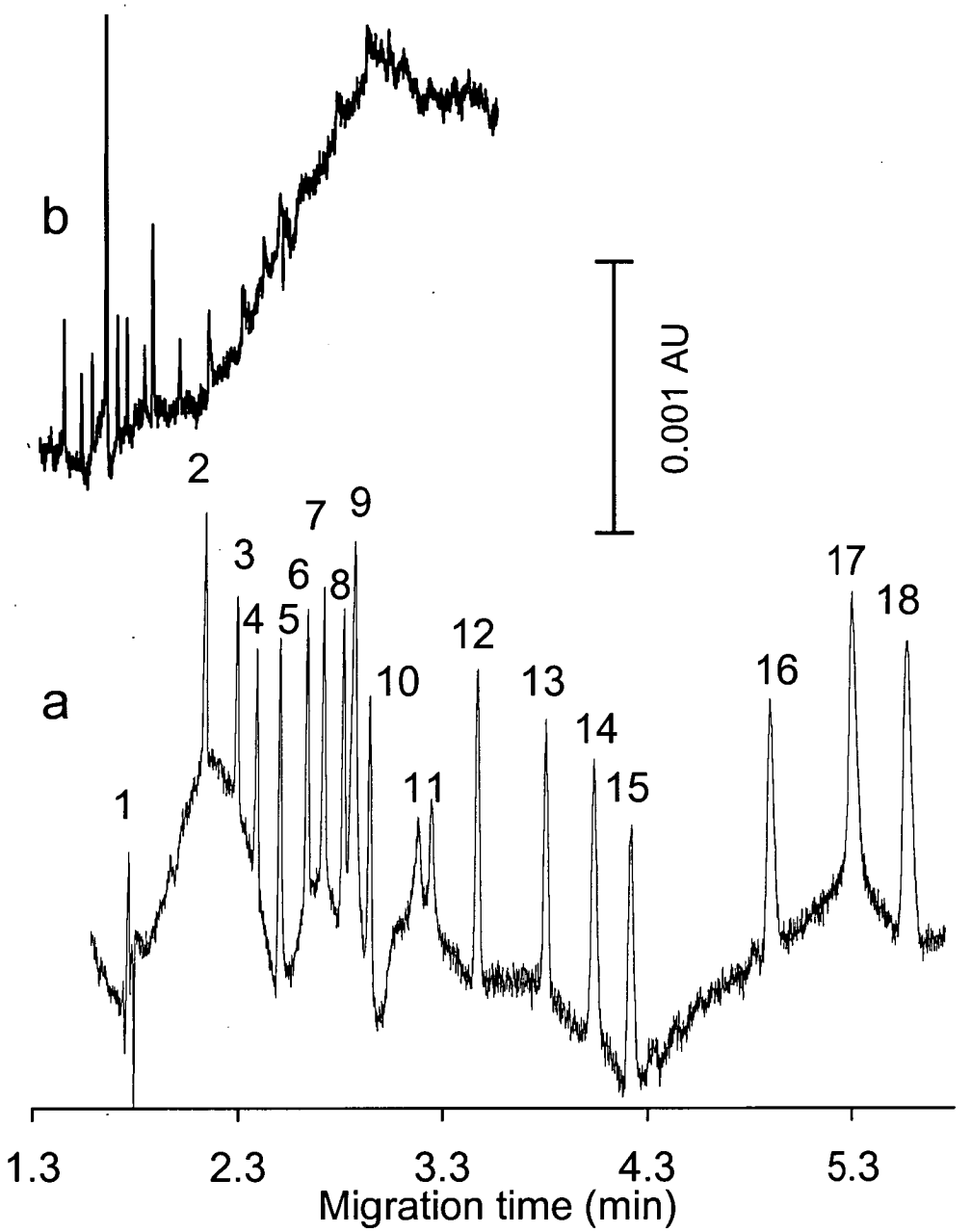

Figure 7-4 Electropherogram of 2 μM cation mixture with (a) 5.0 mM chrysoidine, 5.0 mM HIBA BGE and (b) 5.0 mM imidazole, 6.75 mM HIBA BGE. Conditions- (b) 5.0 mM imidazole, 6.75 mM HIBA, 75 μm ID bare fused silica capillary, injection- (a) 50 mbar for 15 s, (b) 50 mbar for 3 sec. All other conditions as in Figure 7-2.

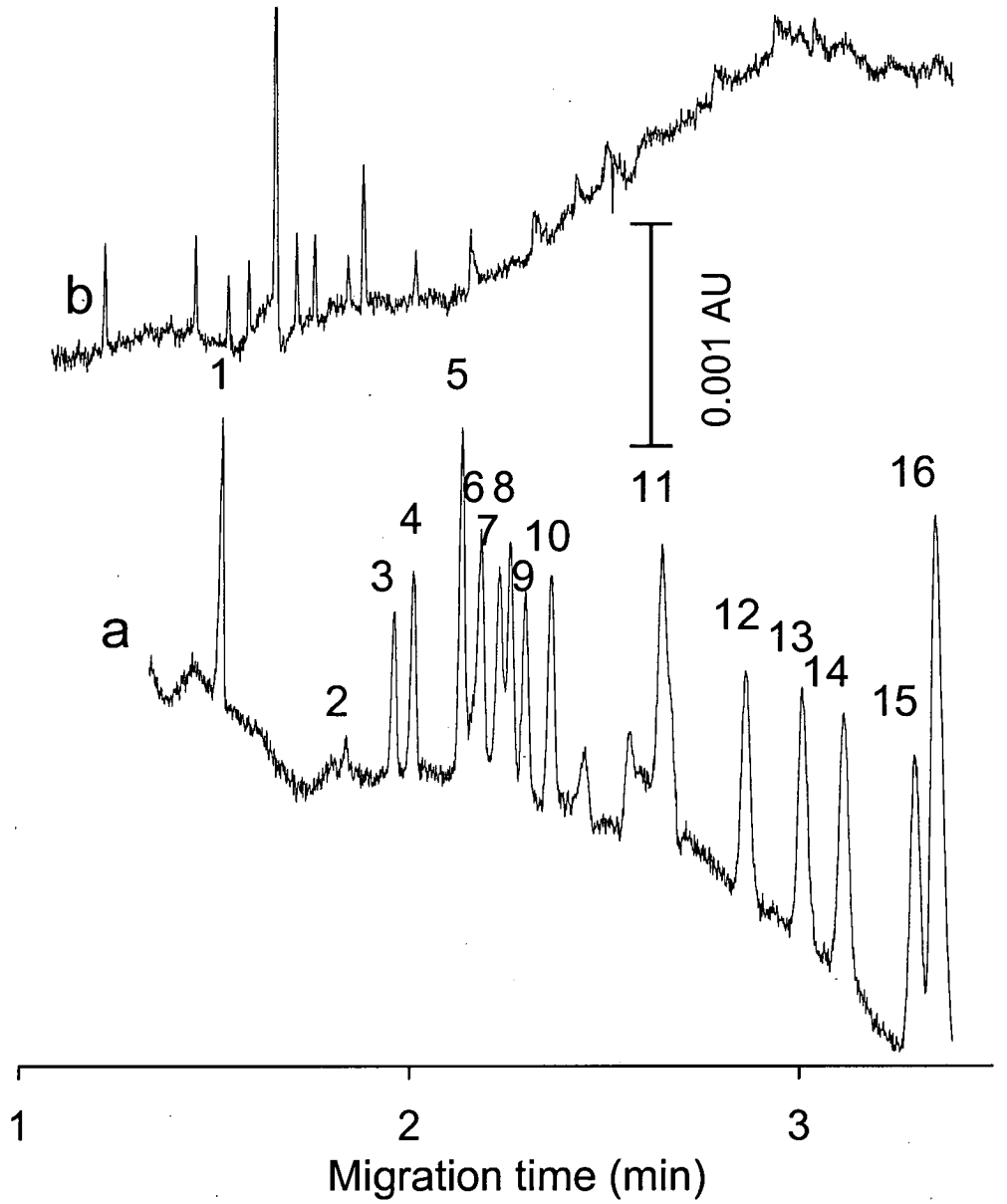

Figure 7-5 Electropherogram of 2 μM cation mixture with (a) 5.0 mM chrysoidine, 10 mM lactic acid BGE and (b) 5.0 mM imidazole, 6.75 mM HIBA BGE. Conditions- (b) 5.0 mM imidazole, 6.75 mM HIBA, pH 4.0, capillary- 75 μm ID bare fused silica capillary, injection- (a) 50 mbar for 15 s, (b) 50 mbar for 3 sec. All other conditions as in Figure 7-3.

Table 7-1 Detection limits (μM) and efficiencies obtained with 5.0 mM chrysoidine electrolytes with (a) HIBA and (b) lactic acid as complexing agents. Conditions- sample: 2 μM of each cation, electrolyte: (a) 5.0 mM chrysoidine, 5.0 mM HIBA, 0.05 % HPMC, pH 4.0 or (b) 5.0 mM chrysoidine, 10.0 mM lactic acid, 0.05 % HPMC, pH 3.8, injection 15 s at 50 mbar. All other conditions as in Figure 7-2.

	HIBA		Lactate	
Analyte	**LOD (μM)**	**Efficiency (N)**	**LOD (μM)**	**Efficiency (N)**
Potassium	0.52	96,180	0.21	83,640
Barium	0.30	132,040	1.43	45,500
Strontium	0.32	137,620	0.36	85,580
Calcium	0.29	135,990	0.29	79,520
Sodium	0.22	99,990	0.19	97,780
Magnesium	0.25	153,350	0.29	78,340
Manganese	0.25	139,000	0.31	61,570
Chromium	0.26	164,210	0.26	100,530
Iron	0.22	59,400	0.31	92,740
Cobalt	0.26	142,660	0.26	87,050
Lithium	0.61	89,930		
Lathanum	0.23	126,620	0.24	40,300
Cerium	0.27	138,270	0.27	64,160
Praseodymium	0.27	88,000	0.24	65,880
Neodymium	0.29	95,870	0.23	55,390
Samarium	0.30	81,580	0.23	82,300
Europium	0.28	75,470	0.12	56,990
Gadolinium	0.25	72,170		

In order to demonstrate that the use of complexing agents operated at a pH value close to their pK_a provided proper buffering, a 50 μM mixture was analysed for 20 consecutive runs without electrolyte replacement or replenishment. From it can be seen that very little change occurred between the first and the 20th runs. Relative standard deviations (RSD's) for migration time, corrected peak area and peak height are recorded in Table 7-2. Migration time reproducibility ranged from 0.22-0.35%, which was less than the values typically reported for CE, particularly considering the large number of consecutive runs used to generate the reproducibility data. Similarly, reproducibility for corrected peak areas (2.08-3.49%) and peak heights (2.13-3.82%) was very satisfactory. The use of a coated capillary and a weak acid complexing agent operated at its pK_a has therefore provided a stable, reproducible, and well buffered system.

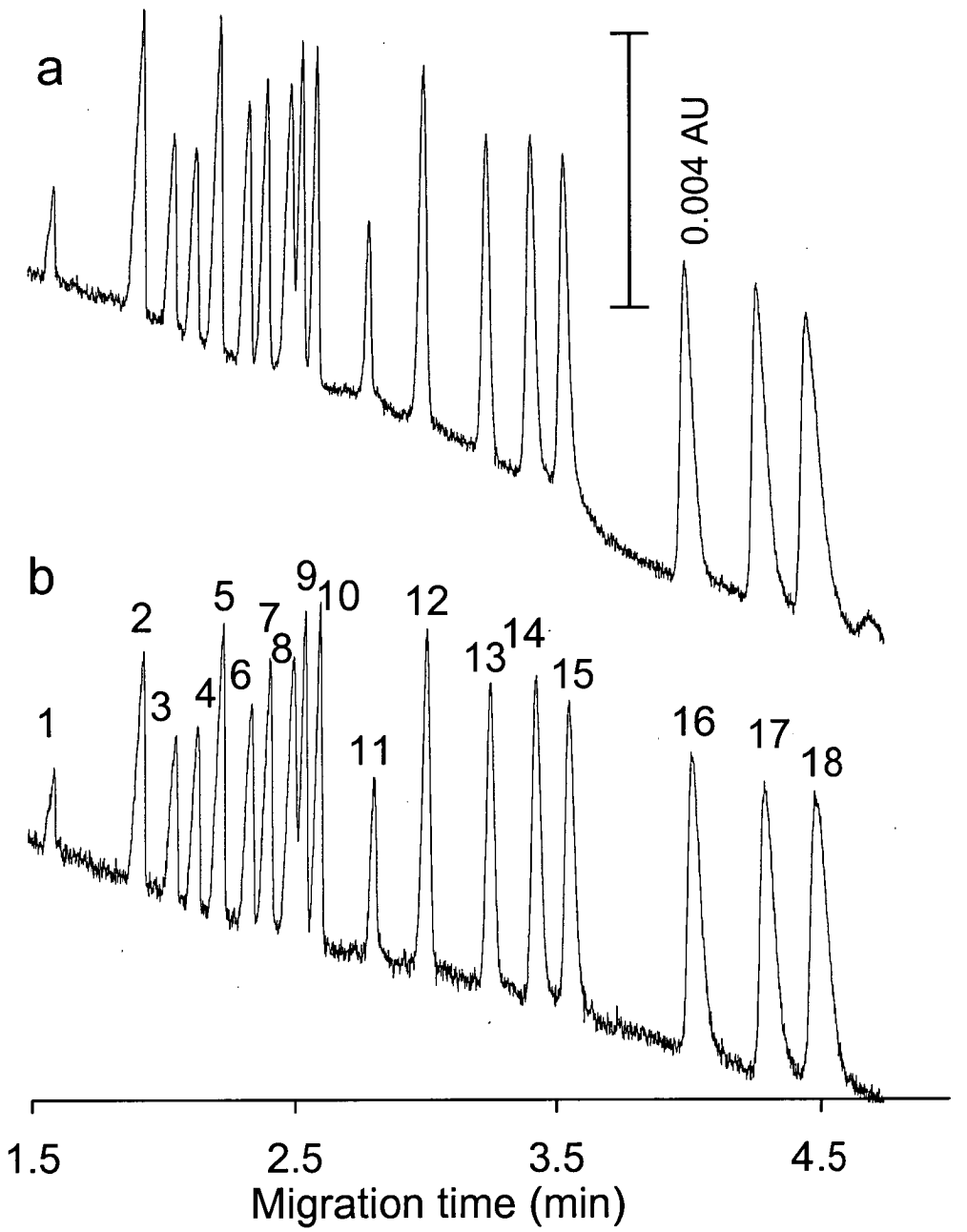

Figure 7-6 Electropherogram of 50 μM cation mixture after (a) 1 and (b) 20 runs without electrolyte replacement or replenishment. Conditions as in Figure 7-2.

Table 7-2 Reproducibility data with 5.0 mM chrysoidine, 5.0 mM HIBA, 0.05 % HPMC electrolyte. Data calculated from 20 successive runs. Conditions- sample: 50 μM of each cation, electrolyte: 5.0 mM chrysoidine, 5.0 mM HIBA, 0.05 % HPMC, pH 4.0. All other conditions as in Figure 7-2.

% RSD	migration time	corrected peak area	peak height
Potassium	0.23	2.67	3.05
Barium	0.27	2.30	2.92
Strontium	0.22	2.79	3.48
Calcium	0.22	2.56	3.02
Sodium	0.24	2.21	3.57
Magnesium	0.24	2.38	3.82
Manganese	0.23	2.08	2.90
Chromium	0.23	2.50	2.89
Iron	0.24	2.76	3.23
Cobalt	0.23	2.42	2.37
Lithium	0.27	3.49	2.95
Lanthanum	0.26	2.92	2.80
Cerium	0.26	2.09	2.53
Praseodymium	0.29	2.12	2.38
Neodymium	0.29	2.60	2.46
Samarium	0.30	2.67	2.98
Europium	0.34	2.56	2.83
Gadolinium	0.35	2.42	2.13

7.4 Conclusions

This work has shown that significant improvements in indirect detection sensitivity for cations can be attained by using a highly absorbing dye as a probe. Associated problems such as baseline stability, lack of probe purity and pH effects can be overcome. Isolation of the cationic dye as a free base was found to be necessary to allow the addition of a weak acid to act as a complexing agent without decreasing pH to a region where competitive displacement with H^+ would become significant. The dye could then be titrated with the weak acid and adjusted to a desired pH. This allowed excellent separations of a metal mixture and highly sensitive detection to be performed. The detection limits achieved were amongst the best reported for indirect detection of cations. Reproducibility and buffering was provided by the use of complexing agents at pH values close to their pK_a's.

It could be expected that further increases in sensitivity could be gained by optimisation of the concentrations of the probe and complexing agent. A significant decrease in detection limits would also occur if the dye could be used at a wavelength at which it absorbs more strongly. This was not possible for chrysoidine with the particular instrument used in this study. Peak heights at the absorption maximum of 453 nm were observed to be roughly twice those at 230 nm, but baseline noise was about 4 times greater due to the lower output of the deuterium lamp at 453 nm. The use of an LED light source operated in the visible region of the spectrum could solve this problem.

In summary, the use of the highly absorbing dye chrysoidine as a probe has led to sensitive detection of a wide range of metal cations. Sensitivity was enhanced compared with less absorbing, commonly used probes for the indirect detection of cations. This study has laid the foundation for further use of dyes for the indirect detection of cations in capillary electrophoresis.

7.5 References

1 F. Foret, S. Fanali, L. Ossicini and P. Bocek, *J. Chromatogr.*, **470** (1989) 299.

2 P. Doble, M. Macka and P.R. Haddad, *J. Chromatogr. A,* **804** (1998) 327.

3 Y. J Xue and E. S. Yeung, *Anal. Chem.,* **65** (1993) 2923.

4 Z. Mala, R. Vespalec and P. Bocek, *Electrophoresis,* **15** (1994) 1526.

5 P.A.G. Butler, B. Mills and P.C. Hauser, *Analyst*, **122** (1997) 949.

6 T. Higashijima, T. Fuchigami, T. Imasaka and N. Ishibashi, *Anal.Chem.*, **64** (1992) 711.

7 Y. Shi and J.S. Fritz, *J. Chromatogr.*, **640** (1993) 473.

8 T.-I. Lin, T.-H. Lee and Y.-C. Chen, *J. Chromatogr. A,* **654** (1993) 167.

9 M. Chen and R.M. Cassidy, *J. Chromatogr.*, **640** (1993) 425.

10 N. Shakulashvili, T. Faller and H. Engelhardt, *J. Chromatogr. A,* **895** (2000) 205.

Chapter 8

Conclusions

The following conclusions can be drawn from this study.

Substantially improved detection limits can be achieved through the use of a highly absorbing indirect detection probe, such as a dye, used in a correctly formulated electrolyte. Increasing the absorptivity of the probe is clearly the easiest and most effective means of decreasing concentration detection limits in indirect photometric detection. Peak shapes are also excellent over a wide analyte mobility range when the appropriate dye is used. This has been demonstrated with a range of anionic dyes for detection of anions and a cationic dye for detection of cations. Dyes are strongly absorbing in the visible region of the spectrum, which provides the chance to perform indirect detection at visible wavelengths.

It is crucial that the introduction of co-ions into the electrolyte is avoided. Unwanted co-ions may be introduced through impurities present in the probe or via incorrect buffering of the electrolyte with a co-ion. Unfortunately, most commercially available dyes contain significant co-ionic impurities, which if not removed will lead to a loss of sensitivity, distorted peak shapes and the presence of system peaks. Suitable purification methods for dyes which are to be used as probes need to be identified and carried out successfully. The use of counter-ionic buffers, or ampholytes at their isoelectric point will provide proper buffering without introducing unwanted co-ions. Properly buffered electrolytes improve method reproducibility and ruggedness significantly. Fortunately, most substances that are likely to be used as buffers can be obtained commercially in high purity.

Most detectors used in capillary electrophoresis instruments retain a linear response far in excess of absorbances which are typically used with indirect detection. As a consequence, probe concentrations can be increased markedly providing excessive separation currents do not occur. This presents the opportunity for highly absorbing dyes to be used at concentrations up to an order of magnitude greater than those employed previously. The

benefits of increased probe concentration are less electromigrational dispersion and improved sample zone stacking, both resulting in improved peak shapes, efficiencies and detection limits.

However, there are problems and limitations in the use of dyes as probes for indirect detection. When the dye concentration exceeds about 1 mM, poor baselines often result due to adsorption of the dye onto the capillary wall. At low concentrations (<1 mM) this can be minimised by the addition of a neutral polymer (HPMC) to the electrolyte which shields the capillary wall from the dye. Additionally, this polymer suppresses EOF almost completely, allowing the separation and detection of anions of a wide range of mobilities. However, at concentrations exceeding 1 mM this approach is not as successful. Two alternative approaches have been used. Firstly, the addition of a zwitterionic surfactant minimised dye adsorption and also provided a relatively high EOF, allowing counter-EOF separation of medium to low mobility anions. This enabled a dye concentration of 3 mM to be used successfully. This method was limited in that high mobility anions could not be detected in the counter-EOF mode with anodic polarity. Coating of the capillary with polyethyleneimine (PEI) and addition of HPMC to the electrolyte suppressed EOF to near zero values, even at probe concentrations approaching 8 mM. However, baseline stability was not acceptable. The application of a small amount of inlet pressure during runs produced a remarkably flat baseline. Separation efficiency was maintained by switching to a narrower ID capillary. Detection limits, peak shapes, efficiency and reproducibility were all enhanced by the use of high probe concentrations.

The use of LEDs as an alternative light source is a viable option. They are particularly suited to visible wavelengths which makes their use in conjunction with highly absorbing dyes an attractive goal. LEDs can provide significantly lower baseline noise in the visible region in comparison with traditional light sources such as deuterium, zinc and mercury lamps. This reduction in baseline noise was used in practice to obtain very good detection limits. The major restriction of the use of LEDs at this time is that there is no commercial instrumentation available that would allow the use of LEDs in a detector offering a high

linear range. Ideally, the combination of an LED which has an emission wavelength at an absorption maximum of a probe dye would provide optimal signal to noise and correspondingly LOD values.

Indirect photometric detection using dyes as probes offers a suitable level of sensitivity for analysis of real samples. It is vital that electrolytes are adequately buffered to handle such samples. The use of highly absorbing dyes at increased probe concentrations provided an ideal combination of high sensitivity for detection of trace ions with the ability to handle more highly concentrated ions. This was highlighted by the analysis of air filter samples containing a range of anions varying in mobilities and concentrations. Determined values agreed quite well with analysis by ion chromatography. Importantly, this CE method required a much shorter run time, presenting the opportunity for higher sample throughput.

Cationic dyes can be used as indirect detection probes for the detection of cations. In a key improvement over the previous work using dyes which has been restricted to the separation of a limited range of analytes due to incorrect buffering (introduction of system peaks in certain mobility regions), it was shown that use of a properly buffered electrolyte containing a weak auxiliary complexing ligand was a viable approach. The cationic dye can be isolated as a free base to allow the addition of a weak acid auxiliary complexing agent without lowering the pH to a value where competitive displacement with H^+ occurred. Limits of detection (without stacking) were comparable or better than those for previously reported methods using indirect photometric detection of cations.

Some general areas that may merit further work are as follows:

- It would be ideal if an LED light source could be fitted to an instrument with superior detector performance in terms of linearity limit and effective pathlength. This would allow LEDs of various emission wavelengths to be easily installed to match absorption maxima of probes. This would hopefully combine low noise and increased signal and allow probes to be used at higher concentrations in order to improve efficiency, peak shapes and detection limits.

- The detection of cations using dyes has not been optimised. This could be performed systematically, possible using a neural network, in order to obtain optimum probe and complexing agent concentrations which would provide highest possible sensitivity and resolution.
- Highly sensitive simultaneous detection of anions and cations may be possible. In order for this to occur without competitive displacement effects, it would be necessary to obtain the dyes as free acids and bases or as a dye-dye ion pair.
- It may also be possible to use highly absorbing metal complexes, such as porphyrins and phthalocyanines, as probes for indirect detection. Detection limits may be improved in a similar fashion to the use of highly absorbing dyes.
- A combination of stacking injection techniques with highly absorbing probe ions for indirect detection could potentially lead to lower limits of detection, providing the stacking technique is compatible with the choice of probe ion.